University of São Paulo
"Luiz de Queiroz" College of Agriculture

Natural genetic variations from the tomato wild relative *Solanum pennellii* associated with domestication and drought resistance

Mateus Henrique Vicente

Thesis presented to obtain the degree of Doctor in Science. Area: Plant Physiology and Biochemistry

Piracicaba
2019

Mateus Henrique Vicente
Bachelor in Agronomy

Natural genetic variations from the tomato wild relative *Solanum pennellii* associated with domestication and drought resistance

versão revisada de acordo com a resolução CoPGr 6018 de 2011

Advisor:
Prof. Dr. **LÁZARO EUSTÁQUIO PEREIRA PERES**

Thesis presented to obtain the degree of Doctor in Science. Area: Plant Physiology and Biochemistry

Piracicaba
2019

Dados Internacionais de Catalogação na Publicação
DIVISÃO DE BIBLIOTECA – DIBD/ESALQ/USP

Vicente, Mateus Henrique

Natural genetic variations from the tomato wild relative *Solanum pennellii* associated with domestication and drought resistance / Mateus Henrique Vicente. - - versão revisada de acordo com a resolução CoPGr 6018 de 2011. - - Piracicaba, 2019.

81 p.

Tese (Doutorado) - - USP / Escola Superior de Agricultura “Luiz de Queiroz”.

1. Tomate 2. Linha de introgressão 3. Domesticação 4. Resistência à seca 5. Condutância hidráulica I. Título

To my father, mother, brother, nephew,

And my love wife,

For all unconditional love, help, friendship

and support, I dedicate...

ACKNOWLEDGEMENTS

I would like to express my sincere feeling of gratitude to everyone who have contributed to the work described in this thesis.

I am deeply grateful to all of you, specially:

My advisor Prof. Dr. Lázaro Peres for the support during my research and for all knowledge shared. Thank you so much for your confidence, patience, friendship and motivation. It was a pleasure to work with you again.

My sincere thanks also to my co-advisor Prof. Dr. Agustin Zsögön, who provided great support during my Ph.D and help me growth as scientist. Thank you for teaching me so many things.

To all the faculties from Plant Physiology and Biochemistry program, thank you for the scientific teachings, in special to professors Dr. Fabio Tebaldi Silveira Nogueira and Dr. Ricardo Ferraz de Oliveira for the transmitted knowledge and collaborations.

I would like to thank Cassia Figueiredo and Francisco Vitti for their assistance, making possible the development of my experiments.

To my labmates, Ariadne Felício, Guilherme Oliveira, Ignácio Achon, Ivan Sestari, James Gattward, Jonata Freschi, Joni Lima, Karla Gasparini, Lilian Pino, Mariana Silva, Mayara Carvalho, Rodrigo Therezan, thank you for all knowledge shared and for all the fun we have had in the last four years. An especially thank to Diego Sevastian, Eloisa Vendemiatti, Frederico de Jesus, João Pedro, Maísa Pinto, Marcela Notini and Stevan Bordignon for the friendship and conviviality outside laboratory. Also, I would like to thank my friends Airton Carvalho, Antoine Gady, Eder Marques, Geraldo Silva, João Paulo Corrêa, for always help me with molecular biology issues and friendship.

My sincere thanks also Gabriel Daneluzzi and Adairo Andrade for all help and support in many experiments presented in this thesis.

I would like to thank the "Luiz de Queiroz" College of Agriculture for the opportunities granted to me along these years, especially to Maria Solizete Granziol Silva for the help, support and availability anytime, and to Prof. Dr. José Laercio Favarin for the knowledge transmitted to me during my teaching training.

I truly thank CAPES (Agency for the Support and Evaluation of Graduate Education, Finance Code 001) and FAPESP (Foundation for Research Assistance of the São Paulo State, FAPESP File 2016/05566-0) for the financial support throughout my doctorate studies.

An especial thank to my love Adriane. My gratitude for all patience, dedication, love and support to my dreams. My heartfelt gratitude also to my family: my parents Lourdes and Nilton, my brother Felipe and our newest member and nephew Guilherme for all love, understanding, and support during this Ph.D. and in all my life.

Finally, my dear God thank you for everything and for bless me everyday.

"The mind that opens to a
new idea never returns to its
original size."

Albert Einstein

"If you don't like your destiny, don't accept it.
Instead, have the courage to change
it the way you want it to be."

Masashi Kishimoto

CONTENTS

RESUMO

Variações genéticas naturais do tomateiro selvagem *Solanum pennellii* associadas à domesticação e resistência à seca

A domesticação das plantas levou a uma perda de variação genética em muitas culturas, devido à ênfase excessiva na seleção de órgãos comestíveis (raiz, folha, caule ou fruto) e a baixa pressão de seleção para outras características no ambiente cultivado. Essa "erosão genética" levou à perda de alelos associados à resistência de diversos estresses ambientais, como seca e salinidade, os quais, por sua vez, podem conduzir a perdas significativas na produtividade das plantas. Entretanto, no tomate (*Solanum lycopersicum* L.), é possível acessar um banco valioso de variação genética nas espécies selvagens relacionadas. Assim, a identificação de variantes genéticas associadas ao processo de domesticação do tomateiro e a mecanismos de resistência a estresses ambientais, os quais podem ter sido perdidos durante a domesticação, pode auxiliar em programas de melhoramento do tomateiro e de outras culturas de interesse comercial. Diante disso, no presente trabalho, o qual foi dividido em dois capítulos, realizamos cruzamentos entre a espécie selvagem, *S. pennellii*, e a cultivar miniatura de tomateiro Micro-Tom (MT) para criamos duas linhas de introgressão (ILs), uma com tamanho de órgão reduzido e outra com maior tolerância à seca. No primeiro capítulo, relatamos a caracterização e mapeamento da IL denominada como *Tiny organs and reduced yield* (*Toy*). O genótipo *Toy* carrega um segmento do genoma de *S. pennellii* no cromossomo 7 e apresenta uma considerável redução em órgãos vegetativos (folhas) e reprodutivos (frutos). Os resultados obtidos conduziram a uma discussão de como esse genótipo pode ser relevante para a domesticação do tomateiro, devido ao seu impacto no tamanho de diversos orgão. Por outro lado, no segundo capítulo, descrevemos o mecanismo de tolerância à seca da IL *Water Economy Locus em Lycopersicon* (*Well*). Plantas *Well* carregam um segmento do genoma de *S. pennellii* no cromossomo 1 e exibem uma menor condutância hidráulica, possivelmente relacionada ao tamanho reduzido do vaso xilemático. A menor condutância hidráulica do genótipo *Well* conduz a perturbações no contínuo solo/planta/atmosfera levando a mudança no comportamento estomático, que, por sua vez, provavelmente está relacionado a maior resistência ao murchamento apresentada por esse material em condições de déficit hídrico.

Palavras-chave: Tomate; Linha de introgressão; Domesticação; Resistência à seca; Condutância hidráulica

ABSTRACT

Natural genetic variations from the tomato wild relative *Solanum pennellii* associated with domestication and drought resistance

Plant domestication led to a loss of genetic variation in many crops, due to the excessive emphasis in the selection of edible organs (root, leaf, stem or fruit) and the low selection pressure for other traits in the cultivated environment. This 'genetic erosion' led to loss of alleles associated with resistance to environmental stresses, such as drought and salinity, which can in turn culminate in productivity losses. In tomato (*Solanum lycopersicum* L.), it is possible to tap into a reservoir of valuable genetic variation in its wild relatives. Identification of genetic variants associated with tomato domestication, and with stress resistance mechanisms which may have been lost during domestication, could be used to aid in breeding programs. In the present work, which was divided into two chapters, we carried out crosses between the wild species *S. pennellii* and the miniature tomato cultivar Micro-Tom (MT) and created two introgression lines (ILs), one with reduced organ size and another with increased drought tolerance. In the first chapter, we report the characterization and mapping of the IL denominated as *Tiny organs and reduced yield* (*Toy*). *Toy* harbors a *S. pennellii* genome segment on chromosome 7 and presents a considerable reduction in both vegetative (leaves) and reproductive (fruit) organs. We discuss how this could be a relevant trait underpinning tomato domestication. In the second chapter, we describe the drought tolerance mechanism of the IL *Water Economy Locus in Lycopersicon* (*Well*). *Well* harbors a *S. pennellii* genome segment on chromosome 1 and shows lower hydraulic conductance, possibly related to decreased xylem vessel size. The results shown suggest that this lower hydraulic conductance promotes a disturbance in the soil-plant-atmosphere hydraulic continuum leading to changes in stomatal behavior, which, in turn, are probably related to the delayed wilting of *Well* under conditions of water deficit.

Keywords: Tomato; Introgression line; Domestication; Drought resistance; Hydraulic conductance

1. A NATURAL GENETIC VARIATION LINKING LEAF AND FRUIT GIGANTISM IN THE TOMATO DOMESTICATION SYNDROME

Abstract

The domestication process involved the selection of traits that differentiate the cultivated and the wild ancestor species. The set of resulting traits is referred to as the domestication syndrome, and includes alterations in growth habit, flowering time and organ size. Increased size of plant structures (gigantism) is evident in many crops. In tomato (*Solanum lycopersicum*), an obvious hallmark of domestication is the massive increase in fruit size in comparison to wild relatives. However, most studies neglect the importance of leaf size, which is also bigger in cultivated tomato cultivars. As a consequence, the genetic basis of leaf size increase during domestication remains relatively unexplored. Here, the tomato wild relative *S. pennellii* was crossed with the cultivated tomato cv. Micro-Tom, aiming to find a possible genetic component associated with leaf size. After successive backcrosses and phenotypic selection, we produced an introgression line (IL) with reduced leaves. The IL also present reduced ovary sizes and fruit weight compared to the MT plants. The IL was thus named *Tiny organs and reduced yield* (*Toy*) and mapped on chromosome 7. Anatomical determinations showed that the organ size reduction in *Toy* plants is due to a decreased cell division. Consistently, genes related to cell division, such as *CYCB2,1* and *FRUIT WEIGHT 2.2* had an heterochronic expression during ovary development in *Toy*. Together, the results presented here suggest that *Toy* may represent a major variation selected during tomato domestication, since it conciliates the increase of fruit size, which are strong sinks, with the necessary increase in the source of photoassimilates.

Keywords: Tomato; Introgression line; Domestication; Leaf size; Fruit size

1.1. INTRODUCTION

The domestication syndrome can be defined as the suite of phenotypic changes that occurred through artificial selection to transform wild species into crops (Evans, 1993). Some of commonly found traits are more vigorous growth, increased apical dominance, determinate growth, loss of natural seed dispersal and larger fruits or grains. (Frary and Doganlar, 2003; Meyer and Purugganan, 2013). Increased size of the whole plant or of certain organs, namely gigantism, is widespread in crops. Gigantism can be also a consequence of allometric alterations in the relative size of certain plant structures (Niklas, 2004). A prime example is the species *Brassica oleracea*, where multiple cultivated strains were produced through selection on the differential growth of edible organs such as stems (kohlrabi), buds (cabbage, Brussels sprouts), leaves (kale) and flowers (broccoli, cauliflower) (Lester, 1989; Gómez-Campo and Prakash, 1999; Prakash et al. 2011). Although increased organ size can be explained by either increased cell size or number, or a combination of both (Krizek, 2009), it also requires developmental alterations to transform larger organs into stronger photosynthetic sinks (Gifford and Evans, 1981).

In tomato (*Solanum lycopersicum* L.), gigantism during domestication is evidenced by the massive increase in fruit size when compared to its wild progenitor *S. pimpinellifolium*, which has

pea-sized fruits (Tanksley, 2004). The genetic basis of fruit gigantism has attracted considerable attention (reviewed in van der Knaap et al., 2014). Increased fruit size in tomato involved mutations in at least five major loci: *fruit weight 2.2* (*fw2.2*), *fruit weight 3.2* (*fw3.2*), *fruit weight 11.3* (*fw11.3*), *fasciated* (*fas*) and *locule number* (*lc*) (Tanksley, 2004). The *FW2.2* gene is a negative regulator of cell division (Guo and Simmons, 2011) and is responsible for up to 30% of the increase on fruit size when comparing lines harboring small- and large-fruit alleles (Frary et al., 2000). The *fw3.2* and *fw11.3* together explained 27% of the phenotypic variance in an F_2 population obtained by crossing the tomato cv. Yellow Stuffer and *S. pimpinellifolium* (van der Knaap and Tanksley, 2003). *FW3.2* and *FW11.3* were identified as a P450 enzyme of the CYP78A subfamily (*SlKLUH*) and a *Cell Size Regulator* (*CSR*), respectively (Chakrabarti et al., 2013; Mu et al., 2017). Unlike *fw2.2, fw3.2* and *fw11.3*, which mostly affect fruit size, *fas* and *lc* also control fruit shape. Hence, the domestication *fas* and *lc* alleles increase the number of carpels (and locules), often resulting in larger and wider fruits with pronounced ribbing (Lippman and Tanksley, 2001; van der Knaap and Tanksley, 2003). The *lc* mutant phenotype is caused by two single-nucleotide polymorphisms (SNPs) downstream the coding region of the *WUSCHEL* gene (Muños et al., 2011). The activity of *WUSCHEL* increases the number of stem cells (Mayer et al., 1998) in the meristem that will form the carpels. The *fas* mutation is a loss-of-function allele caused by an inversion in the regulatory region of the *CLAVATA3* gene (Xu et al, 2015), a negative regulator of *WUSCHEL*. Thus, the *fas* mutation also affects stem cell fate, resulting in an increased number of carpels that derive from the altered meristem. The genetic basis for the gigantism of vegetative organs, on the other hand, is hitherto unknown. Increased stem and leaf size could indirectly have affected fruit size and provided for the necessary balance between photosynthetic sources and sinks accompanying the allometric alterations driven by domestication.

In the carbon economy of the plant, larger fruits represent stronger 'sinks', as they require more photosynthate to achieve a greater size (Gustafson and Stoldt, 1936; Li et al., 2015; Osorio et al., 2014). This, in turn, would necessitate increased photoassimilate export from 'source' tissues, mainly leaves. In tomato, as in other crop plants, this can be achieved by increasing either photosynthetic rate or leaf size. As most domesticated tomato cultivars have bigger leaves than their wild relatives (Milla and Matesanz, 2017), the latter appears to be a more parsimonious possibility. In contrast to fruit size, however, the genetic basis of changes in vegetative organ size remain relatively unexplored in tomato. Given the recently established possibility of performing *de novo* domestication of wild species (Li et al., 2018; Zsögön et al., 2018), the discovery of alleles

responsible for vegetative gigantism would be a valuable addition to the repertoire of traits whose genetic basis is well understood.

We hypothesized that if such a genetic determinant exists, the corresponding non-domesticated alleles could be found through wide crosses between cultivated tomato with any wild relative species. Thus, we crossed *S. pennellii* with the cultivated tomato cv. Micro-Tom (MT). After successive backcrosses and phenotypic selection, we retrieved an introgression line (IL) that presents simultaneous reduction in leaf size and fruit weight, compared to the recurrent parental MT. We mapped this IL on chromosome 7 and named it as *Tiny Organs and Reduced Yield* (*Toy*). *Toy* presented as a single Mendelian locus. We also conducted a literature survey for described QTLs (Quantitative Trait Loci) for leaf size and fruit weight, and screened in the existent collection of introgression lines (ILs), where a defined genomic segment of *S. pennellii* replaces a homologous region in the cultivated tomato cultivar M82 background (Eshed and Zamir, 1994; 1995), and found a similar phenotype in the ILs corresponding to the *Toy* region in chromosome 7. We speculate on the impact of this pleiotropic locus in tomato domestication syndrome and discuss its potential exploitation for crop breeding.

1.2. MATERIALS AND METHODS

1.2.1 Plant material

The wild relatives of tomato used in this work were *S. pennelli* (LA0716), *S. chilense* (LA1969), *S. peruvianum* (LA1537), *S. neorickii* (LA1322), *S. chmieslewskii* (LA1028), *S. habrochaites* f. *glabratum* (PI134417), *S. habrochaites* f. *hirsutum* (LA1777), *S. galapagense* (LA1401), *S. pimpinellifolium* (CNPH384), and *S. lycopersicum* var. *cerasiforme* (LA1320). Domesticated tomatoes of the cultivars Micro-Tom (MT) (LA3911), M82 (LA3475), Ailsa Craig (LA2838A), Moneymaker (LA2706) and Santa Clara (a Brazilian cultivar) were also used. The introgression lines (ILs) *Tiny organs and reduced yield* (*Toy*), *Brilliant corolla* (*Bco*) (Chetelat, 1998) and *Rg7H* (Pinto et al., 2017) were obtained through repeated backcrossing between the cv MT as a pollen receptor and *S. pennellii*, as described in Carvalho et al. (2011).

1.2.2. Growth conditions

Plants were grown in a greenhouse at the Laboratory of Plant Developmental Genetics, ESALQ-USP, (543 m a.s.l., 22º 42' 36" S; 47º 37' 50" W), Piracicaba, SP, Brazil. Automatic irrigation too place four times a day. Growth conditions were: mean temperature of 28°C, 11.5

h/13 h (winter/summer) photoperiod, 250–350 μmol photons m^{-2} s^{-1} PAR irradiance, attained by a reflecting mesh (Aluminet, Polysack Indústrias Ltda, Leme, Brazil). Seeds were germinated in 350 mL pots with a 1:1 mixture of commercial potting mix Basaplant® (Base Agro, Artur Nogueira, SP, Brazil) and expanded vermiculite supplemented with 1 g L^{-1} 10:10:10 NPK and 4 g L^{-1} dolomite limestone ($MgCO_3$ + $CaCO_3$). Upon the appearance of the first true leaf, seedlings were transplanted to pots containing the soil mix described above, except for NPK supplementation, which was increased to 8 g L^{-1}. In addition, MT and *Toy* plants received a supplementary fertilization of 0.5g of NPK formulation 10:10:10 after flowering. Cultivated and wild tomato plants were supplemented with 2g of NPK formulation 10:10:10 per plant.

1.2.3. Phenotypic characterization

Characterization of vegetative phenotypes was performed 40 days after germination (dag). Leaf area and perimeter of the leaf series, length and diameter of third, fourth and fifth internode, and number of leaves before flowering were evaluated. All leaves of the MT and *Toy* plant were scanned and the area and perimeter of leaves were determined using ImageJ software (http://rsbweb.nih.gov/ij/). Internode length and diameter were determined using a digital caliper (Western Ferramentas, São Paulo, SP, Brazil).

For the characterization of reproductive phenotypes, length of petals, sepals, antheridial cones and style; corolla area; and ovary weight, height, and diameter were evaluated. To measure ovary length and height a magnifying glass (Leica S8AP0, Wetzlar, Germany), coupled to a camera (Leica DFC295 Wetzlar, Germany) were used. To determine ovary weight the weight of 1.5 mL Eppendorf microtubes with 1 mL of distilled water, before and after to be filled with 10 ovaries were measured. Ovary weight was then determined as the difference between initial and final tube weight. The leaf area and ovary weight of M82 plants and introgression lines (ILs) from chromosome 7, were also evaluated using the same methodology employed in MT and *Toy*.

1.2.4. MT and *Toy* productivity traits

MT and *Toy* plants were hand-pollinated with pollen from MT plants, because the *Toy* genotype presents low fruit set. Various ovaries were pollinated, but after fruit set confirmation (five days after pollination), we performed selective fruit removal to allow only five fruits to set on each plant.

Productive performance of plants was assessed 90 days after germination. The following parameters were determined: total fruit weight per plant; average weight per fruit; total soluble solids content in fruits (Brix); number of locules and number of seeds per fruit; weight of 10 seeds. Total soluble solids content was assessed in all fruits of plants, using a digital refractometer (PR-101, Atago, Tokyo, Japan).

.

1.2.5. Source-sink ratio in MT and *Toy* plants

To determine whether leaf area of *Toy* plants is a limiting factor for fruit development (since leaves and fruits are the major sources and sinks of photoassimilates, respectively), we manipulated plants creating three categories based on different source-to-sink ratios. Thus, the same amount of source tissue (leaves) in all plants of each genotype was kept and the sink strength by changing fruit number (either three, six or nine per plant, to produce high, medium or low source-to-sink ratios, respectively) was altered. Side branches were removed to prevent them from acting as alternative sinks. The following parameters were then determined: total fruit weight per plant (yield); average fruit weight and leaf area.

1.2.6. Mapping and PCR amplification

Mapping and PCR amplification

Molecular markers were designed to discover polymorphisms between tomato and *S. pennellii* in the region comprising the IL7-2 and part of the IL 7-4. The sequences and types of molecular makers are shown on the Table S1. Two further genotypes harboring genome segments of *S. pennellii* for chromosome 7, *Brilliant corolla* (*Bco*) and *Regeneration 7H* (*Rg7H*), both in the Micro-Tom genetic background were characterized molecularly and phenotypically. Cross-referencing information from these genotypes and the ILs in the M82 background we constructed a map with the putative location of the *TOY* locus.

Genomic DNA extraction from young leaves was performed as described by Fulton et al. (1995). PCR was performed using the following program: a denaturation step at 95°C for 2 minutes, 35 cycles of 30 seconds at 95°C, 30 seconds at 56°C, 90 seconds at 72°C, and finally 7 minutes at 72°C. When required, the enzymatic digestion was performed reactions following the manufacturer's recommendations (NEB, Bethesda, USA). The final PCR

products were analyzed by electrophoresis, using 1.5% (m / v) agarose gel stained with SYBR Gold (Invitrogen).

1.2.7. Histological and microscopic analysis

Samples of MT and *Toy* ovaries (at -8, -4, 0, 4 and 8 days post-anthesis, DPA) and fruit pericarps (12 and 16 DPA), were collected and fixed in Karnovsky solution (Karnovsky, 1965), and vacuum-infiltrated for 15 min. Samples were next dehydrated in an increasing ethanol series (10–100%), and infiltrated into synthetic resin, using a HistoResin embedding kit (Leica, www.leica-microsystems.com), according to the manufacturer's instructions. The tissues were sliced using a rotary microtome (Leica RM 2045, Wetzlar, Germany), stained with toluidine blue 0.05% (Sakai, 1973), and photographed in a Leica DM -LB microscope (Heidelberg, Germany), coupled to a Leica DFC310 camera (Wetzlar, Germany). Histological analysis of ovaries was performed in the central region of the outer pericarp of the fruits, and the area and number of cells were determinate using ImageJ software (http://rsbweb.nih.gov/ij/). This histological analysis also was performed in the mature leaves of these genotypes adopting the procedures described above.

We also evaluated the area and number of cells in leaf epidermis of the MT and *Toy* genotypes. For this, we used the imprinting technique as described by Weyers and Johansen (1985).

The times referred to as -8 and -4 DPA correspond to 8 and 4 days before anthesis, respectively. We based these on the length of the closed flower buds (Faria, 2014).

1.2.8. Maturation rate of meristems and shoot growth

The maturation rate of MT and *Toy* meristems was performed at two, four, six, eight and 10 days after emergence (DAE) of the seedlings from soil. Meristems were characterized according to their stage of development as: vegetative, transition and reproductive (inflorescence + floral meristem) (Park et al., 2012).

Shoot apices were collected at one, two, three and 4 DAE, and photographed with a Leica magnifying glass model S8AP0 (Wetzlar, Germany), coupled to a Leica DFC295 camera (Wetzlar, Germany), for further evaluation of shoot growth by measures of shoot tip length in the ImageJ software.

1.2.9. Quantitative real-time PCR

Total RNA was extracted from young shoot apices (2 days after emergence of soil), young leaves, ovaries (at -8, -4, 0, 4 and 8 DPA) and fruit pericarps (12 and 16 DPA), using Trizol reagent (Invitrogen), according indicated by the manufacturer, and treated with RQ1 RNAse-Free DNAse (Promega). Fruit pericarps were carefully collected from the central region of the outer pericarp of the fruits, at 12 and 16 DPA. After DNase treatment, a single-strand cDNA was synthesized from total RNA (1μg) by reverse-transcription, using RevertAid RT Reverse Transcription Kit (Thermo Fisher Scientific).

Gene expression analyses were performed on a Rotor-Gene Q real-time PCR cycler (Qiagen), using Kapa Sybr Fast qPCR Master Mix (Kapa Biosystems) and gene-specific *CYCB2;1* (Solyc02g082820), *FW2.2* (Solyc02g090730), *EXP5* (Solyc02g088100) primers. The reactions were amplified for 2 min at 95 °C, followed by 40 cycles of 95 °C for 15 s and 60 °C for 30 s. The threshold cycle (CT) was determined. Melt-curve analysis was performed with each primer set to confirm the presence of only a single peak before the gene expression analyses. Two technical replicates were analyzed for each of three or four biological samples. The *CYCB2;1*, *EXPA5* and *FW2.2* expression were normalized to *ACTIN* (Solyc04g011500) gene. The fold changes for each gene were calculated using the equation $2^{-\Delta\Delta CT}$ (Livak and Schmittgen, 2001). Primer sequences used to qRT-PCR are also shown in Table S1.

1.2.10. Statistical analysis

Statistical analysis was performed using SAS software (SAS Institute Inc., Cary, NC, USA). The variables data were submitted to analysis of variance (ANOVA) and the means compared by the Student's t-test. When the data did not meet the assumptions of ANOVA, we performed to non-parametric analysis, using Wilcoxon rank sum test to compare the means. For qRT-PCR data analysis, was used a simplified alternative analysis based on ΔCt values (Yung et al., 2006).

Table S1. Oligonucleotide sequences used for genotyping and quantitative PCR analyses in this work.

Locus ID[1]	Forward	Reverse	Utilization	Enzyme
Solyc02g082820_*CYCB2;1*	GAAGGCAGCAACAGGGAAACTAA	CCCTCTTCTCCTCTATTCTTGTGTC	qPCR	
Solyc02g090730_*FW2.2*	GTTTTGATGACCCTGCTAACTG	CAAAGAGCACAAGGTTCACAG	qPCR	
Solyc02g088100_EXP5	ACCATCGCCTGTAGTGACCTTAAAG	AAGGGTTCAAGAACTCAATGGCAAC	qPCR	
Solyc04g011500_*ACTIN*	GGTCCCTCTATTGTCCACAG	TGCATCTCTGGTCCAGTAGGA	qPCR	
Solyc02g083950_*LC*	GGTCTTGGTCTCTTGGATGATG	AAAATAATGCCTCGTGTCCATTC	Genotyping	EcoRV
Solyc02g090730_*FW2.2*	CCTTGTATCACCTTTGGACAGATT	CGGAGATAGCATTGTCAAAGTTA	Genotyping	MspI
Solyc03g114940_*FW3.2*	GAGATAACGGGTTAAATAGAGT	TAGTTAGGATAGTTATAGTTTGC	Genotyping	BstNI
Solyc07g009130	TCTTACTCTCCGTCATTAGCCT	ATGTCCTGTTTCCTTCGCAA	Genotyping	XhoI
Solyc07g017650	GTAGGTTACCAAGTAGTAGAGGG	AGAGCTACATACCTTATCCAACA	Genotyping	EcoRV
Solyc07g020960	CATTATCTTATTTCCACCCACC	TGAACCTCATCTAACCCTACC	Genotyping	HincII
Solyc07g026680	GTGGATATGGGAAGGAAGT	CGAGGAATATGATGTATGGT	Genotyping	*RsaI*
Solyc07g039570	TGGCAATACTTTCAACCTTCC	CAATGTCTGAGGACGAGCA	Genotyping	PsiI
Solyc07g041190	GTGGACTTGACCTGGAGATG	AAGAGAGAAGGATTGGGGACT	Genotyping	RsaI
Solyc07g041980	GTGGACTTGACCTGGAGATG	AAGAGAGAAGGATTGGGGACT	Genotyping	RsaI
Solyc07g042560	CTGTTAATACCGAATAATCTTGTAAT	GGGACTAAACAAAACAATGAATGG	Genotyping	BstNI
Solyc07g043450	CCATTACATCTTCAAAGCCATCTC	GGCATAGTGACTACAATACATATCG	Genotyping	PagI
Solyc07g045180	GCTTCCAGGGTGTCAATG	ATGTCTAAGTCTGCCAACC	Genotyping	HpyCH4V
Solyc07g047950	GCCATACCTAGACGGGATTT	TATTTCCAGGCACAAGAAGC	Genotyping	DpnII
Solyc07g051830[2]	CAATGAGGACAGACTGATAGC	CACCTGATCTTTGACAACGAG	Genotyping	

Table S1. Continuation…

Solyc07g052970[2]	TGGATGTCAATGGTGAACAAG	GCCCCACACATGAACAATG	Genotyping	
Solyc07g054090	TTTGTCAACCTTCATCAGCCTT	AGAGAAAAAGCAGGTAAGGAGAG	Genotyping	Hpy188I
Solyc07g055020	CCGCCATCTTGACCCATTTATA	CTTTCTTCCGCAATCCACTCAT	Genotyping	HincII
Solyc07g055400	GCAACCCAAAATCCAAATCAAC	ATCTCCCTGTAGACACCATG	Genotyping	Hpy188I
Solyc07g056060	GCAAGAAGGCAATCAACTAC	CACTTGTAAAGACTTCCTGC	Genotyping	PsiI
Solyc07g056580	CCACGACTGTTATGCTTTATG	GGGTATCAGTTCACTTTCTTG	Genotyping	TaqI
Solyc07g062600	AAGCCATTCACCTTATGTCAG	CCACCAGGAGAACTTGATTCA	Genotyping	EcoRI
Solyc07g062750	GGGTTTGTTGTGTCCTATGTG	TGGGTTGGTGTGATGCTTC	Genotyping	ApaLI
Solyc07g062930	CCTTTCTCCTACCTCCCAGAT	GAATTGTGGTCCTGAGTGTAGA	Genotyping	MspI and HaeIII
Solyc07g063010[2]	GTGATGATTTGAAGGAGGATTGA	TTATCAGTCACCTCTCTGCCAG	Genotyping	
Solyc07g063080	GTGTCCAGGGAGAAGGTA	GACGTTCTCGACTGTTGA	Genotyping	RsaI
Solyc07g063130	GCAGAAAAGACAAGGTCAATCC	CAAACTCCCTCAACTCACCCTT	Genotyping	HpyCH4V
Solyc07g063300	CCATTGTAGGTGTTACGGTGC	CAGAACCAATAGATGCGAGTAGT	Genotyping	DraI
Solyc07g063390	GTCTTACTGGCTTAAAACTTGG	CTTGGGAACTCGATCTAATGTA	Genotyping	EcoRV
Solyc07g063480	GCCTTTATTTCTATCCTCTCC	GCTAGACCTTGTTCAGATCTC	Genotyping	PsiI
Solyc07g063590	GGTGCTATGAAGGTGAAAGGA	GTTGTGAAGAACAGATGGCTC	Genotyping	HinfI
Solyc07g064080	TCTAAGTTGAGAGTTATGGATGATGT	TGGAACGAATCATGAAGGAA	Genotyping	EcoRV
Solyc07g064300	AGCATCTTAATATAGGGGGCTTA	CTCTTATTCGGGCAAGCAAG	Genotyping	DraI
Solyc07g064550	TCGTCTCCTTGTTGATCCTGT	TCCAAACACCATCCAGCATA	Genotyping	PstI
Solyc07g064830	AATGGGCTCCAGGTTCAAAT	TTGTTGACCACCCATTGAAG	Genotyping	EcoRV

Table S1. Continuation…

Solyc07g065050	TGTGGGCATTTTGTTGACTG	CAATAGCAAAACAAAAGGCATC	Genotyping	PstI
Solyc07g065270	GTCGGGTAACAGTTCGTGCT	CCCTGAGCAATCTGGAAATC	Genotyping	MspI
Solyc07g065440	CTCAGAAGAAGAACGAGCACAG	TGGTGCATCCTGTGTAACATC	Genotyping	HinfI
Solyc07g066630	TGATAGCTTAAATGTTGTGGGAAG	GCAACCAAGCAACTAACCAAA	Genotyping	HindII
Solyc11g071940_*FW11.3*	CAATAGTCTCCATGCTCAACG	CTGTCATAGAAACATCTCAAAAGG	Genotyping	HaeIII + SmlI

[1] Locus according to the Sol Genomics Network database (http://solgenomics.net/).

[2] SCAR (sequence characterized amplified regions) markers.

1.3 RESULTS

1.3.1. Natural allelic variation that reduced leaf area and diameter stem

Most wild relatives of the tomato have small leaves (Figure 1), so we decided to look for the genetic determinants of leaf size in the wild species. *S. pennellii* was crossed with the tomato cv. Micro-Tom (MT). *S. pennellii* has a fully sequenced genome (Bolger et al., 2014), and a collection of introgression lines (ILs) (Eshed and Zamir, 1994; 1995), which can facilitate the mapping of possible candidate genes. Upon self-fertilization of the F1 population, we selected plants with the size of MT, but with smaller leaves, from which we collected pollen to backcross (BC) to MT. After six rounds of backcrosses, self-fertilization (BC_6F_3), and phenotypic screening, we produced an introgression line (IL) with reduced leaf size in the MT background, which we named as *Tiny organs and reduced yield* (*Toy*) (Figure S1A). *Toy* plants present a very conspicuous phenotype for leaf size (Figure S1B).

Monogenic segregation of *Toy* was verified by a crossing between MT and *Toy*. The F1 plants presented intermediate phenotype between MT and *Toy* plants (Figure S2). In an F_2 population, the leaf size of 28 plants was scored as MT, 31 plants were scored as *Toy* and 73 plants presented and intermediate phenotype. A χ^2 test indicated no significant deviation from a 1:2:1 segregation ratio (P=0,445; χ^2=2.26), suggesting that *Toy* may behave as a semi-dominant gene.

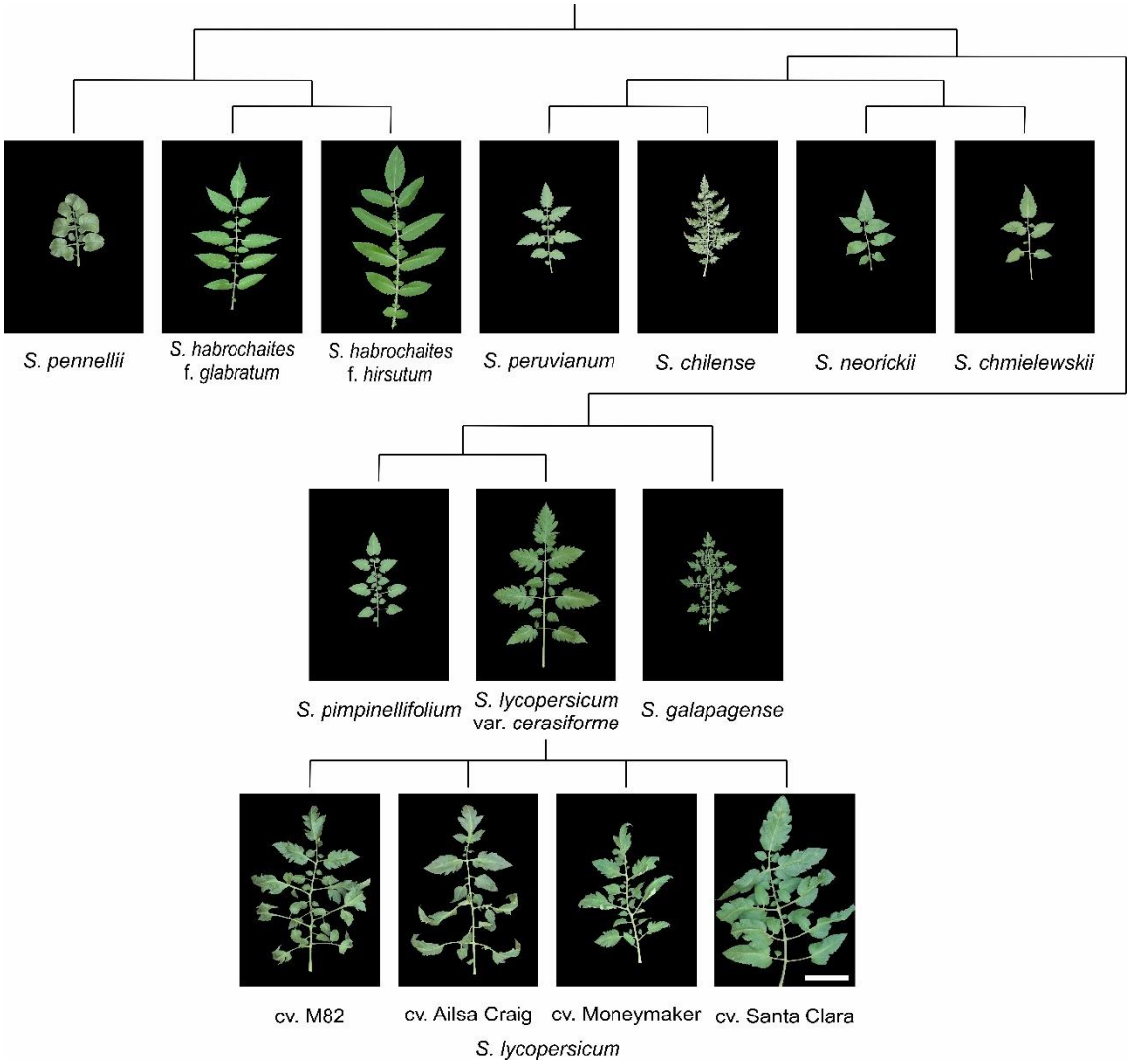

Figure 1. Representative leaf of tomato cultivars and its wild relatives. A. *Solanum pennelli* (LA0716). **B.** *S. chilense* (LA1969). **C.** *S. peruvianum* (LA1537). **D.** *S.neorickii* (LA1322). **E.** *S. chmieslewskii* (LA1028). **F.** *S. habrochaites* f. *glabratum* (PI134417). **G.** *S. habrochaites* f. *hirsutum* (LA1777). **H.** *S. galapagense* (LA1401). **I.** *S. pimpinellifolium* (CNPH384). **J.** *S. lycopersicum* var. *cerasiforme* (LA1320). **K.** *S. lycopersicum* cv. M82 (LA3475). **L.** *S. lycopersicum* cv. Ailsa Craig (LA2838A). **M.** *S. lycopersicum* cv. Moneymaker (LA2706). **N.** *S. lycopersicum* cv. Santa Clara (local variety). Scale bar= 10 cm.

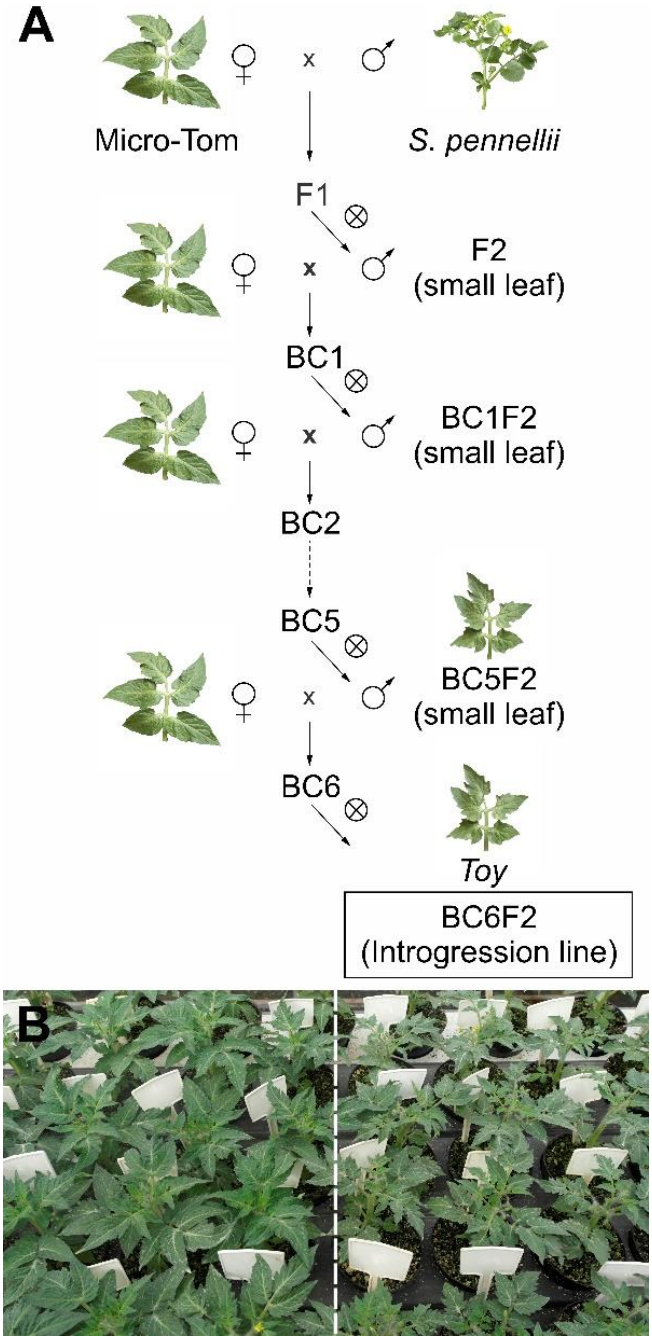

Figure S1. Introgression of a natural variation to leaf size from *S. pennellii*. A. Crossing sequence to create an introgression line with small leaf in MT background, here denominated as *TINY ORGANS AND REDUCED YIELD* (*Toy*). **B** Homogenous population of MT (left) and *Toy* (right) plants, 25 days after germination (dag). Note the considerable difference in leaf size of MT and *Toy* plants.

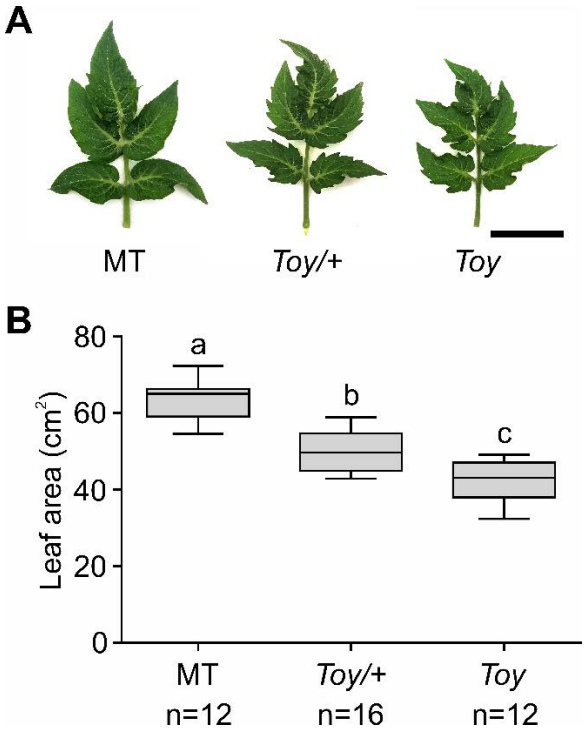

Figure S2. F1 population (*Toy/+*) presents intermediate leaf phenotype. A. Representative leaf from MT, *Toy*/+ and *Toy* plants. **B.** Leaf area of representative leaves of the genotypes, 50 dag. *n* at the bottom of the graphic represents the leaf number on each evaluation). Statistical significance was tested by Student's t-test ($p<0.001$).

The difference in leaf size between MT and *Toy* was consistent across all leaves and developmental stages (Figure 2A and 2B). The reduced size of *Toy* leaves appears to be due to a decrease in cell proliferation (Figure 2C and 2D). We verified a significant increase in epidermal pavement cell area (Figure 2E) with reduced cell numbers (Figure 2F) in *Toy* mature leaf epidermis compared to MT (Figure 2G). Remarkably, stomatal density (Figure S3A), the number of stomata per area of leaf surface, was not altered in *Toy*. Leaf dry mass also was lower in *Toy* than MT for all leaves (Figure S3B). *Toy* palisade parenchyma showed bigger cells than MT, both in cell height and width, but in a smaller number (Figure 2G to 2L). Greater palisade parenchyma cell size promoted an increase in leaf thickness in *Toy* (Figure 2M). *Toy* plants also showed a reduction in stem diameter compared to MT (Figure S3C). On the other hand, no evidence difference was observed in *Toy* internode length (Figure S3D), root system (Figure S4A), and root dry mass (Figure S4B) compared to MT.

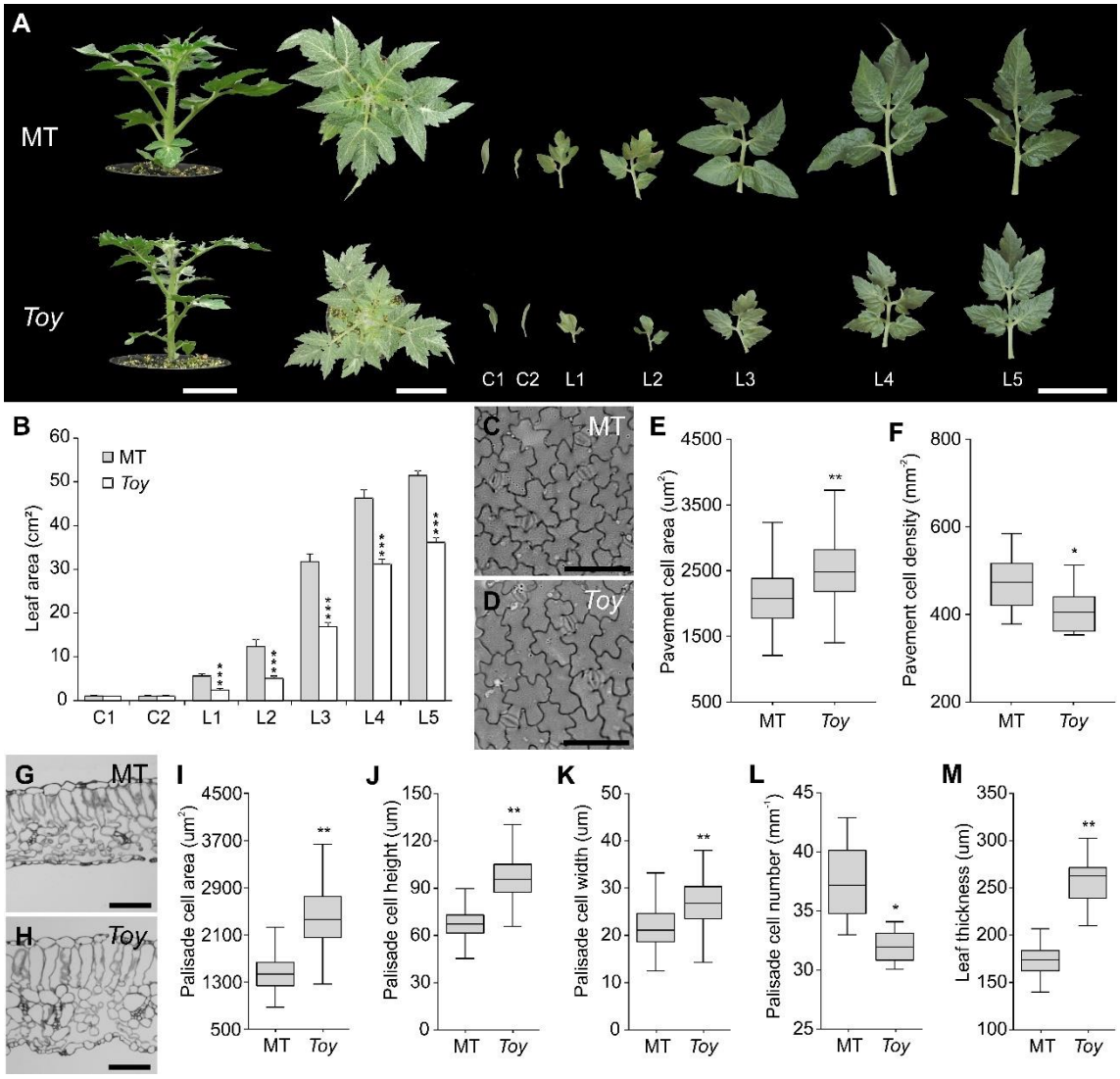

Figure 2. A tomato introgression line (IL) from *S. pennellii* with reduced leaf size. A. Side and top view of MT (top) and *Toy* (bottom) plants, as well as the heteroblastic leaf series of both genotypes from cotyledons (C1) to fifth leaf (L5). Scale bars=5 cm. **B.** Leaf area of heteroblastic leaf series of MT (gray bar) and *Toy* (white bar) genotypes, 40 dag. Data are presented as mean±s.e.m. (n=14 leaves). **C** and **D.** Representative imprints of adaxial side from MT (C) and *Toy* (D) leaves. Note the difference in cell size. Scale bar=100μm. **E.** Cell area in adaxial side of MT and *Toy* leaves (n=320 cells). **F.** Number of pavement cells per mm^2 in adaxial side of MT and *Toy* leaves (n=14 sections). **G** and **H.** Representative cross-sections of MT (G) and *Toy* (H) leaves. Scale bar=100μm. **I-L.** Characterization of palisade tissue. Palisade cell area (I), height (J), width (K) and number (M) from MT and *Toy* leaves (n=5 cross-sections). **M.** Leaf thickness (n=5 cross-sections). Data are mean±s.e.m. Statistical significance was tested by Student's t-test (*$p<0.05$, **$p<0.01$, ***$p<0.001$).

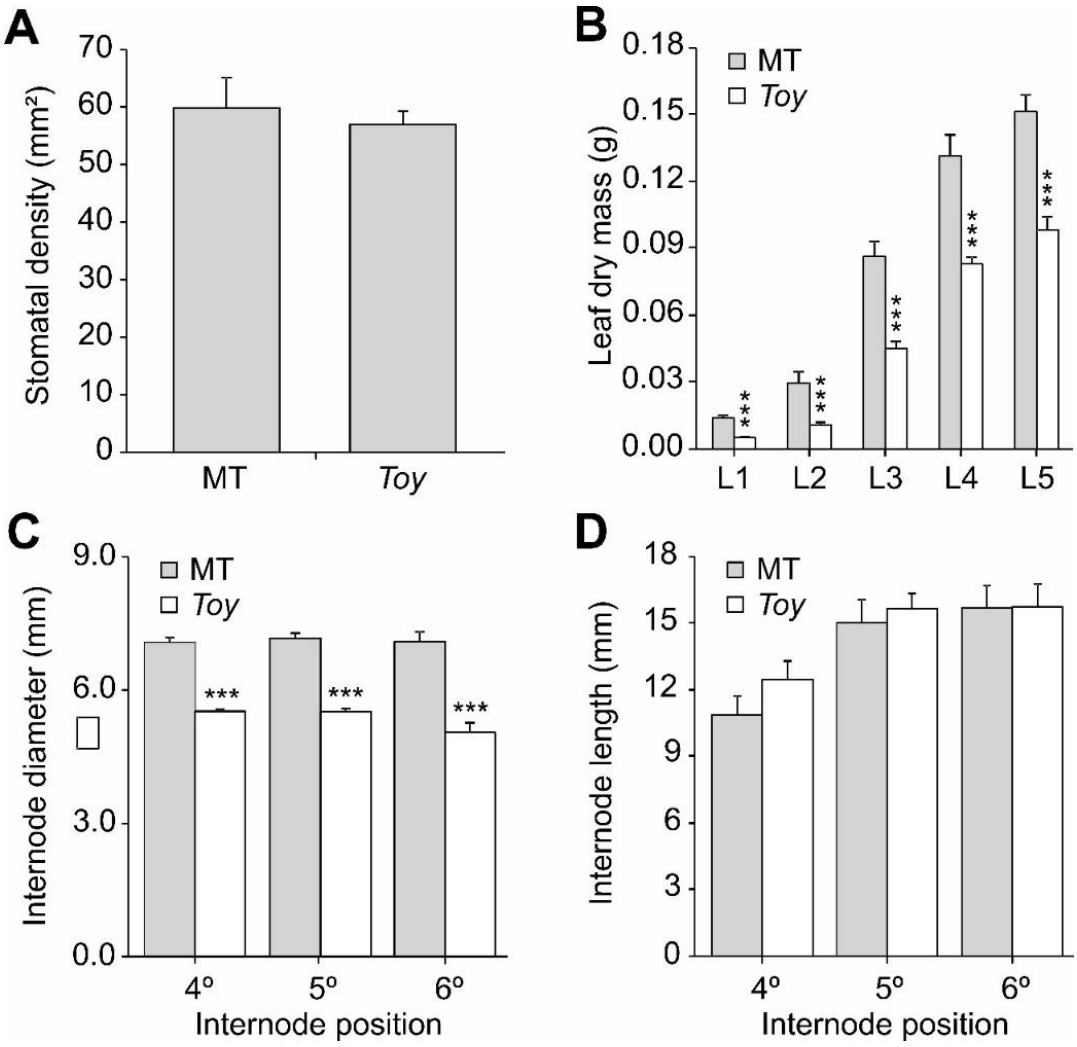

Figure S3. ***Toy*** **characterization. A.** Stomatal density per mm^2 in adaxial side of MT and *Toy* leaves. **B.** Leaf dry mass of heteroblastic leaf series of MT (gray bar) and *Toy* (white bar) leaves. **C** and **D.** Internode diameter (C) and length (D) of the MT and *Toy* plants, 40 dag. Data are mean±s.e.m. (n=14). Statistical significance was tested by Wilcoxon rank sum test, being the significance levels indicated by asterisks (**$p<0.01$, ***$p<0.001$).

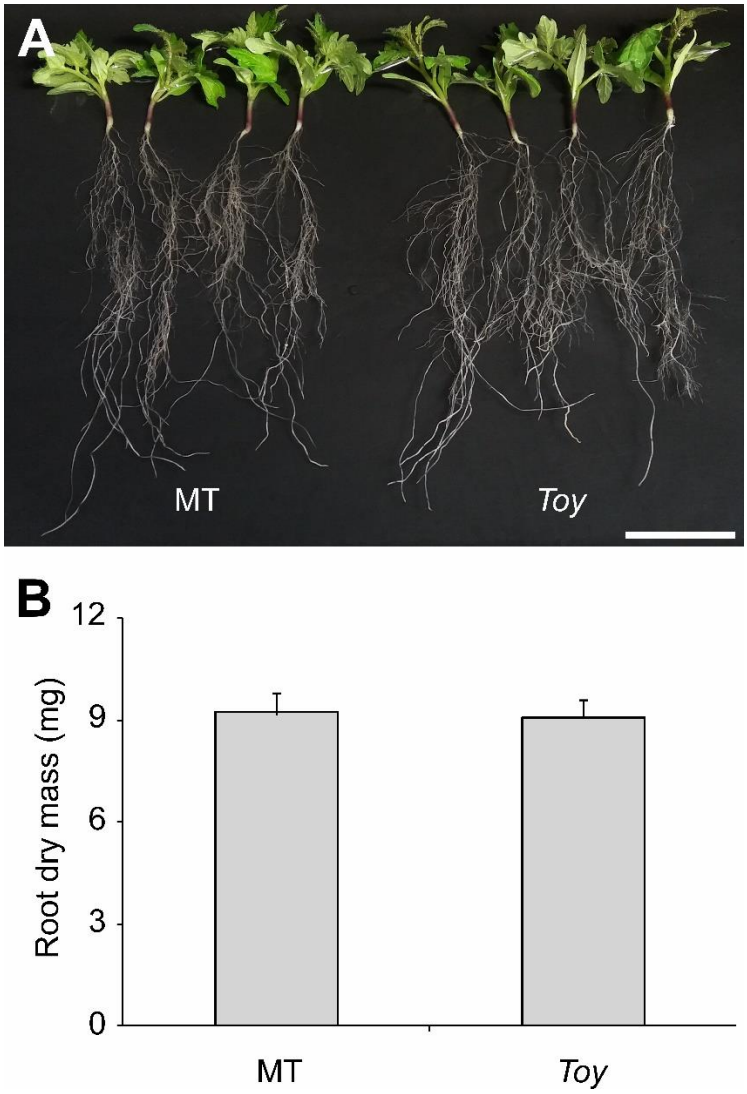

Figure S4. Root size is not affected in *Toy*. A. MT (left) and *Toy* (right) genotypes showed no evident differences in the root system, 20 dag. Scale bar = 5 cm. **B.** Root dry mass of MT and *Toy* seedlings. Data are mean±s.e.m. Statistical significance was tested by Student's t-test.

1.3.2. *Toy* affects all flower whorls

Toy plants also show alterations in reproductive organ size (Figure 3A). We verified a significant decrease in the size of all whorls, namely, petal length, corolla area and sepal length in *Toy* flowers compared to MT (Figure 3B-3D). *Toy* also showed smaller anther cones and pistils than MT (Figure S5). The reduction in the anteridial cone length appears to be more severe, which explains the high incidence of exserted styles in the *Toy* flowers. *Toy* also showed smaller fresh weight, length, and diameter of ovaries (Figure 3E-3H). Therefore, *Toy* promotes a reduction in all flower whorls, which may strong consequence on the plant yield, since its impact in the ovary size.

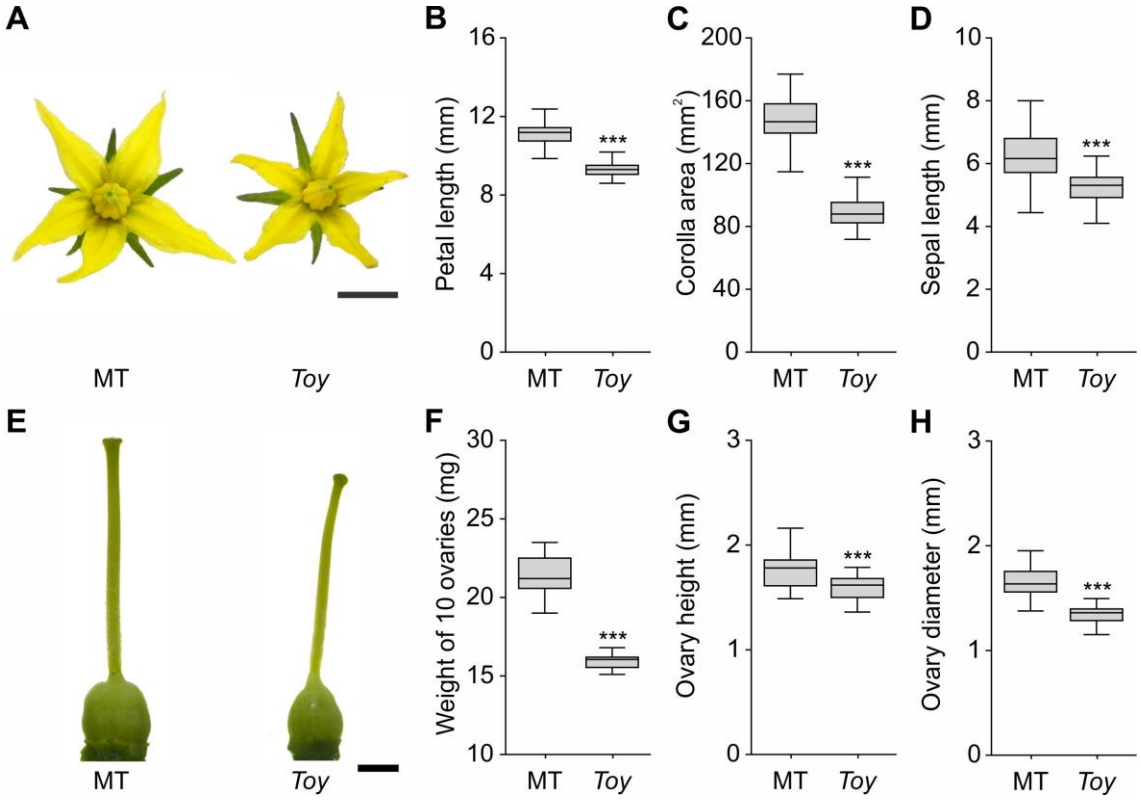

Figure 3. ***Toy*** **reduces organ size in all whorls. A.** Representative MT (left) and *Toy* (right) flower at anthesis. Scale bar=0.5 cm. **B-D.** Petal length (B). **C.** Corolla area. **D.** Sepal length of MT and *Toy* flowers. n=45 flowers. **E.** Representative MT (left) and *Toy* (right) ovary at anthesis. Scale bar=1 mm. **F.** Fresh weight of 10 ovaries at anthesis (n= 13 repetitions). **G** and **H.** Ovary height (G) and diameter (H), at anthesis (n= 25 flowers). Data are mean±s.e.m. *** indicate significant differences by Wilcoxon rank sum test ($p<0.001$).

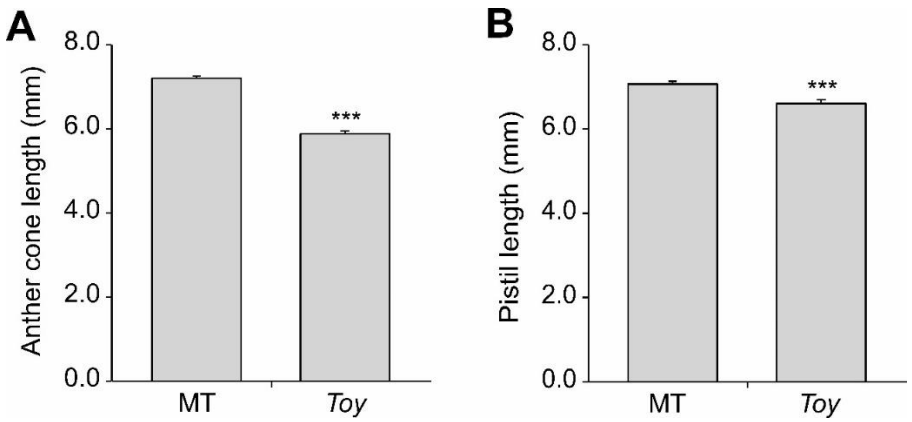

Figure S5. ***Toy*** **flowers display reduction in anther cone and pistil length. A.** Anther cone length. **B.** Pistil length. Data are mean±s.e.m. (n=45 flowers). *** indicate significant differences by Wilcoxon rank sum test ($p<0.001$).

1.3.3. Ovary reduction results in reduced fruit size in *Toy*

Ovary size is strongly related to final fruit size (Nesbitt and Tanksley, 2001; Hamada et al., 2008; Rosati et al., 2009). Thus, we analyzed whether the *Toy* ovary reduction could have an impact on fruit weight and, potentially, in yield of plants. As fruit set is reduced in heterostylic *Toy* flowers, we hand-pollinated *Toy* with MT pollen. Several ovaries per plant were pollinated, but after fruit set confirmation (five days after pollination), we performed selective fruit removal to allow only five fruits to set on each plant. The results confirmed that the ovary size has a substantial impact on the final fruit size (Figure 4A). When we compare *Toy* and MT fruits, the difference in fruit weight between them is 43% (Figure 4B), which promotes a drastic consequences on total fruit weight per plant (Figure 4C). Although MT presents large fruits, they show a decrease in soluble solids (°Brix) compared to *Toy*, which is 21% higher (Figure 4D). Another interesting feature we observed, in *Toy* plants, was a reduction in fruit locule size, which was accompanied by a reduction in seed number (Figure 4A). *Toy* plants presented a greater frequency of fruits with two locules (Figure 4E), and a reduction in seed production and size compared to MT fruits (Figure 4F and 4G).

We next investigated whether reduced seed set in *Toy* was due to gametophytic incompatibility with MT. We hand-pollinated MT and *Toy* plants with *Toy* pollen. *Toy* plants also produced fewer seeds per fruit than MT (Figure S6), indicating that *Toy* plants do no show incompatibility with MT pollen.

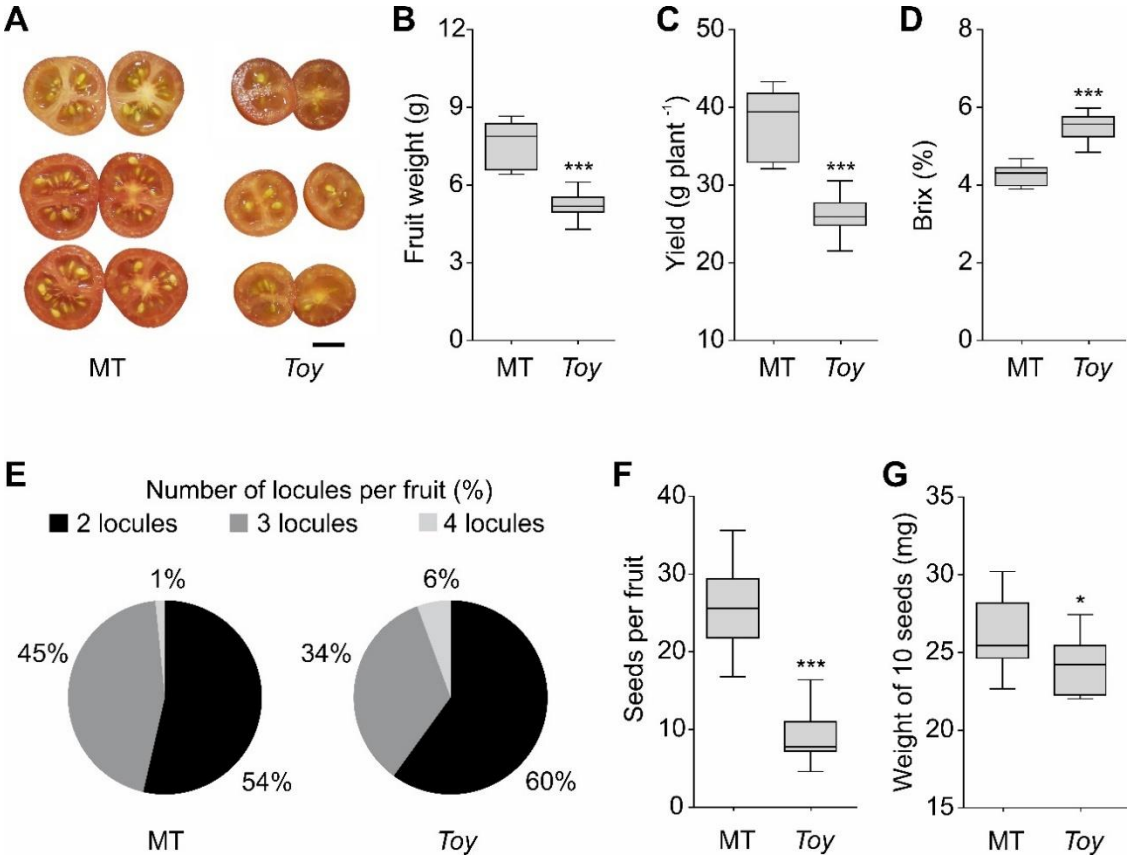

Figure 4. Fruit traits are altered in *Toy*. A. Representative MT (left) and *Toy* (right) ripe fruits. Scale bar=1 cm. **B.** Average values of fruit weight in ripe fruit. **C.** Average fruit yield per plant of each genotype. **D.** The average total soluble solids content in ripe fruits (Brix) (n = 10 plants with 5 fruits on each). **E.** Frequency of locule number per fruit in MT and *Toy* fruits (n=125 fruits). **F** and **G.** Average seeds number (F) and weight of 10 seeds (G) from MT and *Toy* fruits (n=11 plants, here we weigh all seeds of the 5 fruits on each plant and divide by the total seeds number). Data are mean±s.e.m. Statistical significance was tested by Student's t test, being the significance levels indicated by asterisks (*$p<0.05$, ***$p<0.001$).

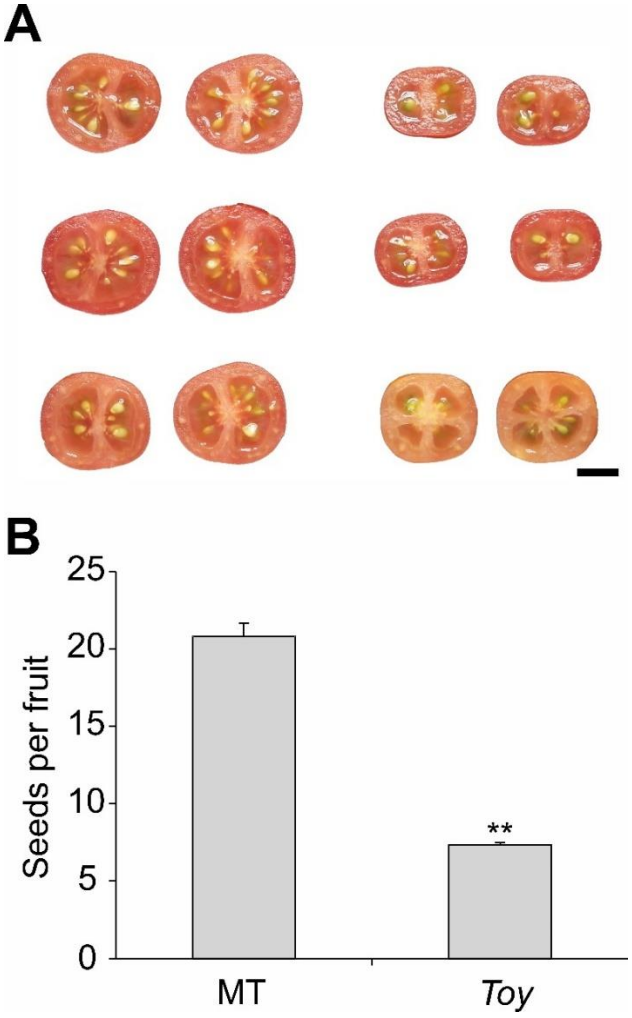

Figure S6. MT and *Toy* fruits pollinated with *Toy* pollen. A. Representative MT (left) and *Toy* (right) ripe fruits. Scale bar=1 cm. **B.** Average seeds number per fruit (n=15 fruits). Data are mean±s.e.m. ** indicate significant differences by Wilcoxon rank sum test ($p<0.01$).

We next addressed the possibility that reduced fruit size could be the consequence of altered photosynthetic source-sink relationships due to reduced leaf area. We thus manipulated the plants to maintain source strength constant and altered the source:sink ratio by changing the sinks as follows: 1) Plants with three fruits (high source:sink ratio); 2) Plants with six fruits (medium source:sink ratio); and 3) Plants with nine fruits (low source:sink ratio). To ensure that side branching did not interfere in the results, we pruned all the plants in the three treatments.

Toy plants produced smaller fruits than MT in all treatments (Figure 5A). The increase in fruit number, from three to six, promoted a significant reduction in fruit weight only in MT plants, suggesting that the leaf area and ovary size were limiting factors to the final fruit weight in MT and *Toy* genotypes, respectively, since the leaf area was similar in both experimental conditions (Figure 5B). On the other hand, when we increased the number of fruits, from six to

nine, there was a significant reduction in the final fruit weight for both genotypes, probably by the source limitation. This reduction was more pronounced in *Toy* plants, since MT genotype showed an increase in yield (approximately 10%), which was not observed for *Toy* plants (Figure 5C).

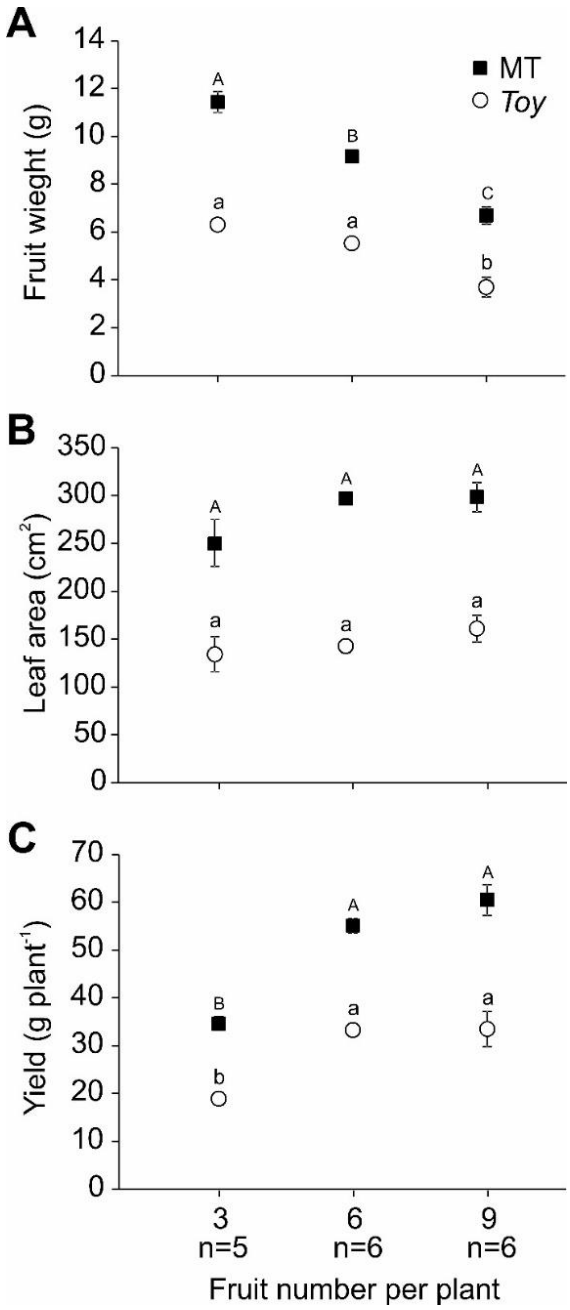

Figure 5. Fruit weight differences as a result of the source-sink relationship. A. Average values of fruits weight; **B.** Leaf area and **C.** Yield from MT (dark square) and *Toy* (white circle) plants with three, six and nine fruits. Data are mean±s.e.m.. n at the bottom of the figure represents the plant number on each evaluation. Statistical significance was tested by Student's t-test ($p<0.001$). Different capital and lowercase letters on the symbols indicate significant difference between the treatments in MT and *Toy* genotypes, respectively.

1.3.4. Toy affects cell number and size during fruit development

Toy presented alterations in ovary/fruit size before and after anthesis. A time-course comparison of ovary/fruit development from -8 DPA to 16 DPA (Figure 7A) exposed the differences in the *Toy* ovary/fruit growth. This difference is explained, at least in part, by pericarp development. *Toy* plants always presented an ovary/fruit pericarp thinner that MT throughout the evaluation period (Figure 7B).

Increase in organ size is due to either increased cell proliferation or expansion, or a combination of both (Krizek, 2009). Thus, we measured the number of cell layers and the cell area of MT and *Toy* ovary/fruit pericarps. The measurements revealed that the reduction in the *Toy* pericarp may be due to a combined decrease in the cell number and size during fruit development (Figure 7C and 7D). The number of cell layers was lower in *Toy* than MT pericarps from -8 DPA to 16 DPA. Cell size was also reduced in *Toy* fruit pericarps compared to MT from the flower anthesis (0 DPA). Noteworthy, both genotypes followed the same pattern of division and expansion, i.e., a drastic increase in cell division from anthesis to 8 DPA (Figure 7C) and a quick expansion after 8 DPA (Figure 7D), which is the norm in tomato fruit development (Gillaspy et al., 1993).

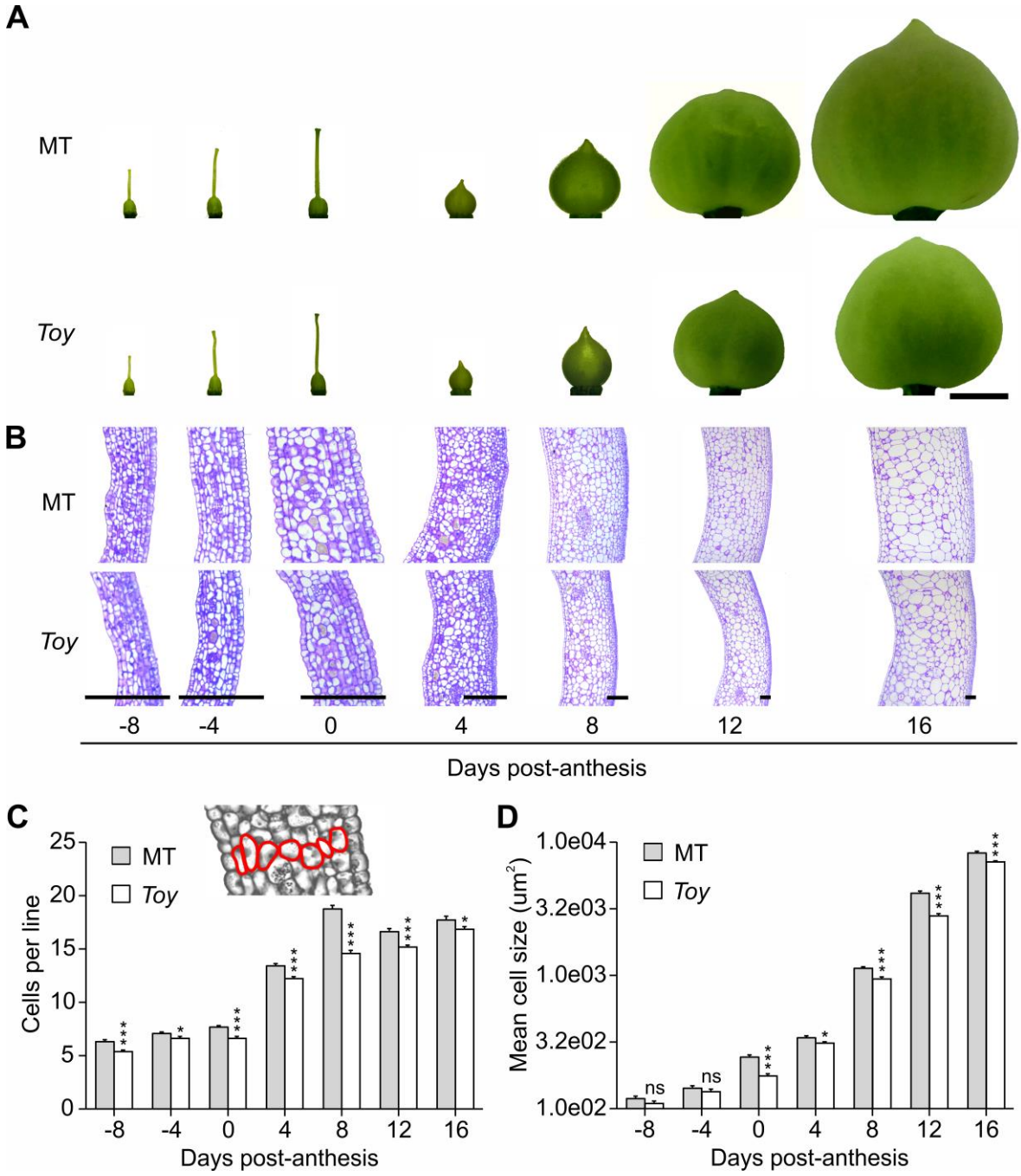

Figure 7. Histological analysis of pericarp development of MT and *Toy* fruits. A. Developing ovary/fruit at -12, -8, -4, 0, 4, 8, 12 and 16 days post-anthesis (DPA). MT (top) and *Toy* (botton). Scale bar=5mm. **B.** Longitudinal sections of MT (top) and *Toy* (botton) pericarp at -12, -8, -4, 0, 4, 8, 12 and 16 days post-anthesis. Scale bar = 150µm. **C.** Time course of cell number per line in the longitudinal sections of MT (dark bar) and *Toy* (white bar) fruit pericarp. Insert in top of this figure represents how the counting of the cells was performed and red lines delimited cell perimeter (n=30). **D.** Time course of average cell area in the line of the MT (dark bar) and *Toy* (white bra) genotypes (n=30). Data are mean±s.e.m. Statistical significance was tested by Student's t-test (**p<0.05*, ***p<0.001,* ****p<0.001*, *ns* indicate similar means).

1.3.5. The *Toy* locus is located on chromosome 7

Given that *Toy* is an IL from *S. pennellii*, we took advantage of the existing collection of introgression lines (ILs) from *S. pennellii* in tomato cv. M82 as a tool to identify its chromosomal position (Zamir and Eshed, 1994; 1995). We performed a survey of the existing literature and found that six QTLs responsible for fruit reduction were found in chromosomes *2*, *3*, *5*, *7* and *10* (Causse et al 2004). Interestingly, an independent study showed decreased leaflet size in ILs 2-6, 7-2 and 7-3 (Chitwood et al 2013). These results restricted our search in two region of chromosomes *2* and *7*, so we next conducted an *in silico* analysis of these chromosomes to identify candidate genes for *Toy* (Tomato Genome Consortium, 2012).

Chromosome *2* harbors the *FW2.2* gene (Solyc02g090730), which is responsible for approximately 30% of the increase on tomato fruit size between the wild relative S. *pimpinellifolium* and cultivated tomato, and is present in the IL2-5/2-6 (Frary et al., 2000). Furthermore, the *S.pennellii* allele of this gene (*Spfw2.2*) promotes reduction in ovary size when introgressed in the cultivated tomato (Nesbitt and Tanksley, 2001). Thus, we designed molecular markers to investigate whether the *FW2.2* allele from *S. pennellii* underlies the *Toy* phenotype. Our results showed that *Toy* harbors the cultivated tomato allele of *FW2.2*. Concomitantly, we verified that *Toy* genotype also presents all MT alleles for other known genes for fruit size, such as *FW3.2*, *FW11.3* and *LC* (Figure S7). Thus, we focused our subsequent analyses on chromosome 7.

We cultivated all ILs harboring *S. pennellii* genomic segments on chromosome 7 (IL7-1; IL7-2, IL7-3; IL7-4 and IL7-5) and determined their leaf area. IL7-2 showed a consistently lower leaf area than the parental line M82 (Figure 6 and S8A). We next analyzed ovary size, another *Toy* phenotype, and found a reduction in the ovaries of both IL7-2 and IL7-3 compared to M82 (Figure S8B and S8C), suggesting a common genetic basis for the phenotype of these ILs and *Toy*. These data corroborate our literature survey describe above.

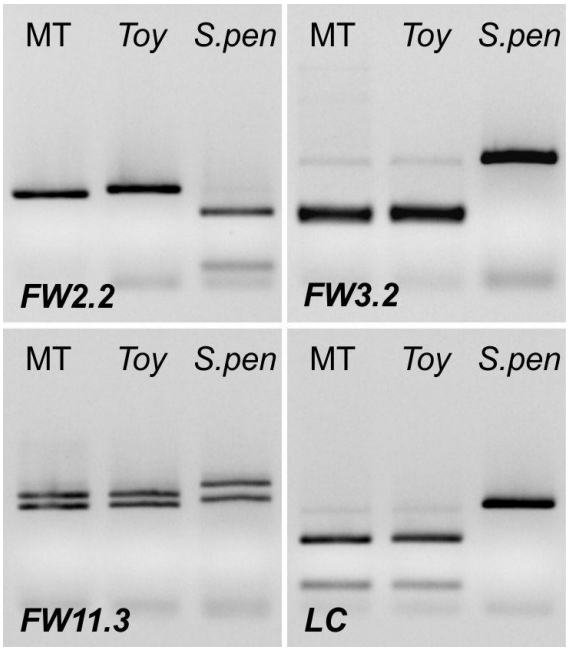

Figure S7. *Toy* plants harboring alleles of known genes for fruit size from MT. PCR genotyping for the *FW2.2* (top, right), *FW3.2* (top, left), *FW11.3* (bottom, right) and *LC* (bottom, left) alleles. Micro-Tom (MT) and *S. pennellii* (*S.pen*) were used as control.

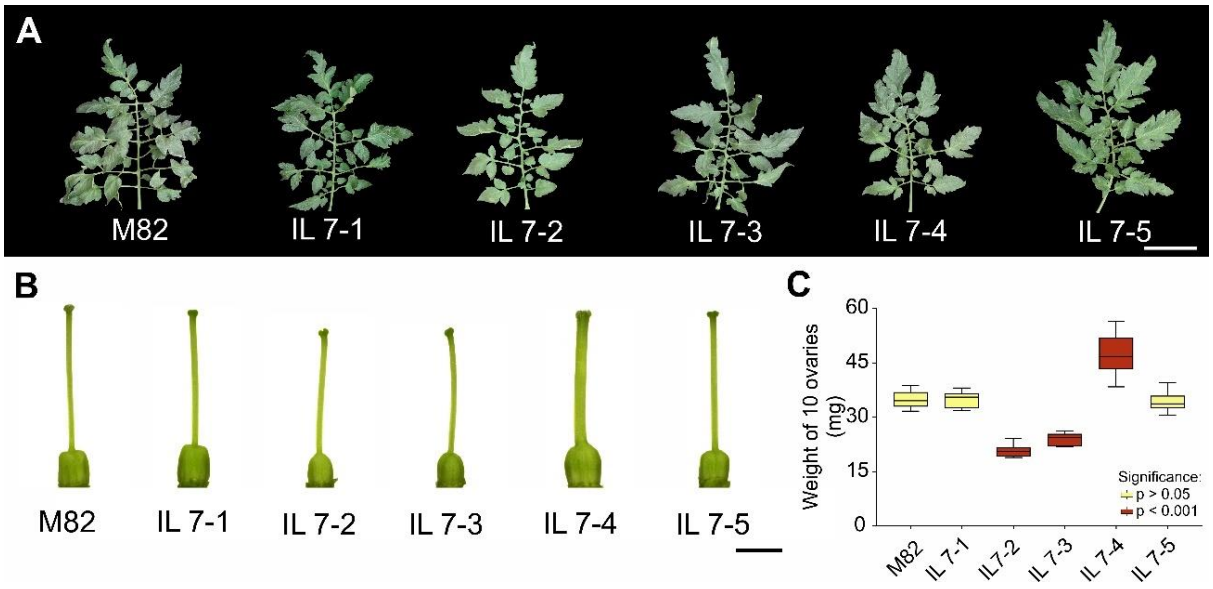

Figure S8. Characterization of introgression lines from chromosome 7. A. Representative leaf. Scale bar=10 cm. B**.** Representative ovary at anthesis. Scale bar=2 mm. **C.** Weight of 10 ovaries of M82 and introgression lines from chromosome 7 (n=10 repetitions). Statistical significance was tested by Wilcoxon rank sum test. Colors indicate the significance level in comparisons of each IL with M82.

We next used a set of genetic markers to analyze chromosome *7* of *Toy*. Thus, we found an introgression from *S. pennellii* encompassing approximately 11 Mbp on the long arm of chromossome 7. This region encompasses 1169 genes between the Solyc07g042560 and Solyc07g065440 markers. To refine the mapping results, we made use of two other ILs of *S. pennellii* in the MT background previously generated in our laboratory: *Brilliant corolla* (*Bco*) and *Regeneration 7H* (*Rg7H)*, neither of which shows the reduced organ phenotype of *Toy* (Figure 6 and S9). Our mapping and comparison helped us reduce the genomic region responsible for the *Toy* phenotype to a region harboring 250 genes, which located between the Solyc07g042560 and Solyc07g065440 markers (Figure 6).

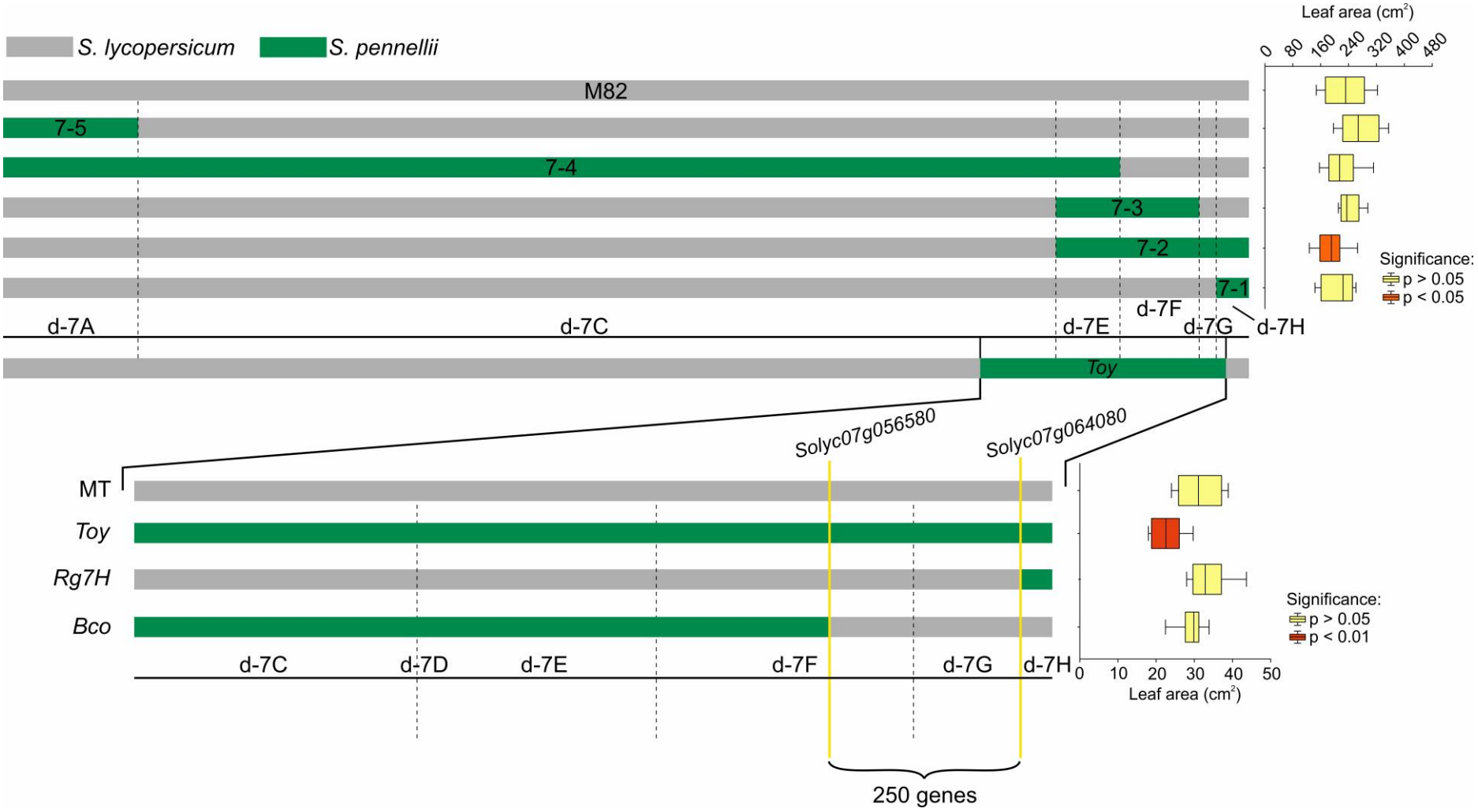
S. lycopersicum
S. pennellii
M82
7-5
7-4
7-3
7-2
7-1
d-7A
d-7C
d-7E
d-7F
d-7G
d-7H
Toy
Leaf area (cm²)
0 80 160 240 320 400 480
Significance:
p > 0.05
p < 0.05
Solyc07g056580
Solyc07g064080
MT
Toy
Rg7H
Bco
d-7C
d-7D
d-7E
d-7F
d-7G
d-7H
0 10 20 30 40 50
Leaf area (cm²)
Significance:
p > 0.05
p < 0.01
250 genes

Figure 6. Mapping of *Toy* allelic natural variation. *Toy* plants harboring a genome segment from *S. pennellii* that presents in the IL 7-1, 7-2, 7-3 and 7-4 (top). This segment was mapped between the *Solyc07g042560* and *Solyc07g065440* markers. IL7-2 showed a consistently reduction in leaf area compared to parental line, M82 (graphic in top, statistical significance was tested by Wilcoxon rank sum test and colors indicate the significance in comparisons of each IL with M82, n=14 leaves). Two ILs in the MT background that lodge a segment from *S. pennellii* on the chromosome 7 (*Bco* and *Rg7H*) were also mapped. *Toy* presented a drastic reduction in leaf area compared to MT, *Rg7H* and *Bco* genotypes (graphic in bottom, Statistical significance was tested by Student t test and colors indicate the significance level between genotypes, n=10 leaves). The data and the overlapping of the *Bco*, *Rg7H* and *Toy* genotype mapping indicate that the *Toy* gene might be in one region with 250 genes localized in the bins d-7F and d-7G. In the construction of this figure, we searched data from The Tomato Genome Consortium (2012) and Chitwood et al. (2013).

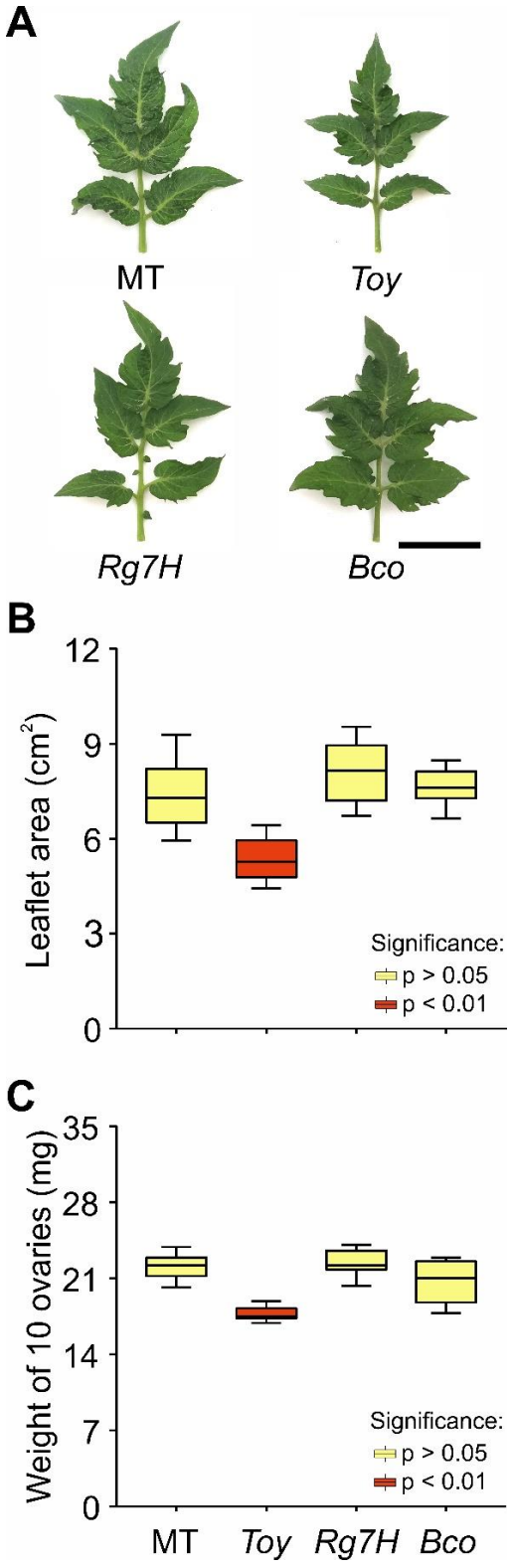

Figure S9. *Toy* plants present reduced leaves and ovaries. A. Representative leaf of MT, *Toy*, *Rg7H* and *Bco* genotypes. Scale bar=5 cm **B.** Terminal leaflet area (n=10 leaflet). **C.** Ovary weight (n=8 repetitions with 10 ovaries on each). Statistical significance was tested by Student's t-test. Colors indicate the significance level between genotypes.

1.3.6. *Toy* affects genes related to cell division and expansion

The results presented so far suggest that the transcriptional activity of genes related to cell division and expansion could be altered in *Toy*. To assess this, we extracted mRNA from ovaries/fruits (at -8, -4, 0, 4 and 8 DPA), fruit pericarps (12 and 16 DPA) and young leaves to analyze the transcriptional profile of a set of genes. Genes analyzed were *CYCB2;1* (Solyc02g082820), *FW2.2* (Solyc02g090730), and *EXP5* (Solyc02g088100). The results are shown in Figure 8.

In ovary/fruit tissues, we verified that the mRNA levels of the cell-cycle gene *CYCB2;1* presented greatest expression peak in both genotypes at 4 DPA (Figure 8A). *CYCB2;1* was higher in MT than *Toy* at anthesis (0 DAP) and at 16 DPA. On the other hand, *FW2.2*, another cell-cycle gene, was highly expressed at 4 DPA and 8 DPA in both genotypes. No quantitative variation in *FW2.2* expression was observed between genotypes during fruit devolvement, except at 8 DPA, where *Toy* ovaries presented increased levels of this transcript compared than MT (Figure 8B). After 4 DPA, the expression of cell-expansion gene *EXPA5*, a member of the α-expansin gene family, increased in in both genotypes (Figure 8C). However, ovaries of *Toy* plants presented a significant decrease in the expression of this gene at anthesis. Similar behavior was observed at 16 DPA. In contrast, we observed similar expression of *CYCB2;1* and *EXP5* genes in MT and *Toy* young leaves (Figure 8D).

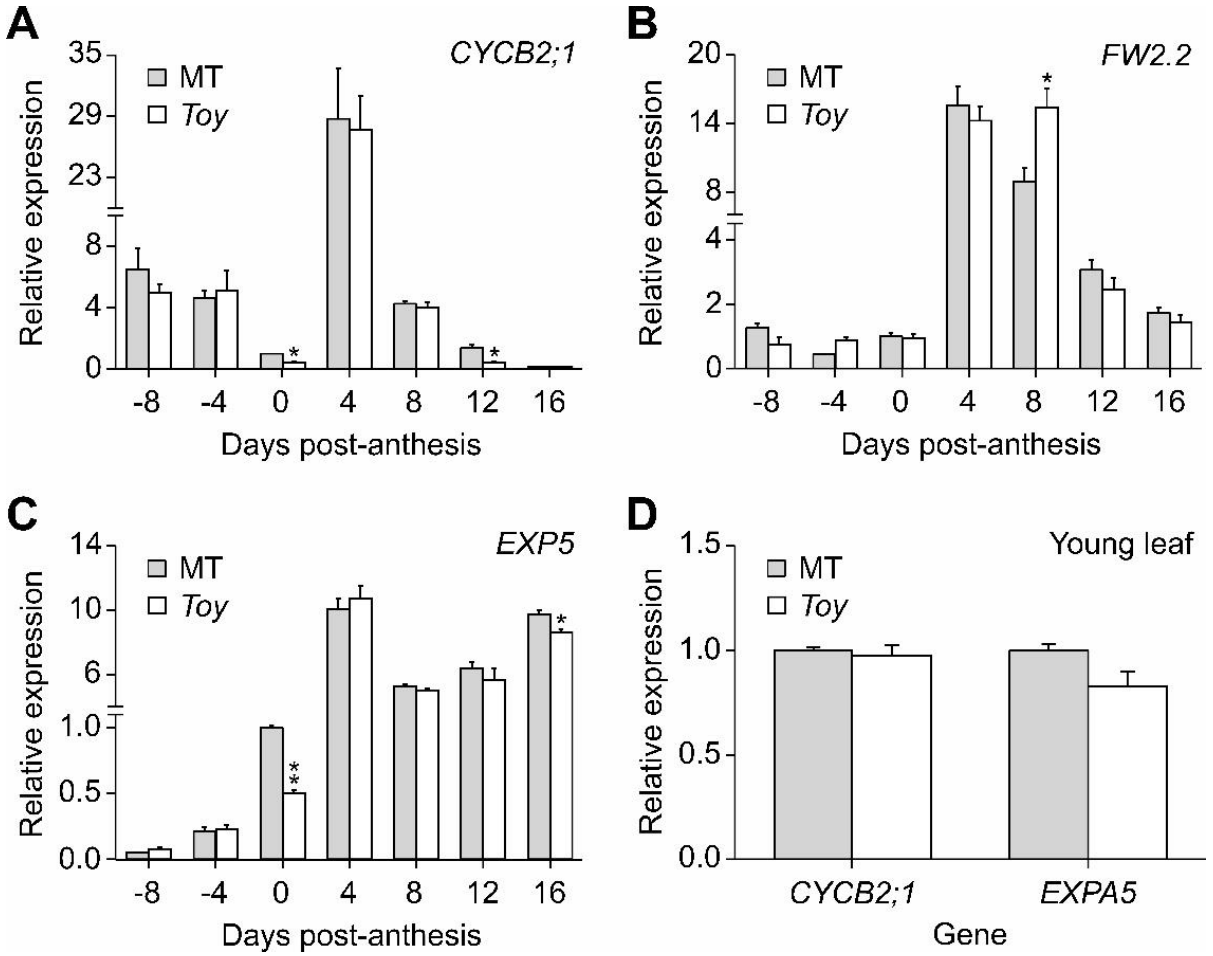

Figure 8. Time course of transcript levels of cell division- and expansion-related genes in ovaries/fruits and young leaves of MT (gray bar) and *Toy* (white bar). **A-C.** Relative transcript levels of *CYCB2;1* (A), *FW2.2* (B) and *EXP5* (C) in ovaries/fruit at -8, -4, 0, 4, 8 DPA and fruit pericarp at 12 and 16 DPA. **D.** Relative expression of *CYC2;1* and *EXPA5* genes in young leaves. Data are mean±s.e.m (n= 3 biological replicates). Statistical significance was tested by Student's t-test (*$p<0.05$, **$p<0.01$).

1.3.7. *Toy* plants present early flowering

Toy genotype exhibited a consistent early flowering compared to MT confirmed by distinct experiments. The analysis of the rate of shoot apical meristem maturation showed that *Toy* seedling present transition of all vegetative meristem at six days after emergence of same from soil (DAE), whilst MT present vegetative meristem same after 10 DAE (Figure 9A). This precocious transition affects the flowering time and the number of leaves in the primary shoot of *Toy* plants, which bloomed earlier and produce less leaves to the first inflorescence than MT genotype (Figure 9B and 9C).

Interestingly, although the *Toy* genotype exhibits a reduction in vegetative and reproductive organs it shows an initial growth more pronounced than MT, which corroborates

with precocious flowering. This differentiated growth was observed when we evaluated the shoot tip length of MT and *Toy* seedlings from emergence to 4 DAE (Figure 9D). Thus, we next collected apices from seedlings at 2DAE, where all meristems are vegetative in MT and *Toy* genotypes (Figure 9A), to evaluate the expression levels of cell division and expansion genes. However, we found no significate difference in the expression of *CYCB2;1* and *EXP5* genes between genotypes (Figure 9E). Together, these results suggest that the *Toy* genotype may exhibits a heterochronic behavior.

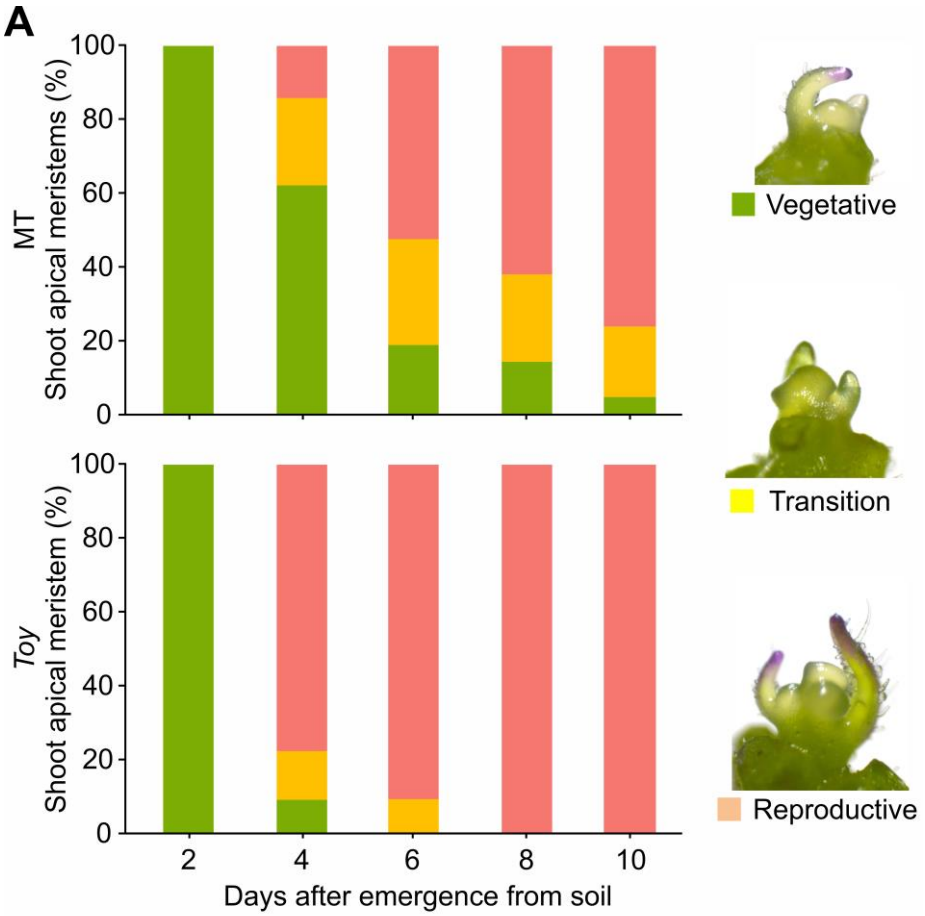
A
MT
Shoot apical meristems (%)
Toy
Shoot apical meristem (%)
100
80
60
40
20
0
2
4
6
8
10
Days after emergence from soil
Vegetative
Transition
Reproductive

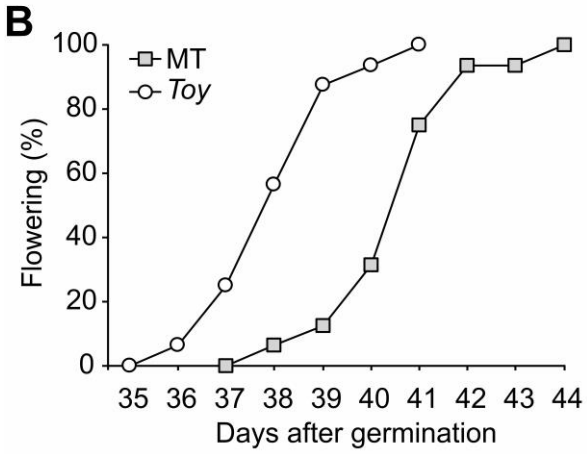
B
MT
Toy
Flowering (%)
100
80
60
40
20
0
35 36 37 38 39 40 41 42 43 44
Days after germination

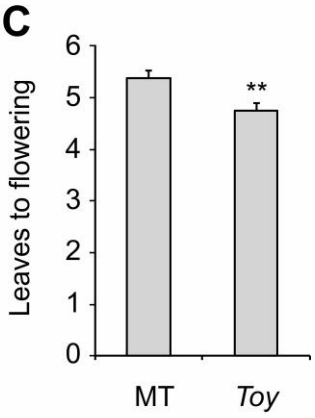
C
Leaves to flowering
6
5
4
3
2
1
0
**
MT
Toy

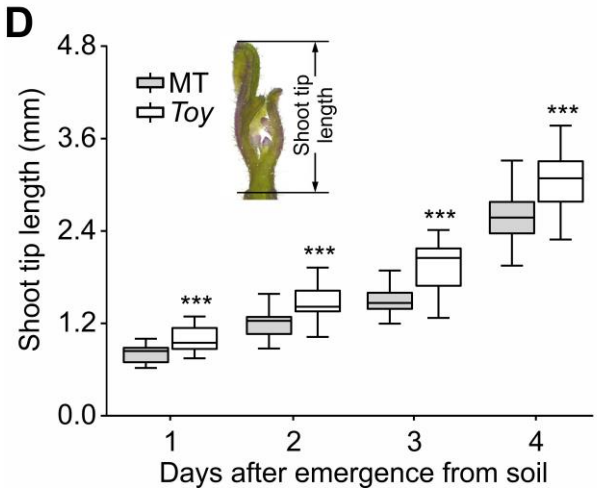
D
MT
Toy
Shoot tip length
Shoot tip length (mm)
4.8
3.6
2.4
1.2
0.0
***
1
2
3
4
Days after emergence from soil

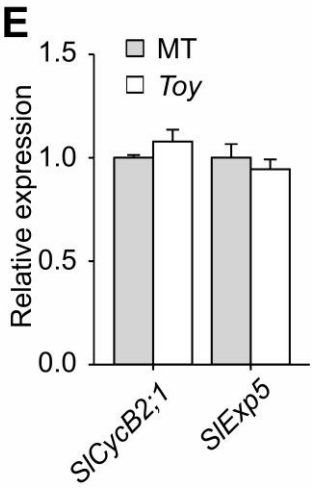
E
MT
Toy
Relative expression
1.5
1.0
0.5
0.0
SlCycB2;1
SlExp5

Figure 9. Flowering partner of MT and *Toy* plants. A. Rate of shoot apical meristem maturation. Percentage of MT (top panel) and *Toy* (bottom panel) seedlings (n=21), whose meristems were visually recognized as: vegetative meristem (vegetative; green bars); transition meristem (transition; yellow bars) or inflorescence/floral meristem (reproductive; pink bars). Representative images of meristem types are shown to the right of the figure. Seedlings were assessed two, four, six, eight and ten days after emergence from soil of seedling. **B.** Chronological time to flowering of the MT and *Toy* genotypes, in days. Percentage of plants with at least one open flower (n= 16). **C.** Development time to flowering (days) of the MT and *Toy* genotypes. Number of leaves formed before the vegetative meristem transition. Data are mean±s.e.m (n= 16). **D.** Time course of MT (gray bars) and *Toy* (white bars) shoot tip development in the first days after seedling emergence. Insert in top of this figure represents how measure was performed. **E.** Relative expression of *CYC2;1* and *EXPA5* genes in shoot apices at 2 DAE. Data are mean±s.e.m (n= 3 biological replicates). Statistical significance was tested by Student's t test, being the significance levels indicated by asterisks (***p<0.01*, ****p<0.001*).

1.4. DISCUSSION

Increased organ size, or gigantism, is a recurrent domestication trait observed in many crops (Evans, 1993; Frary and Doganlar, 2003). In this study, we set out to discover genetic determinants for gigantism of vegetative organs in the tomato. We characterized *TINY ORGANS AND REDUCED YIELD* (*Toy*), a novel introgression line from *S. pennellii* in the tomato cv. Micro-Tom background. Besides reduced leaves, *Toy* also showed reduction in the stem diameter, flower whorls, fruit weight, seed number per fruit, and seed weight. These differences in plant structure indicate that either one gene, or multiple closely linked genes, are potentially responsible for a key domestication trait in tomato, namely, increased plant size and vigor. Possibly, *Toy* may harbor gene with pleiotropic effects that contribute to domestication-related characteristics.

Among the many genes influencing fruit size, tomato domestication was marked by a change in the expression pattern of the *FW2.2* gene. When present in cultivated tomato, the *FW2.2* allele from *S. pennellii* promotes reduction not only in fruit weight but also in ovary size (Nesbitt and Tanksley, 2001). *Toy* plants also showed reduction in fruit and ovary size, however, this IL harbors the cultivated tomato allele (Figure S7). This suggests that the increase in the expression of *FW2.2* gene, at 8 DPA (Figure 8B), is a consequence of the change in the temporal expression of division-related genes during *Toy* fruit cell division phase.

Changes in temporal expression patterns during plant ontogeny promoting heterochronic alterations may entail several consequences in the final organ (Cong et al. 2002; Chuck et al., 2007; Eloy et al., 2011; Jiang et al., 2015; Vendemiatti et al., 2017). In Arabidopsis, the increase in leaf size of the *apc10* mutant was ascribed to enhanced cell proliferation during the early stages of leaf development, due to changes in expression timing of these genes (Eloy et al., 2011). In tomato, the temporal variation in expression of *FW2.2* gene was suggested as the responsible for

the fruit gigantism associated with the wild and domesticated alleles of this gene (heterochronic allelic variation) (Cong et al., 2002). Domestication of several crops entailed different heterochronic alterations (Takhtajan, 1991) and some may be linked with gigantism phenotypes. Thus, changes in the transcript levels of cell division- and expansion-related genes in particular moments of *Toy* fruit development shown here (Figure 8), suggest that *Toy* could be an allelic variation, which results in a decrease of organ size through heterochronic alterations in plant development. In addition, it is widely known that changes in flowering time and development rate may be interpreted as heterochrony (Geuten and Coenen, 2013), such as occurs in *Toy* plants (Figure 9).

Increased organ size, or gigantism, is a recurrent characteristic of the domestication process and promotes several phenotypic differences between cultivated and wild ancestor species (Darwin, 1868; Evans, 1993). Most tomato cultivars have bigger leaves than their wild relatives (Figure 1), suggesting that plants with greater leaves were selected during domestication. It is probably that this selection was unconscious, since human interest was mostly focused on the fruit. However, the successful production of larger fruits may necessitate proportionally increased vegetative organs to supply sufficient photosynthates.

Several studies highlight the importance of leaf size for growth and productivity of plants (Gifford et al., 1984; Li et al., 1998; Vos et al., 2005; Koester et al., 2014), since the leaves are the major organ for carbon fixation. *Toy* plants exhibit a drastic reduction in photosynthetic sources. When we evaluated the impact of this leaf area reduction on fruit size (sink), we found that under high and medium source-to-sink ratio, the leaf area was not a limiting factor for fruit size in *Toy* plants, but rather the ovary size, which was found to be smaller than MT (Figure 3). On the other hand, when we decreased the source-to-sink ratio, increasing the fruit number per plant, it was evident that the reduced leaf area of *Toy* became a major limiting to factor for fruit size and yield (Figure 5). Previous works demonstrated an increase in fruit size when the inflorescence number per plant and/or the fruit load per inflorescence are reduced, which probably occurs by increasing the source-to-sink ratio (Veliath and Ferguson, 1972; Fisher, 1977; Nesbitt and Tanskely, 2001; Baldet et al., 2006).

Although the segregation data indicate that *Toy* behaves as a Mendelian, semi-dominant gene, we cannot exclude the possibility that the IL harbors two or more genes controlling similar traits (i.e., organ size) on chromosome 7. Several studies indicate that may exist of two QTLs for fruit weight in the region corresponding to the introgression of the *S. pennellii* segment in the *Toy* plants (Grandillo et al., 1999; Van der Knaap and Tanksley, 2003; Causse et al., 2004; Barrantes et al. 2016). Moreover, it has been demonstrated that different elements of the domestication

syndrome may be regulated by the same genomic regions, indicating pleiotropy or linkage among several loci (Koinange et al., 1996; Cai and Morishima, 2002; Poncet et al., 2002; Bomblies and Doebley, 2006; Weeden, 2007).

The probable ancestor of cultivated tomato is the cherry tomato (*S. lycopersicum* var. *cerasiforme*). This tomato was structured into two groups and one of them is resulting from the admixture of the *S. lycopersicum* and *S. pimpinellifolium* genomes (Ranc et al., 2008). Several accessions of *S. pimpinellifolium*, *S. lycopersicum* var. *cerasiforme* and cultivated tomatoes were sequenced by Lin et al. (2014). Based on the single nucleotide polymorphism (SNP) occurrence between these genotypes, the authors classified the putative genes in domestication or improvement genes. Interestingly, the region that *Toy* was mapped to contains both putative domestication and improvement genes (Figure 10). Thus, our results would not be invalidated by the existence of more than one genetic determinant behind the *Toy* phenotype, as co-selection could have occurred through linkage drag over the course of domestication.

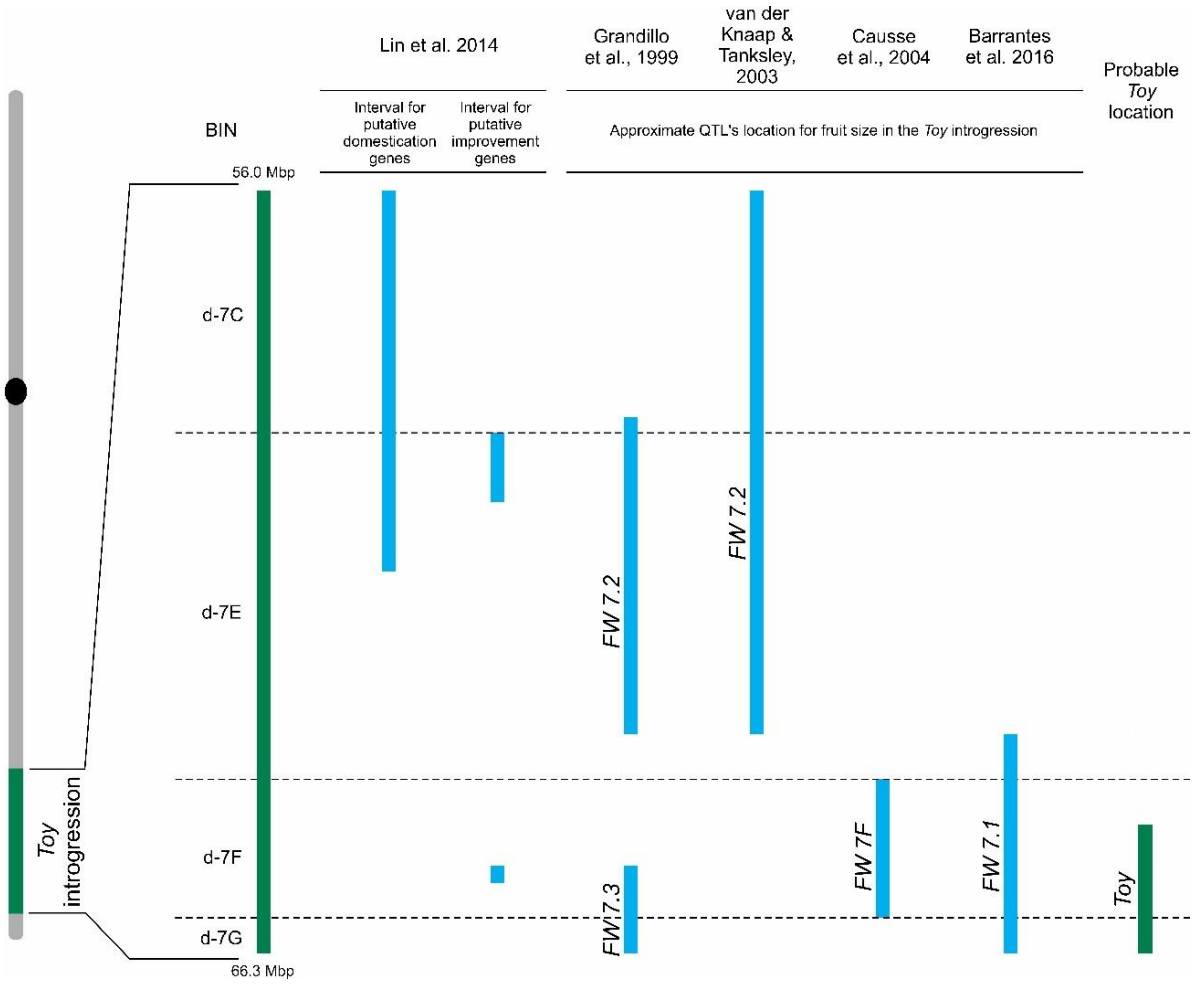

Figure 10. QTLs (Quantitative Trait Loci) affecting fruit weight on chromosome 7. The interval of putative domestication and improvement genes identified by Lin et al. (2014) occur at least in same region where *Toy* was mapped. Some QTL mapping works for fruit weight on the chromosome 7, more specifically in the *Toy* location region, are also shown, as well as the possible region may harboring *Toy* locus. Bars indicate approximately QTL intervals.

1.5. CONCLUSION

Based on the analysis of natural genetic variation, we presented a potential genetic determinant for increased leaf size in cultivated tomato. Furthermore, our results could unveil a novel link in the genetic basis of fruit and leaf size in tomato. Fruit gigantism in tomato is a hallmark domestication trait, however, less attention has been paid to the increase in vegetative organ size, which represents a necessary source of photosynthates to supply larger fruits.

Further research should determinate the molecular identity of the gene(s) underlying the *Toy* phenotype. This would place one more piece in the tomato domestication puzzle and provide new information that could be harnessed to improve both tomatoes as well as other species, as gigantism is recurring theme in most extant crops. In addition, the pleiotropic effect presented by

Toy plants, credits this locus as a good candidate for the implementation of the *de novo* domestication (Zsogon et al. 2017; 2018) in several species.

REFERENCES

Bai YL, Lindhout P. 2007. Domestication and breeding of tomatoes: what have we gained and what can we gain in the future? Annals of Botany , 100, 1085-1094.

Baldet P, Hernould M, Laporte F, Mounet F, Just D, Mouras A, Chevalier C, Rothan C. 2006. The expression of cell proliferation-related genes in early developing flowers is affected by a fruit load reduction in tomato plants. Journal of Experimental Botany, 57, 961-970.

Barrantes W, Lopez-Casado G, García-Martínez S, Alonso A, Rubio F, Ruiz JJ, Fernández-Muñoz R, Granell A, Monforte AJ. 2016. Exploring new alleles involved in tomato fruit quality in an introgression line library of *Solanum pimpinellifolium*. Frontiers in Plant Science. DOI:10.3389/fpls.2016.01172.

Bolger A, Scossa F, Bolger ME, Lanz C, Maumus F, Tohge T, Quesneville H, Alseekh S, Sorensen I, Lichtenstein G, Fich EA, Conte M, Keller H, Schneeberger K, Schwacke R, Ofner I, Vrebalov J, Xu Y, Osorio S, Aflitos SA, Schijlen E, Jimenez-Gomez JM, Ryngajllo M, Kimura S, Kumar R, Koenig D, Headland LR, Maloof JN, Sinha N, van Ham RCHJ, Lankhorst RK, Mao L, Vogel A, Arsova B, Panstruga R, Fei Z, Rose JKC, Zamir D, Carrari F, Giovannoni JJ, Weigel D, Usadel B, Fernie AR. 2014. The genome of the stress-tolerant wild tomato species *Solanum pennellii*, Nature Genetics, 46, 1034-1038.

Bomblies K, Doebley JF. 2006. Pleiotropic effects of the duplicate maize *FLORICAULA/LEAFY* genes *zfl1* and *zfl2* on traits under selection during maize domestication. Genetics, 172: 519-531.

Cai H, Morishima H. 2002. QTL clusters reflect character associations in wild and cultivated rice. Theoretical and Applied Genetics, 104, 1217-1228.

Carvalho RF, Campos ML, Pino LE, Crestana SL, Zsögön A, Lima JE, Benedito VA, Peres LEP. 2011. Convergence of developmental mutants into a single tomato model system: 'Micro-Tom' as an effective toolkit for plant development research. Plant Methods, 7, 18.

Causse M, Duffe P, Gomez MC, Buret M, Damidaux R, Zamir D, Gur A, Chevalier C, Lemaire-Chamley M, Rothan C. 2004. A genetic map of candidate genes and QTLs involved in tomato fruit size and composition. Journal of Experimental Botany, 55, 1671-1685.

Chakrabarti M, Zhang N, Sauvage C, Muños S, Blanca J, Cañizares J, Diez MJ, Schneider R, Mazourek M, McClead J, Causse M, van der Knaap E. 2013. A cytochrome P450 regulates a domestication trait in cultivated tomato. Proc. Natl Acad. Sci. USA, 110, 17125–17130.

Chetelat RT. 1998. *Bco*, a corolla pigment intensifier on chromosome 7. Report of the Tomato Genetics Cooperative, 48, 10-12.

Chitwood DH, Kumara R, Headlanda LR, Ranjana A, Covingtona MF, Ichihashia Y, Fulopa D, Jiménez-Gómeza JM, Pengb J, Maloofa J, Sinha NR. 2013, A quantitative genetic basis for leaf morphology in a set of precisely defined tomato introgression lines. Plant Cell, 25, 2465-2481.

Chuck G, Cigan AM, Saeteurn K, Hake S. 2007. The heterochronic maize mutant *Corngrass1* results from overexpression of a tandem microRNA. Nature Genetics. 39, 544-549.

Cong B, Liu J, Tanksley SD. 2002. Natural alleles at a tomato fruit size quantitative trait locus differ by heterochronic regulatory mutations. Proceedings of the National Academy of Sciences of the United States of America, 99, 13606-13611.

Darwin C. 1868. The Variation of Animals and Plants Under Domestication. London: John Murray.

Doebley JF, Gaut BS, Smith BD. 2006. The Molecular Genetics of Crop Domestication. Cell, 127, 1309-1321.

Eloy NB, de Freitas Lima M, Van Damme D, Vanhaeren H, Gonzalez N, De Milde L, Hemerly AS, Beemster GTS, Inzé D, Ferreira PCG. 2011. The APC/C subunit 10 plays an essential role in cell proliferation during leaf development. Plant Journal, 68, 351-363.

Eshed Y, Zamir D. 1994. A genomic library of *Lycopersicon pennellii* in *L. esculentum*: a tool for fine mapping of genes. Euphytica, 79, 175-179.

Eshed Y, Zamir D. 1995. An Introgression line population of *Lycopersicon pennellii* in the cultivated tomato enables the identification and fine mapping of yield-associated QTL. Genetics, 141, 1147-1162.

Evans LT. 1993. Crop evolution, adaptation and yield. Cambridge Univ. Press, Cambridge. 500p.

Faria JPB. 2014. Alterações hormonais no mutante *ovate* de tomateiro (*Solanum lycopersicum* L. cv Micro-Tom) e seu impacto na morfologia, qualidade do fruto, produtividade e partenocarpia. Dissertação (Mestrado em Fisiologia e Bioquímica de plantas). Escola Superior de Agricultura "Luiz de Queiroz", Universidade de São Paulo, Piracicaba, 68p.

Fisher KJ. 1977. Competition effects between fruit trusses of the tomato plants. Science Horticulture, 8, 37-42.

Frary A, Nesbitt TC, Grandillo S, van der Knaap E, Cong B, Liu J, Meller J, Elber R, Alpert KB, Tanksley SD. 2000. Cloning and transgenic expression of *fw2.2*: a quantitative trait locus key to the evolution of tomato fruit. Science, 289, 85-87.

Frary A, Doganlar S. 2003. Comparative genetics of crop plant domestication and evolution. Turkish Journal of Agricultural Forestry, 27, 59-69.

Fulton TM, Chunwongse J, Tanksley SD. 1995. Microprep protocol for extraction of DNA from tomato and other herbaceous plant. Plant Molecular Biology Reporter, 13, 207-209.

Gómez-Campo C, Prakash S. 1999. Origin and domestication. In: Gómez-Campo, C. (Ed.), Biology of Brassica Coenospecies. Elsevier Science, Amsterdam, pp. 59–106.

Gifford RM, Evans L. 1981. Photosynthesis, carbon partitioning, and yield. Annual Review Plant Physiology, 32, 485-509.

Gifford RM, Thorne JH, Hitz WD, Giaquinta RT. 1984. Crop productivity and photoassimilate partitioning. Science, 24, 801-808.

Grandillo S, Ku HM, Tanksley SD. 1999. Identifying loci responsible for natural variation in fruit size and shape in tomato. Theoretical and Applied Genetics, 99, 978-987.

Gillaspy G, Ben-David H, Gruissem W. 1993. Fruits: a developmental perspective. The Plant Cell, 5, 1439-1451.

Geuten K, Coenen H. 2013. Heterochronic genes in plant evolution and development. Frontiers in Plant Science. 4, 381.

Gustafson, FG; Stoldt, E. 1936. Some relations between leaf area and fruit size in tomatoes. Plant Physiology, 11, 445-451.

Guo M, Simmons CR. 2011. Cell number counts—the *fw2.2* and *CNR* genes and implications for controlling plant fruit and organ size. Plant Science 181, 1-7.

Hamada K, Hasegawa K, Kitajima A, Ogata T. 2008. The relationship between fruit size and cell division and enlargement in cultivated and wild persimmons. The Journal of Horticultural Science and Biotechnology, 82, 218-222.

Jiang LB, Clavijo JA, Sun LD, Zhu XL, Bhakta MS, Gezan SA, Carvalho M, Vallejos CE, Wu R. 2015. Plastic expression of heterochrony quantitative trait loci (hQTL) for leaf growth in the common bean (*Phaseolus vulgaris* L.). New Phytologist, 207, 872-882.

Karnovsky MJ. 1965. A formaldehyde-glutaraldehyde fixative of high osmolality for use in electron microscopy. Journal of Cell Biology, 27: 137-138.

Krizek, BA. 2009. Making bigger plants: key regulators of final organ size. Current Opinion in Plant Biology, 12: 17-22.

Koester RP, Skoneczka JA, Cary TR, Diers BW, Ainsworth EA. 2014. Historical gains in soybean (*Glycine max* Merr.) seed yield are driven by linear increases in light interception, energy conversion, and partitioning efficiencies. Journal of Experimental Botany, 65, 3311-3321.

Koinange EMK, Singh SP, Gepts P. 1996. Genetic control of the domestication syndrome in common bean. Crop Science, 36, 1037-1045.

Krizek BA. 2009. Making bigger plants: key regulators of organ size. Current Opinion in Plant Biology, 12, 17-22.

Lester RN. 1989. Evolution under domestication involving disturbance of genic balance. Euphytica, 44, 125-132.

Li T, Heuvelink E, Marcelis LFM. 2015. Quantifying the source-sink balance and carbohydrate content in three tomato cultivars. Frontiers in plant science, 6, 416.

Li T, Yang X, Yu Y, Si X, Zhai X, Zhang H, Dong W, Gao C, Xu C. 2018. Domestication of wild tomato is accelerated by genome editing. Nature Biotechnology. doi:10.1038/nbt.4273.

Li Z, Pinson SRM, Stansel JW, Paterson AH. 1998. Genetic dissection of thesource-sink relationship affecting fecundity and yield in rice (*Oryza sativa* L.). Molecular Breeding, 4, 419-426.

Lin T, Zhu G, Zhang J, Xu X, Yu Q, Zheng Z, Zhang Z, Lun Y, Li S, Wang X, Huang Z, Li J, Zhang C, Wang T, Zhang Y, Wang A, Zhang Y, Lin K, Li C, Xiong G, Xue Y, Mazzucato A, Causse M, Fei Z, Giovannoni JJ, Chetelat RT, Zamir D, Stadler T, Li J, Ye Z, Du Y, Huang S. 2014. Genomic analyses provide insights into the history of tomato breeding. Nature Genetics, 46, 1220-1226.

Lippman Z, Tanksley SD. 2001. Dissecting the genetic pathway to extreme fruit size in tomato using a cross between the small-fruited wild species *Lycopersicon pimpinellifolium* and *L. esculentum* var. Giant Heirloom. Genetics, 158, 413-422

Livak KJ, Schmittgen TD. 2001. Analysis of relative gene expression data using real-time quantitative PCR and the $2^{-\Delta\Delta CT}$ method. Methods, 25, 402-408.

Mayer KF, Schoof H, Haecker A, Lenhard M, Jürgens G, Laux T. 1998. Role of WUSCHEL in regulating stem cell fate in the Arabidopsis shoot meristem. Cell, 95, 805–815.

Meyer RS, Purugganan MD. 2013. Evolution of crop species: genetics of domestication and diversification. Nature Reviews Genetics, 14, 840-852.

Mizukami Y. 2001. A matter of size: developmental control of organ size in plants. Current Opinion in Plant Biology, 4, 533–539.

Mu Q, Huang Z, Chakrabarti M, Illa-Berenguer E, Liu X, Wang Y, Ramos A, Knaap EVD. 2017. Fruit weight is controlled by cell size regulator encoding a novel protein that is expressed in maturing tomato fruits. PLoS Genetics, 13:e1006930.

Muños S, Ranc N, Botton E, Berard A, Rolland S, Duffe P, Carretero Y, Le Paslier MC, Delalande C, Bouzayen M, Brunel D, Causse M. 2011. Increase in tomato locule number is controlled by two single-nucleotide polymorphisms located near WUSCHEL. Plant Physiology, 156, 2244-2254.

Nesbitt TC, Tanksley SD. 2001. *fw2.2* directly affects the size of developing tomato fruit, with secondary effects on fruit number and photosynthate distribution. Plant Physiology, 127, 575-583.

Niklas KJ. 2004. Plant allometry: is there a grand unifying theory? Biological reviews of the Cambridge Philosophical Society, 79, 871-89.

Osorio S, Ruan YL, Fernie AR. 2014. An update on source-to-sink carbon partitioning in tomato. Frontiers in plant science, 5, 516.

Pinto MS, Abeyratne CR, Benedito VA, Peres LEP. 2017. Genetic and physiological characterization of three natural allelic variations afecting the organogenic capacity in tomato (*Solanum lycopersicum* cv. Micro-Tom Plant Cell, Tissue and Organ Culture, 129, 89-103.

Poncet V, Martel E, Allouis S, Devos M, Lamy F, Sarr A, Robert T. 2002. Comparative analysis of QTLs affecting domestication traits between two domesticated x wild pearl millet (*Pennisetum glaucum* L., Poaceae) crosses. Theoretical and Applied Genetics, 104, 965-975.

Prakash S, Wu XM, Bhat SR. 2011. History, evolution, and domestication of *Brassica* crops. Plant Breeding Reviews, 35, 19-84.

Ranc N, Munos S, Santoni S, Causse M. 2008. A clarified position for *Solanum lycopersicum* var. *cerasiforme* in the evolutionary history of tomatoes (Solanaceae). BMC Plant Biology, 8, 130.

Rosati A, Zipanćič M, Caporali S, Padula G. 2009. Fruit weight is related to ovary weight in olive (*Olea europaea* L.). Sci. Hortic., 122, 399-403.

Sakai WS. 1973. Simple method for differential staining of parafilm embedded plant material using toluidine blue O. Stain Technology 48: 247–249.

Takhtajan A. 1991. Evolutionary Trends in Flowering Plants, Columbia University Press, New York City, 241p.

Tanksley SD. 2004. The genetic, developmental, and molecular bases of fruit size and shape variation in tomato. The Plant Cell, 16, S181–S189.

The Tomato Genome Consortium. 2012. The tomato genome provides insights into fleshy fruit evolution. Nature, 485, 635–41.

van der Knaap E, Tanksley SD .2003. The making of a bell pepper shaped tomato fruit: identification of loci controlling fruit morphology in yellow stuffer tomato Theoretical and Applied Genetics, 107, 139-147.

van der Knaap E, Chakrabarti M, Chu Y, Clevenger JP, Illa-Berenguer E, Huang Z, Keyhaninejad N, Mu Q, Sun L, Wang Y, Wu S. 2014. What lies beyond the eye: the molecular mechanisms regulating tomato fruit weight and shape. Frontiers in Plant Science, 5, 227.

Veliath JA, Ferguson AC. 1972. The effect of deblossoming on fruit size, yield, and earliness in tomato. Journal of Horticultural Science 7: 278–279

Vendemiatti E, Zsögön A, Silva GFF, Jesus FA, Cutri L, Figueiredo CRF, Tanaka FAO, Nogueira FTS, Peres LEP. 2017. Loss of type-IV glandular trichomes is a heterochronic trait in tomato and can be reverted by promoting juvenility. Plant Science, 259, 35-47.

Vos J, Van Der Putten PEL, Birch CJ. 2005. Effect of nitrogen supply on leaf appearance, leaf growth, leaf nitrogen economy and photosynthetic capacity in maize (*Zea mays* L.). Field Crops Research, 93, 64-73.

Weyers JDB, Johansen LG. 1985. Accurate estimation of stomatal aperture from silicone rubber impressions. New Phytology, 101, 109-15.

Weeden NF. 2007. Genetic changes accompanying the domestication of Pisum sativum: is there a common genetic basis to the 'domestication syndrome' for legumes? Annals of Botany, 100, 1017-1025.

Xu C, Liberatore KL, MacAlister CA, Huang Z, Chu YH, Jiang K, Brooks C, Ogawa-Ohnishi M, Xiong G, Pauly M, Van Eck J, Matsubayashi Y, van der Knaap E, Lippman ZB. 2015. A cascade of arabinosyltransferases controls shoot meristem size in tomato. Nature Genetic, 47, 784-792.

Zsögön A, Cermak T, Voytas D, Peres LEP. 2017. Genome editing as a tool to achieve the crop ideotype and de novo domestication of wild relatives: case study in tomato. Plant Science 256, 120-130.

Zsögön A, Čermák T, Naves ER, Notini M M, Edel KH, Weinl S, Freschi L, Voytas DF, Kudla J, Peres LEP. 2018. *De novo* domestication of wild tomato using genome editing. Nature Biotechnology. doi:10.1038/nbt.4272.

2. THE *WATER ECONOMY LOCUS IN LYCOPERSICON* (*WELL*) HAS A LOWER HYDRAULIC CONDUCTANCE, WHICH IS LINKED TO ITS DELAYED WILTING AND FAST RECOVERY FROM DROUGHT

Abstract

The search for drought-resistant plants is becoming increasingly relevant, especially in light of future predictions of climate change. Tomato (*Solanum lycopersicum*) is an important crop that presents a great source of drought resistance in its wild relatives, such as *S. pennellii*. However, studies exploring the genetic components and physiological mechanisms involved in this resistance are still incipient. In the present work the physiological mechanisms responsible for the drought resistance of an introgression line (IL) named *Water Economy Locus in Lycopersicon* (*Well*) were studied. *Well* was obtained by crossing *S. pennellii* and the miniature tomato cultivar Micro-Tom (MT), and further mapped on chromosome 1. This IL presents a noteworthy delay in wilting upon water withdrawal and a great control of water loss compared to MT. Measurements of stomatal conductance (g_s) showed no significant difference between MT and *Well* plants under well-hydrated and moderate stress conditions, but a significant g_s reduction in *Well* plants was verified after the resuming of irrigation. *Well* plants also presented midday depressions in leaf patch pressure (P_p) curve, which is inversely proportional to the leaf turgor pressure, as well as a smaller "wrong-way responses" (WWR) duration compared to MT. These results suggest that *Well* plants exhibit a differential stomatal behavior. *Well* stomatal behavior was associated with a lower hydraulic conductance (*K*), which is probably ascribed to a decreased xylem vessel size observed in its stem. The further molecular identification of the *Well* gene will provide for our understanding of drought-resistance mechanisms and allows its faster use in breeding programs.

Keywords: Tomato; Introgression line; Drought resistance; Hydraulic conductance; Xylem vessel

2.1. INTRODUCTION

Water has a fundamental role in biomass accumulation in plants, namely photosynthesis, and its lack may beget irreparable losses in crop production (Boyer, 1982; Mueller et al., 2012; van Ittersum et al., 2013). The importance of water is undeniable for current agriculture. Hence, climate change has caused significant impacts on the global water cycle, leading to concerning prospects for food security, mostly due to changes in crop yield (Kang et al., 2009; Sun et al., 2012; Najafi et al. 2018). In this context, the investigation of the genetic basis and the physiological mechanisms that improve drought resistance or water-use efficiency (WUE, amount of carbon fixed per unit water transpired) in plants is required. In addition, the manipulation of such parameters might be essential for modern agriculture, which requires more sustainable crop production.

Noteworthy, the process of crop domestication has generated a bottleneck in genetic diversity (Doebley et al., 2006), which has made it difficult to search for putative genes and mechanisms involved in biotic and abiotic stress tolerance. However, wild progenitors and/or

related species of crops represent an excellent alternative for breeding, as they are a rich reservoir of natural genetic variation (Rick, 1973; Zamir, 2001; Koornneef et al., 2004; Juenger, 2013). Such genetic variation can directly contribute to improve crop performance under resource-limited conditions (e.g. low water availability). Among domesticated crops, the tomato (*Solanum lycopersicum* L.) stands out as a useful model for natural genetic variation studies (Rick, 1973; Zsögön et al., 2017). Tomato has a fully sequenced genome and a broad repository of natural genetic variation in the form of 12 closely related wild species (Rick, 1976, 1983; The Tomato Genome Consortium, 2012; Bolger et al, 2014). Each of these relatives presents peculiarities according to the conditions that they experience in their natural habitat, including water availability. The major genetic sources for drought resistance in tomato are *S. chilense* and *S. pennellii* (Rick, 1973). Although some features of S. chilense preclude its use in genetic and physiological studies (e.g. fertility barriers with cultivated tomato) (Zsögön et al, 2017), *S. pennellii* has attracted the interest of plant biologists around the world (Bolger et al, 2014).

S. pennellii exhibits a remarkable capacity of surviving, maintaining water status and growth in environments with low water availability (Yu, 1972; Rick, 1973; Martin and Thorstenson, 1988). Besides, a high-quality, fully annotated genome sequence of *S. pennellii* is already publicly available (Bolger et al., 2014). Thus, determination of the genetic basis of its drought resistance is highly desirable, and some progress has been made by identification and characterization of *S. pennellii´s* individual genes (Wei and O'Connell, 1996; Treviño and O'Connell, 1998; Ziaf et al., 2011; Loukehaich et al., 2012; Li et al., 2015; Li et al., 2018). Furthermore, *S. pennellii* has a higher WUE than cultivated tomatoes (Kebede et al., 1994; Martin et al., 1999; Xu et al., 2008).

Drought resistance is sometimes treated as synonymous with high WUE, and although drought can increase WUE (Franks et al 2015), they are not physiologically equivalent (Blum 2005; 2009). Different from WUE, drought resistance is more complex than the relationship between two physiological variables, transpiration and photosynthesis (Blum, 2005). Instead, it is a trait strongly linked to all aspects of plant development, including phenology and morphology. In line with this, Levitt (1972) pointed out that the mechanisms of drought resistance can be drought escape, dehydration avoidance and dehydration tolerance. Drought escape consists of phenological modifications that make plants capable of completing their life cycle before the onset of severe water stress, such as earlier flowering (Kooyers, 2015). Drought avoidance involves morphological adaptations such as deep root systems or stomatal modifications (Pinheiro et al. 2005; Basu et al. 2016). Both drought scape and avoidance comprise mechanisms that maintain plant tissues with high water potentials in dry environments (Levitt, 1972). In

dehydration tolerance, biochemical mechanism allows plants to withstand severe water scarcity through the protection of membranes and other cellular components (Serraj and Sinclair, 2002; Basu et al. 2016). Drought tolerance can lead to a growth reduction and thus lower yields. Therefore, despite the fact that drought resistance is a trait long sought by breeders, it is important to determine the kind of mechanism involved and its impact on productivity.

Herein, we use an introgression line (IL) produced by successive backcross between *S. pennellii* and the tomato model system Micro-Tom (MT), which was denominated as *Water Economy Locus in Lycopersicon* (*WELL*) (Zsögön, 2011). *WELL* was mapped on chromosome 1 and characterized as both drought resistant (Zsögön, 2011) and more effective in water use (Vicente et al., 2015). Probably, *Well* plants harbor one of the genetic components of *S. pennellii's* drought resistance, whose physiological mechanism has not yet been explored. The aim of this work was to investigate the physiological mechanisms involved in the drought-resistance presented by the *Well* genotype. The data presented here indicate a putative mechanism of drought resistance in the *Well* plants involving decreased xylem conductance, which promotes changes in the stomatal behavior and dehydration avoidance.

2.2. MATERIALS AND METHODS

2.2.1 Plant material and growth conditions

The tomato model system Micro-Tom (MT) cultivar (Meissner et al., 1997) and the *Water Economy Locus in Lycopersicon* (*Well*) genotype, an introgression line into MT from *Solanum pennellii* (LA716) were used for this study. The introgression and initial characterization of *Well* genotype was described in Zsögön (2011) and Vicente et al. (2015).

Plants were grown in a greenhouse at the Laboratory of Hormonal Control of Plant Development, ESALQ-USP, (543 m a.s.l., 22º 42' 36" S; 47º 37' 50" W), Piracicaba, SP, Brazil. Growth condition were mean temperature of 28°C, 11.5 h/13 h (winter/summer) photoperiod, 250–350 μmol photons m^{-2} s^{-1} PAR irradiance, attained by a reflecting mesh (Aluminet, Polysack Indústrias Ltda, Leme, Brazil). Seeds were sown in trays containing a 1:1 mixture of commercial substrate (Basaplant®, Base Agro, Artur Nogueira, SP, Brazil) and expanded vermiculite, supplemented with 1 g L^{-1} 10:10:10 NPK and 4 g L^{-1} dolomite limestone ($MgCO_3$ + $CaCO_3$). Ten days after germination, seedlings were transplanted to pots containing the soil mix described above but supplemented with 8 g L^{-1} 10:10:10 NPK. However, the pots capacity varied according to the experiments, as described below.

Experiments conducted to measure the time course of plant growth, water loss, leaf transpiration, transient wrong way response (WWR) of stomata, anatomical analyses, stem and leaf hydraulic conductance were performed with plants grown individually in 250 mL pots. To determine the degree of leaf rolling, gas exchange and water potential under three condition (watering, drought and rewatering), and turgor pressure by the LPCP (leaf patch clamp pressure) probes were conducted in 350 mL pots with two plants per pot, one of each genotype (MT and *Well*). Lastly, experiments of wilting and stem and leaf relative water content in seedling were conducted in 6 L pots containing 60 seedlings, 30 of each genotype (MT and *Well*).

2.2.2. Leaf rolling and time course of plant growth

The leaf rolling degree (LRD) of MT and *Well* plants was calculated according to Premachandra et al. (1993). The blade width was measured daily in a terminal leaflet of a fully expanded leaf from watering interruption to rewatering of plants. Measurements were taken in the leaflet median region of plants initially 45 days old. LRD was determined as the percentage reduction of leaf width by rolling.

In a separate experiment, plant growth was determined by the weekly measurement of MT and *Well* plant height. The measurements were taken from the tenth day after germination and the height was considered as distance between of the cotyledon insertion and apex of plants.

2.2.3. Gas exchange and leaf water potential determinations

Gas-exchange measurements were performed with a portable photosynthesis system (LI-6400XT, LI-COR, Lincon, USA) to obtain the net CO_2 assimilation rate (A), stomatal conductance (g_s), transpiration rate (E), and transpiration efficiency (A/E). The analyses were performed in three different conditions of water supply: before water interruption, moderate visual wilting and one week after rehydration of plants. All gas exchange measurements were performed on a same fully expanded terminal leaflet. The measurements before water interruption were performed in plants with 45 days after germination (DAG). Leaf temperature (27 ± 0.5°C), photosynthetic photon flux density (1000 μmol m^{-2} s^{-1}), flow rate (350 μmol s^{-1}), CO_2 concentration (400 ppm) into the leaf chamber were held constant. Evaluations were taken after ~20 minutes equilibration to measure steady-state gas exchanges.

At the end of the gas exchange evaluation of each plant, the water potential was determined. A small leaf disc (~6 mm diameter) was collected and quickly taken to a

thermocouple psychrometer (PSYPRO, WESCOR, Logan, USA) coupled to C-52 sample chambers. All measurements were performed on the lateral leaflet of the leaf used to obtain the gas exchange.

2.2.4. Leaf water loss and transpiration in detached leaves

Leaf water loss and transpiration were determined using fully expanded leaves from five plants per genotypes at 40 DAG. Detached leaves were photographed for area determination using ImageJ software (http://rsbweb.nih.gov/ij/). Leaf petioles were excised, then re-cut under water (to prevent embolism) and placed in a solution of "artificial xylem sap" (AX) in 10mL scintillation vials. The vials were sealed with plastic film, in which was made a small hole to introduce the petioles. The AX solution contained 3 mM KNO_3, 1 mM $CaCl_2$, 1 mM KH_2PO_4, 1 mM K_2HPO_4, 0.1 mM $MnSO_4$ and 0.1 mM $MgSO_4$ as described by Carvalho et al. (2011). Samples were maintained in this solution over-night at room temperature for maximum hydration.

The leaves used to evaluate water loss were taken from the solution of AX and left on the laboratory bench. Leaves that were used to determine detached leaf transpiration rate remained in the scintillation vials. An analytical balance was used to weight hourly the leaves (06:00 h to 18:00 h). Water loss was normalized according to the initial weight (%). Transpiration was determined through the following equation: $E = (W_i - W_n)/\text{Leaf area}$ (g cm^{-2}), where W_i represents the initial weight of the experimental set (leaf + vial + AX solution) and W_n the weight of this set after one hour.

2.2.5. Wrong Way Response by leaflet excision

MT and *Well* plants were brought to the laboratory two days before the evaluation for acclimation. The laboratory condition was mean temperature of 25°C, 12 h photoperiod, 200 μmol photons m^{-2} s^{-1} PAR irradiance. A fully expanded terminal leaflet from fourth to sixth leaf was chosen for gas exchange analysis and measurements were performed with a portable photosynthesis system (LI-6400XT). After stomatal conductance (g_s) reached a steady state, measurements were taken every minute and after 10 minutes the leaflet was excised from the rachis and gas exchange continued to be logged until a new steady state of at least 5 minutes. Leaf temperature (27 ± 0.5°C), photon flux density (800 μmol m^{-2} s^{-1}), air flow rate (300 μmol s^{-1}) and CO_2 concentration (400 ppm) into the leaf chamber were kept constant.

The quantification of the parameters of stomatal opening during wrong way response (WWR) of plants was as described by Buckley et al. (2011). Briefly, the initial and maximum g_s value (g_{si} and g_{smax}, respectively) logged after leaflet excision and the time required for it to happen, i.e., the time at the end of the WWR (t), were recorded. Then, the absolute size of WWR (W = g_{smax} - g_{si}), duration of WWR (L= t) and rate of opening during WWR (V=W/L) were calculated. All g_s values were normalized using the initial g_s from each sample, which was logged right before the excision.

2.2.6. Stem anatomic, stomatal and vein density analyses

Internodes of MT and *Well* stem were collected (between fourth and fifth leaves) and immediately sliced in a sliding microtome (Leica RM 2045, Wetzlar, Germany). Cross-sections were placed in distilled water and clarified with 1.0% sodium hypochlorite solution. The clarification time varied according to each sample. Samples were stained with 0.5% aqueous Safranin and for one minute with 1% alcian blue. Afterwards, the analyses and the pictures were acquired using the light microscope (Nikon Eclipse E200, Tokyo, Japan). The xylem vessels were measured in the ImageJ software (http://rsbweb.nih.gov/ij/).

The stomatal density in adaxial and abaxial sides of terminal leaflet of fully expanded leaf of the MT and *Well* genotypes were also evaluated. For this, the imprinting technique was used, as previously described by Vicente et al. (2015).

Leaf vein length per unit leaf area (VLA; also known as vein density) was determined in photographs of terminal leaflet using ImageJ software. Firstly, leaflets were cleared using 70% ethanol aqueous solution and the images were collected with a Leica magnifying glass model S8AP0 (Wetzlar, Germany), coupled to a Leica DFC295 camera (Wetzlar, Germany).

2.2.7. Stem and leaf hydraulic conductance

To determinate stem hydraulic conductance, stem internodes were excised, and the distal end was tightly sealed to a silicone hose, using dental low-viscosity addition silicone (Futura AD). The opposite extremity was immersed in a container filled with deionized water. The container was maintained in a thermal bath at 25ºC. The internodes were maintained in the same vertical orientation as in situ.

The silicone hose was connected to a metal cylindrical piece of 4 cm^3 filled with a dry cotton previously weighted. The metal piece was connected to a polyurethane tube that was

connected to a computer-controlled pump. A suction pressure (vacuum) was applied in the excised stems to drive water across the system, simulating the plant transpiration. The pressure applied to the internode was maintained constant at 30 KPa, being this value determined in preliminary tests (data not shown). Measurements were started at the time in which the silicone hose was completely filled with water, avoiding any interference of the internode length.

Water flow was determined by weighing the water absorbed by the cotton piece, which was renewed after each measurement.

Leaf hydraulic conductance (K_{leaf}) was performed according Zsögön et al. (2015). Briefly, K_{leaf} was estimated by the relationship between transpiration rates and the difference in water potential between the transpiring leaflet (Ψ_L) and the opposite non-transpiring leaflet (Ψ_X) on the same leaf. Leaflet transpiration (*E*) was measured using a portable photosynthesis system (LI-6400XT), and water potential using a Scholander pressure chamber (Soil Moisture Equipment Corp 3005; Santa Barbara Corp, Santa Barbara, CA, USA). K_{leaf} was calculated according to Ohm's Law as:

$$K_{leaf} = E / (\Psi_L - \Psi_X)$$

2.2.8. Determination of leaf turgor pressure by leaf patch clamp pressure (LPCP)

The relative changes of turgor pressure of leaves were measured by the leaf patch clamp pressure (LPCP) probes (formerly Zim-probes, now Yara Water Sensor – Yara, Oslo, Norway). The measuring principles of the LPCP probe together with the theoretical background are described in detail elsewhere (Zimmermann et al., 2008; Westhoff et al., 2009; Zimmermann et al., 2013). Briefly, two magnets are oppositely placed on the leaf and a pressure sensor in the magnet positioned on the leaf abaxial side. This sensor captures variations in the attraction between the magnets (known as patch pressure) in response to changes in water status of leaf (leaf turgor pressure). Thus, the patch pressure (P_p) is inversely proportional to the leaf turgor pressure, i.e., when leaf dehydrates during stomatal opening, P_p values increases, and conversely, decreases when the leaf rehydrates (Bramley et al, 2013).

The clamped leaf was a fully expanded terminal leaflet from fourth to sixth leaf in the primary stem, always considering leaves of similar physiological growth. The clamping was made as recommended by Westhoff et al., (2009) and Zimmerman et al. (2010). The LPCP probe readings were recorded in real time during 10 days. Measurements of ambient temperature (T)

and relative humidity (RH) were also taken simultaneously by temperature and humidity sensors (Yara, Oslo, Norway). The plants were kept well-watered during the experiment.

2.2.9. Seedling wilting and relative water content

Six-liter pots were filled with three liters of gravel, two liters of the transplanting soil mix, and one liter of the substrate used for sowing. Fifty seeds of MT and *Well* genotypes were sown on each half side of the pot. Thirty seedlings of each genotype were left per pot after germination. Three pots (90 seedlings of each genotype) were used for these experiments. A daily watering regime was adopted for 10 DAG with subsequent water withholding.

The seedling wilting experiment was conducted after irrigation interruption. The percentage of wilted seedlings was evaluated after the wilting onset on the first seedling in the pot, regardless of its genotype. Seedlings were considered as wilted when they presented wilting of the first leaf below the shoot apex. The evaluations were performed twice a day (12:00h and 17:00h). We rewatered the pot when 100% of the seedlings had wilted. The percentage of seedlings that recovered the leaf turgor was determined next.

Aiming to record the seedling water status from the interruption of irrigation to the wilting onset, the leaf and stem relative water content (RWC_{leaf} and RWC_{stem}, respectively) were determined. RWC in leaves and stem were performed every two days, sampling at noon. For RWC evaluation, four MT and *Well* seedlings were collected and the fresh weight of the stem and the first two true leaves above the cotyledons were determined. Then, stems and leaves were immediately placed in distilled water for 3-4 hours to hydrate to full turgidity. After complete rehydration, excess water was removed using filter paper and the turgid weight of samples was obtained. Next, stems and leaves were oven dried at 80°C for 24 hours and weighed to determine the dry weight. RWC was calculated using the equation:

$$RWC\ (\%) = [(FW - DW) / (TW - DW)] \times 100$$

The parameters FW, DW and TW correspond to the fresh, dry and turgid weight of the samples, respectively. The protocol used here to determine relative water content was adapted from http://plantstress.com/methods/RWC.htm.

2.2.10. Statistical analysis

All data significance was tested by the Student t-test when the data using SAS software (SAS Institute Inc., Cary, NC, USA). When the data did not meet the assumptions of ANOVA, we performed to non-parametric analysis, using Mann–Whitney U test. Each experiment had different number of sample units (as indicated in the figure legends).

2.3 RESULTS AND DISCUSSION

To explore the drought resistance of *S. pennelli* (Figure 1A), we used the genotype *Well*, which was generated by an initial cross between *S. pennellii* and the miniature tomato cultivar Micro-Tom (MT). After successive backcrosses with MT, a near isogenic line, that presents a remarkable resistance to wilting after water withdrawal, was obtained (Figure 1B). Noteworthy, during the introgression of *Well*, we noticed that plants displaying delayed wilting were always taller than MT, even after five backcrosses (Zsögön, 2011). From the seedling stage, the *Well* plants were already taller than MT and such phenotype was kept during all the plant growth (Figure S1). Previous studies also showed that *Well* plants present longer internodes when compared to MT plants (Zsögön 2011; Vicente et al., 2015).

We next performed an experiment to verify if the drought resistance of *Well* is displayed at the early growth stage. MT and *Well* seedlings were grown in the same pot and water supply was interrupted 10 days after germination (DAG). We verified that *Well* seedlings had a delayed wilting compared to MT, particularly in the first 48 hours (Figure S2A). When all seedlings of both genotypes in the same pot were wilted (Figure S2B), irrigation was resumed, and an increased recovery of *Well* seedling in comparison to MT was observed (Figure S2C and S2D).

Plants under water deficit usually show a progressive decrease in leaf width due to leaf rolling (Kadioglu and Terzi, 2007; Saglam et al., 2008; Puglielli et al., 2017). *Well* plants had a reduced leaf rolling after water withdrawal when compared to MT (Figure 1C). Since both genotypes were placed in the same pot, they experienced similar soil water potential (Figure 1B). These results suggest that *Well* presents a mechanism that allows plants to reduce water loss and to resist drought stress.

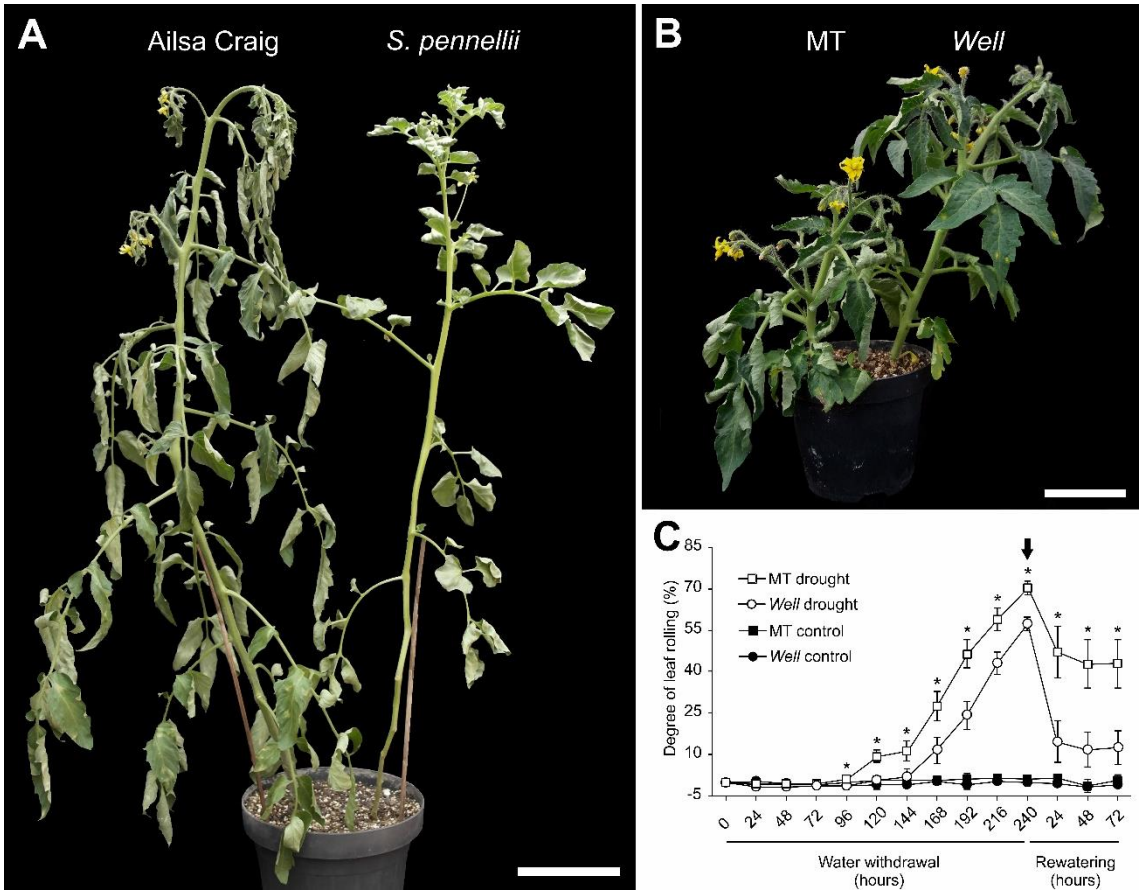

Figure 1 – Phenotype of the *Water Economy Locus in Lycopersicon* (*Well*), an introgression line for drought resistance from the tomato wild relative *S. pennellii*. A. Tomato (*S. lycopersicum* cv. Ailsa Craig) (left) and *S. pennellii* (right) plants under drought stress cultivated on the same pot. Scale bar = 10 cm. Note that the cultivated tomato tip is already drooping where the wild species is not. **B.** Representative 40-days old MT (left) and *Well* (right) plants cultivated in the same pot after 5 days of water withdrawal. Note that *Well* leaves look more turgid (presenting less rolling) than MT ones. Bar scale = 5 cm. **B.** Changes in leaf rolling (degree of leaf rolling) in MT (squares) and *Well* (circles) plants cultivated on the same pot under two conditions: well-watered (control, full symbols, n=8 terminal leaflets) or water-deficient (drought, open symbols, n=12 terminal leaflets). Water supply was interrupted during 10 days, when plants were 45-days old. Arrow indicates the point of rewatering of the plants. Data are mean±s.e.m.. * indicates statistical significances between MT and *Well* plants in drought conditions (Student t test; $p<0.05$). No significant differences were observed between genotypes under well-watering conditions.

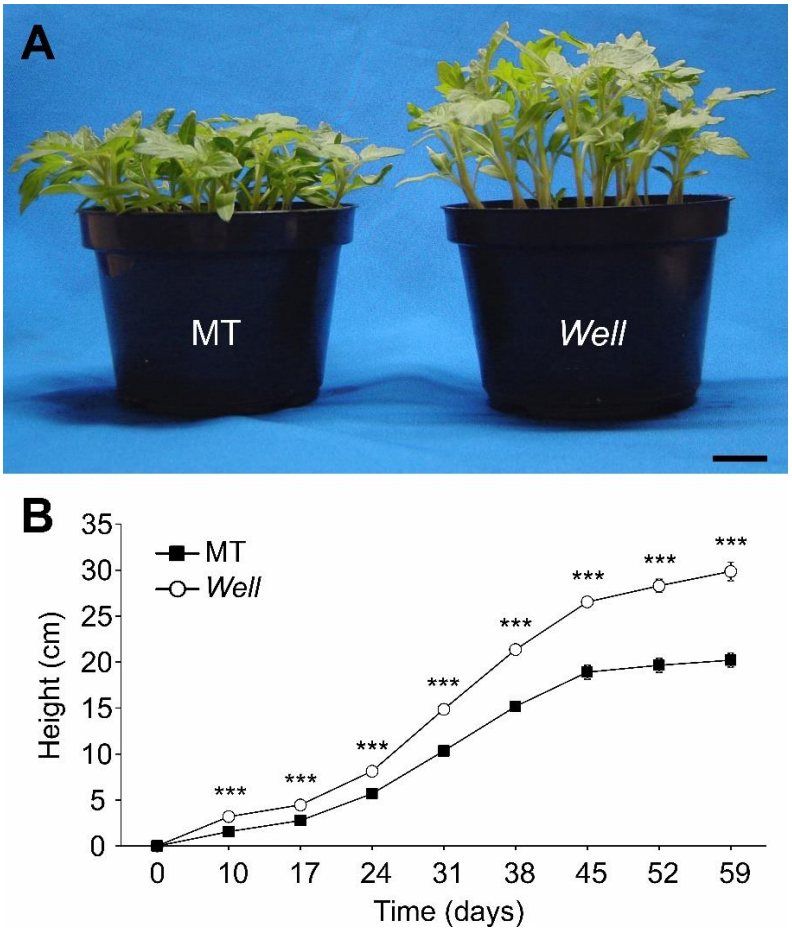

Figure S1. *Well* seedlings are taller than MT ones. **A.** 10-days old seedlings of MT (left) and *Well* (right). Scale bar = 2 cm. **B.** Time course of MT (full square) and *Well* (open circle) plants growing during 59 days after germination. Data are mean±s.e.m.. *** indicates significant differences by Student t test ($p<0.001$).

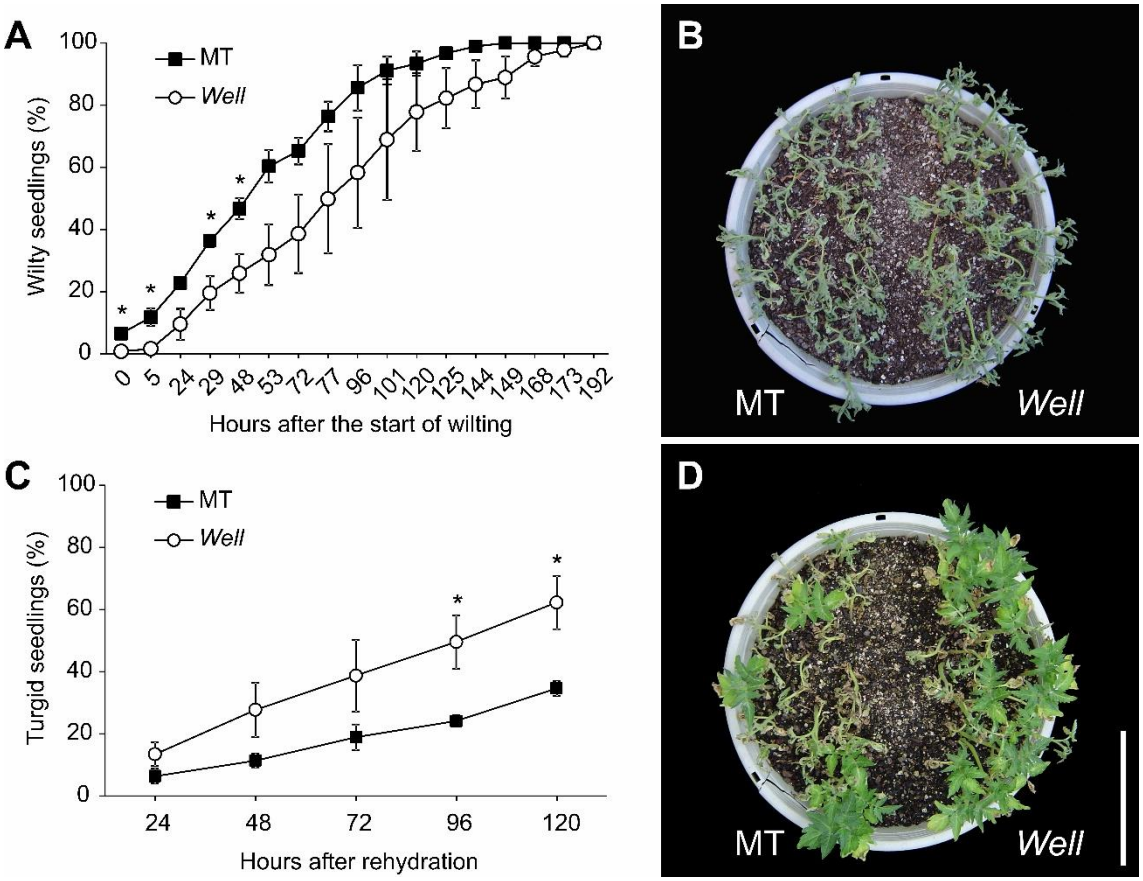

Figure S2 – *Well* plants wilt slower and recover faster from water withdraw, when compared to MT. **A.** Time course of wilted seedlings in MT (full square) and *Well* (open circle) after the start of wilting in each pot. Wilted seedlings were scored when presenting the curvature of the shoot apex. **B.** Representative image at the time when 100% of MT (left) and *Well* (right) seedlings were wilted. **C.** Time course of turgor recovery in MT (full square) and *Well* (open circle) seedlings after resuming irrigation. **D.** Representative image after 120 hours of resuming irrigation in MT (left) and *Well* (right) seedlings. Water supply was interrupted when seedlings were 15 days old. Scale bar = 15 cm. Data are mean ± s.e.m. (n = 3 pots with 60 seedlings, 30 of each genotype). * indicates significant differences by Student t test ($p<0.05$).

In order to test whether the reduced water loss in *Well* is due to the regulation of stomatal aperture, the stomatal conductance (g_s) was measured in three situations: well-watered plants, during drought stress (after water withdrawal) and after rewatering. Although no differences were verified before and during drought stress, *Well* plants showed a significant reduction in g_s after rewatering, when compared to MT plants (Figure 2A). However, the lower g_s of *Well* after rewatering did not affect CO_2 assimilation (A), which presented similar values in both genotypes (Figure 2B). *Well* plants showed a higher A than MT before water interruption. *Well* plants also presented a lower transpiration rate (E) than MT after the restoration of water supply (Figure 2C). The reduced E in *Well* genotype promoted an increase in the instantaneous WUE ($WUE_{instantaneous}$), which was obtain by the relationship between CO_2 assimilation and transpiration rate.

No difference in $WUE_{instantaneous}$ was observed before and during drought stress among the genotypes (Figure 2D).

The reduction in leaf water potential (Ψ_L) is usually accompanied by a decrease in photosynthetic activity and stomatal conductance in response to drought stress (Brix, 1962; Hsiao, 1973; Pasteirnak and Wilsoon, 1974; Boyer, 1976). Ψ_L was determined in both genotypes in each situation during gas exchange measurements and no difference was verified between MT and *Well* leaves (Figure 2E). These results suggest that the reduced wilting phenotype of *Well* plant does not involve a mechanism of water potential modification (*e.g.* osmotic adjustment) and that the genotypes experienced the same soil water potential when placed in the same pot. As expected, we observed a significant decrease in Ψ_L of plants under drought condition (Ψ_{PD} = -1.48 ± 0.081) compared to those under control and rewatering conditions (Ψ_{PD} = -0.83 ± 0.079 and Ψ_{PD} = -0.92 ± 0.083, respectively; Student's t-test, $p<0.001$).

Fully expanded leaves of both genotypes were placed on the laboratory bench for drying and the weight was evaluated hourly. In a total period of 12 h, the water loss was significantly lower in *Well* leaves than MT ones only in the first three hours (Figure 2F).

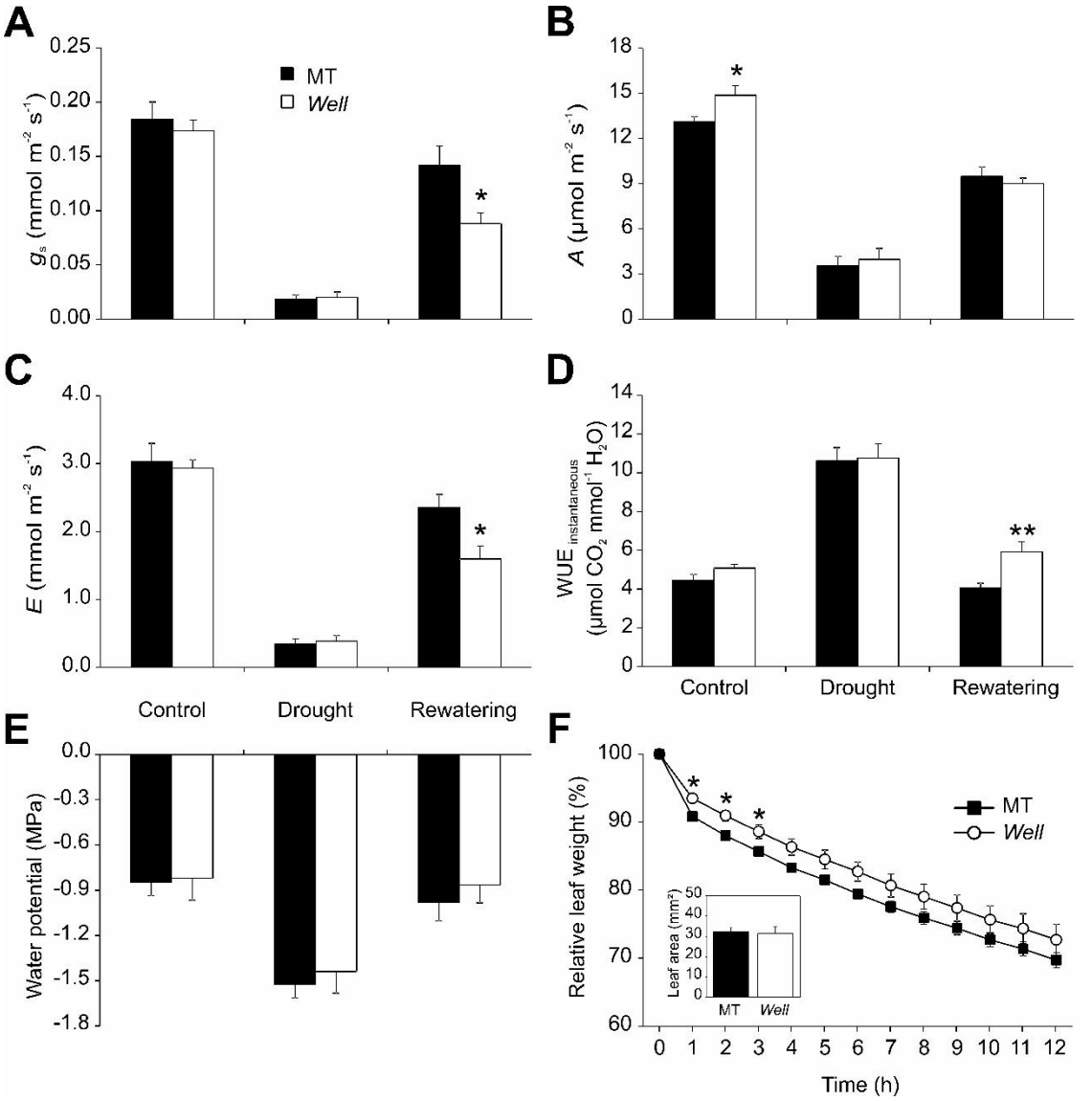

Figure 2 – Stomatal conductance (g_s) is reduced in *Well* plants after rehydration. **A-E.** MT (full bars) and *Well* (open bars) stomatal conductance (A), CO_2 assimilation (B), transpiration (C), instantaneous WUE (D) and water potential (E) in three different conditions. Control, drought and rehydrated condition represent the moment before the water interruption, moderated visual wilting and one week after rehydration of plants, respectively (n=6 plants to gas exchange and n=4 to water potential determination). MT and *Well* were cultivated in the same pot and the evaluation was conducted in plants 45 DAG. **F.** Water loss in MT (full square) and *Well* (open circle) detached leaves left on a laboratory bench under environment condition (n=5 leaves). Insert presents the area of leaves used to perform this experiment. Data are mean±s.e.m.. Statistical significance was tested by Student t test (*$p<0.05$, **$p<0.01$).

The transpiration rate was also measured in detached leaves with petioles immersed in a solution of artificial xylem sap. The reduced water loss in *Well* leaves compared to MT ones was evidenced shortly in the first hour of the experiment and the differences became greater during the 12 h of measurements (Figure 3A). Normally, reduced transpiration rate is associated with reduced stomatal density (Xu and Zhou, 2008; Farber et al., 2016). However, the comparison of stomatal density in *Well* and MT leaves showed increased values for *Well* in the adaxial surface

and no differences in the abaxial surface (Figure 3B), where tomato has the higher stomatal density (Gay and Hurd, 1975). These results suggest that the reduced *Well* transpiration and wilting are more related to stomatal sensitivity than density.

In most plants, stomatal closure occurs in response to changes in evaporative demand or water supply. However, transient g_s increases before closure lead to a new, lower steady-state value of gs, known as "wrong-way responses" (WWR) (Buckley et al., 2011). These responses occur after any disruption in the soil-plant-atmosphere hydraulic flow continuum (Powles et al., 2006). Since this disruption may be achieved by leaf excision (Darwin, 1898; Raschke, 1970; Powles et al., 2006), we evaluated WWR in MT and *Well* terminal leaflet after excision and verified that these genotypes present different kinetics of stomatal closure (Figure 3C).

The WWR parameters were also calculated as described by Buckley et al. (2011) and a smaller WWR duration in *Well* compared to MT was observed. This indicates a faster response to water content variation (Table S1). WWR is a phenomenon useful to investigate the kinetics of guard cell osmoregulation, because it involves two distinct phases: an initial hydropassive phase followed for a hydroactive one. The later hydroactive phase needs metabolic energy to reduce the guard cell osmotic pressure (Darwin 1898; Raschke 1970; Buckley et al. 2003; Powles et al., 2006). These data suggest that *Well* plants have a mechanism to induce or sense water status variations, promoting stomatal closure, and consequently regulating the water loss under stress conditions.

Table S1. Wrong-Way Response parameters of MT and *Well* terminal leaflets as described by Buckley et al. (2011). W corresponds to WWR absolute size and L to WWR duration (n=5).

	WWR absolute size (relative g_s)	**WWR duration (time_min)**	**WWR rate opening (W/L)**
MT	36.26 ± 10.56 a	4.60 ± 0.40 a	7.74 ± 2.01 a
Well	20.08 ± 4.08 a	3.00 ± 0.00 b	6.69 ± 1.36 a
***p*-value**	0.690	0.004	0.222

*Different letters indicate significant differences among genotypes (Mann–Whitney U test).

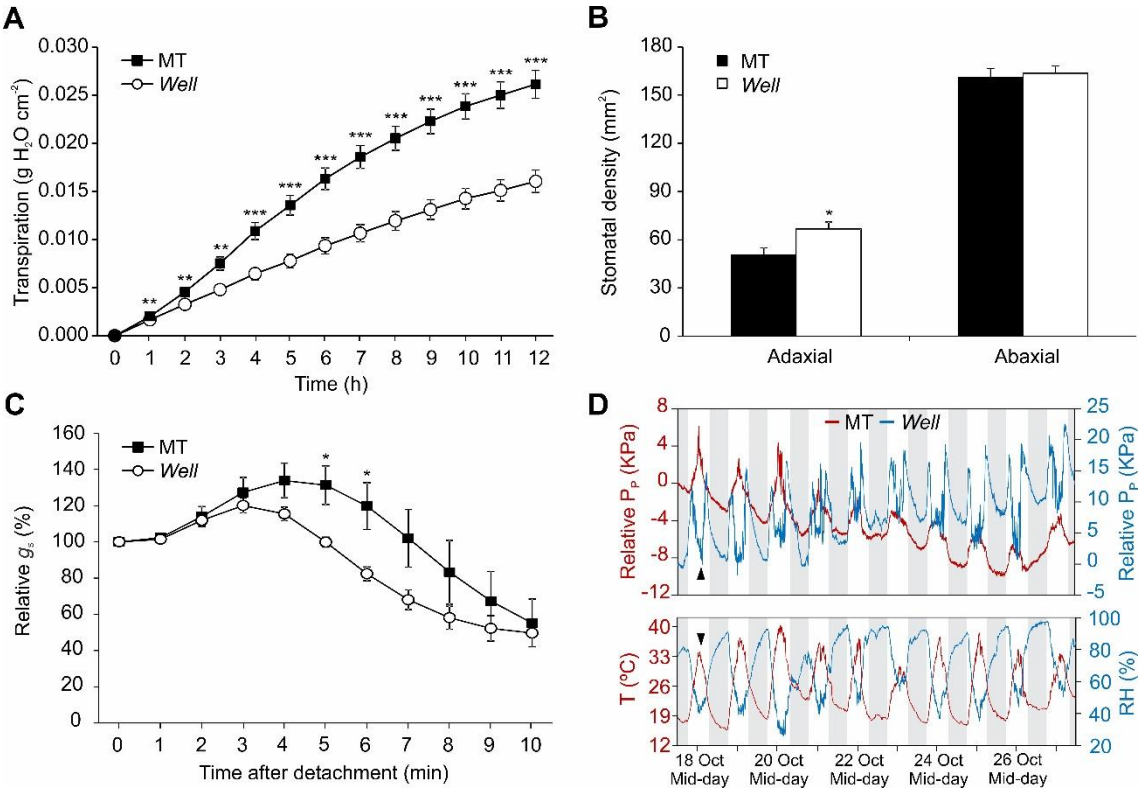

Figure 3 – *Well* plants present higher stomatal sensitivity. **A.** Transpiration of MT (full square) and *Well* (open circle) leaves (n=5) with petioles immersed in a solution of artificial xylem sap during 12 hours. **B.** Stomatal density in adaxial and abaxial side of MT (full bar) and *Well* (open bar) leaves (n=12). **C.** Wrong-way response (WWR) of stomatal conductance (g_s) of MT (full square) and *Well* (open circle) plants after terminal leaflet excision at the rachis (n=5). The WWR parameters described by Buckley et al. (2011) are shown in Table S1. Data are mean±s.e.m.. Statistical significance was tested by Student t test (*$p<0.05$, ***$p<0.001$). **D.** Relative changes in leaf patch pressure (P_p) (upper panel) on MT (red line) and *Well* (blue line) representative plants cultivated in the same pot, and concomitant changes in local air temperature (lower panel; T; red line) and relative humidity (lower panel; RH; blue line). Relative P_p values were normalized to the first value evaluated in each plant using the non-invasive leaf patch clamp pressure probe (Zimmermann et al., 2008; Westhoff et al., 2009). P_p is inversely proportional to the leaf turgor pressure, *e.i.*, leaf dehydrated presents higher P_p values, which decrease with the rehydration of leaves. In the graphic background, white and gray bars represent day and night periods, respectively. The black arrow heads indicate the midday depression of P_p curve on *Well* plant (upper panel) and that this depression correspond to higher temperatures (lower panel).

The water status of MT and *Well* plants was also evaluated using non-invasive leaf patch clamp pressure (LPCP) probes (Zimmermann et al. 2008; Westhoff et al. 2009; Zimmermann et al., 2013). LPCP probe is an alternative method to keep track, in real time, leaf hydration, and water temporal and spatial dynamics in the plants by measuring patch pressure (P_p), which is inversely proportional to the leaf turgor pressure (Zimmermann et al. 2008; Fernández et al., 2011; Bramley et al., 2013; Zimmermann et al., 2013; Fernández, 2014; Padilla-Díaz et al., 2016). The evaluation of changes in leaf patch pressure in MT and *Well* plants cultivated in the same pot under well-watered condition showed similar patterns of P_p values. In plants under well-watered

or low stress conditions, P_p curves presented maximum and minimum values at day and night, respectively (Westhoff et al., 2009; Ehrenberger et al., 2012; Bramley et al, 2013). Interestingly, the totality of *Well* plants evaluated presented midday depressions in the daily P_p curve over the all evaluation period, mainly in the hours of greater evapotranspirational demand (Figure 3D). Sporadically, some MT plants also showed midday depressions, but in a much lower frequency. Ehrenberger et al. (2012) observed a midday depression in olive plants under moderate water stress, *i.e.*, higher P_p values in the morning followed by decreased values on the hours around midday and increased values in the afternoon.

The stomatal closure of *Well* plants observed during the midday is likely to explain, at least in part, the higher water-use efficiency (WUE) of this genotype previously verified through gravimetric and carbon isotope discrimination ($\Delta^{13}C$) determination (Vicente et al., 2015). Several studies demonstrated a reduction in the CO_2 leaf concentration and an improvement in the assimilation of the ^{13}C isotope under conditions that promotes stomatal closure, such as reduced water supply (Farquhar et al., 1982; Martin and Thorstenson, 1988; Farquhar et al., 1989). Under non-limiting condition for gas exchange, the enzyme Ribulose-1,5-bisphosphate carboxylase/oxygenase (Rubisco) normally catalyses ^{12}C fixation, which is lighter than ^{13}C (Farquhar et al., 1989).

Together, these results showed that *Well* genotype, under well-watered conditions, exhibits responses similar to plant under moderate stress (Ehrenberger et al., 2012), which evidences the *Well* greater stomatal sensitivity to variations in water availability. Therefore, the reduced wilting observed in *Well* plants is likely to be due to its capacity to perceive differences in the water status and to respond by closing stomata, allowing a better recovery of *Well* when compared to MT after severe drought stress (Figure 1 and S2).

The water status variation in 10-days old MT and *Well* seedlings were also monitored. The relative water content (RWC) in leaves and stem was measured in both genotypes from the interruption of irrigation to the beginning of seedling wilting. The measures were taken every two days at midday, since all *Well* plants presented a drastic variation in P_p curves during this period (Figure 3D). Significant differences in RWC between MT and *Well* leaves were verified only at 0 and 10 days after irrigation interruption (Figure 4A). MT presented higher leaf RWC values at 0 days and *Well* at 10 days. On the other hand, the *Well* genotype maintained the stem RWC higher than MT plants when submitted to the same dry stress conditions (Figure 4B). These results indicate that the stem may act as a water reservoir in *Well* plants. This observation, coupled to the greater stomatal sensitivity, is likely to contribute to the better recovery from drought stress presented by *Well*.

Several studies demonstrated that the stomatal closure occurs in response to variations in the plant hydraulic conductance (K_{plant}) (Saliendra et al., 1995; Cochard et al., 2002; Brodribb and Holbrook, 2003; 2004; Sack and Holbrook, 2006; Scoffoni et al., 2017a), due to the disruption in the soil/plant/atmosphere water flux continuum. The major determinant of K_{plant} is the leaf hydraulic conductance (K_{leaf}), since it forms a considerable part of hydraulic resistance in the plant structure (Sack and Holbrook, 2006). The K_{leaf} was measured in MT and *Well* plants, and *Well* plants presented reduced values (Figure 4C). This suggests that the diurnal variation on the stomatal behavior in this genotype (Figure 3D), may be a consequence of its lower hydraulic conductance. These findings are corroborated by Fletcher et al., (2007), which reported that soybean genotypes exhibiting slow-wilting in response to drought stress presented little or no further increase in transpiration rate under high vapor pressure deficit (VPD). Later, it was demonstrated that this limiting transpiration rates is associated with a low K_{leaf} (Sinclair et al., 2008).

The vein density (Vein length per unit area, VLA) in MT and *Well* leaves was characterized, since the leaf vein system has a crucial role on water supply across the leaf, as well as a strong influence on stomatal aperture and, consequently, on leaf hydraulic conductance (Sack & Holbrook, 2006; Sack and Scoffoni, 2013). High VLA can enable higher K_{leaf}, stomatal conductance and higher rates of gas exchange per unit leaf area (Sack and Scoffoni, 2013). However, *Well* plants showed higher vein density than MT (Figure S3). Another K_{plant} component, shoot hydraulic conductance (K_{stem}), was also measured and a lower conductance in *Well* stem when compared to MT (Figure 4D) was observed. Thus, there is strong evidence that the wilting responses verified in *Well* plants are caused by a differential xylem hydraulic conductance.

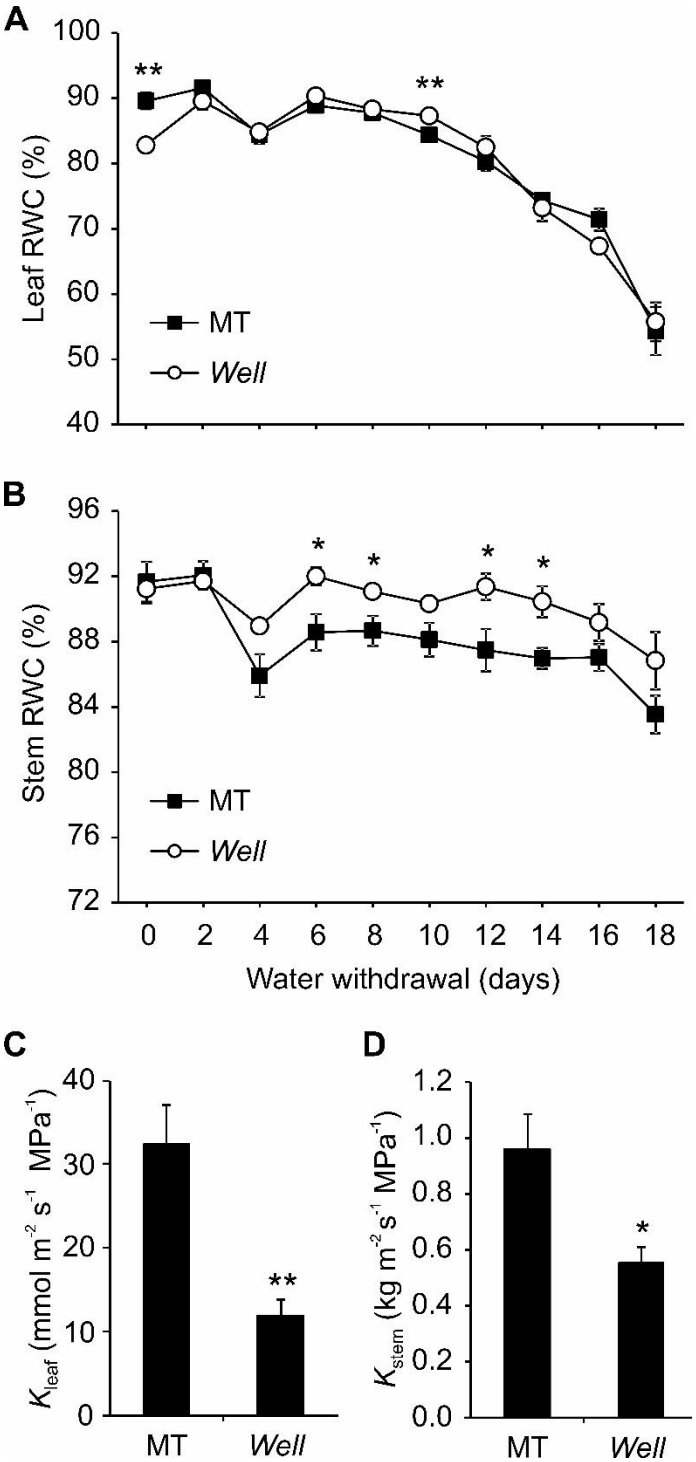

Figure 4 – *Well* plants maintain a higher stem relative water content (RWC) than MT under water withdrawal. **A and B.** Variation on the leaf (A) and stem (B) RWC in MT (full square) and *Well* (open circle) seedlings after the interruption of the water supply. Water supply was interrupted when seedlings were 10 days old (n = 4 seedlings). The seedlings were collected from 3 pots with 30 seedlings of each genotype on the same pot. **C and D.** *Well* presents a significant reduction in leaf (C) and stem (D) hydraulic conductance, which may affect water transport via xylem (n = 8 leaves and 5 stem segments). Data are mean±s.e.m.. Statistical significance was tested by Student t test (*$p<0.05$, **$p<0.01$).

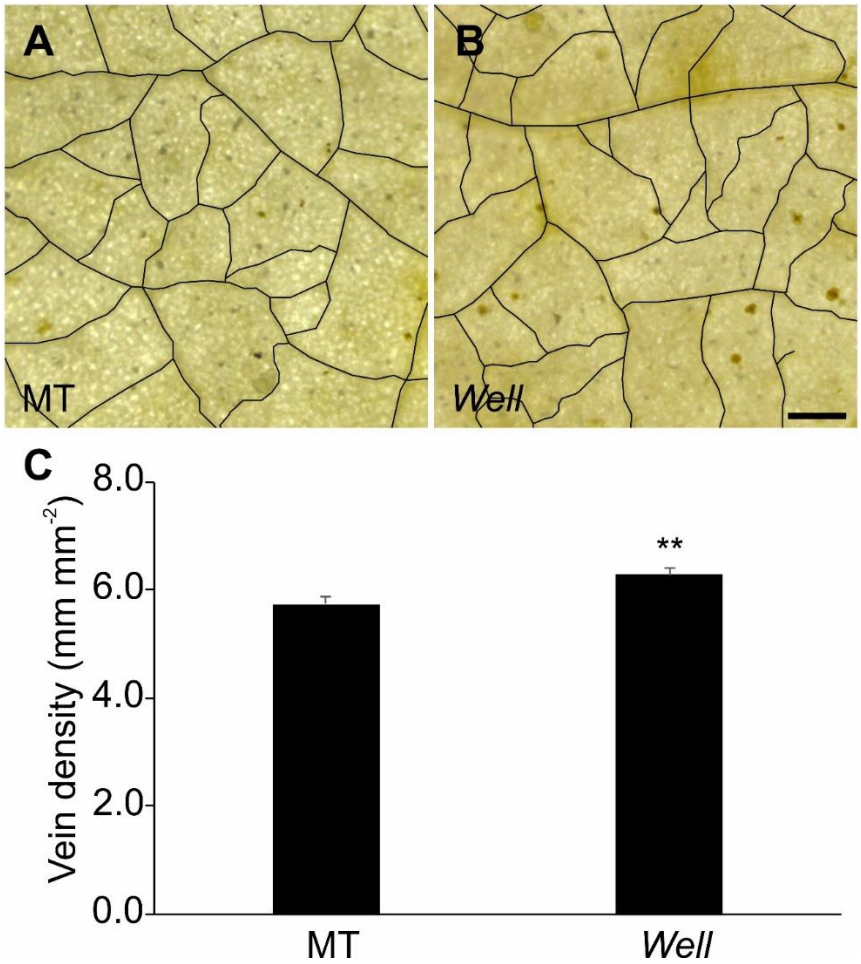

Figure S3 – *Well* plants exhibit an increase in vein density compared to MT. **A and B.** Representative image of MT (A) and *Well* (B) clarified leaves used to vein density measurement. All veins were measured in each leaflet. Scale bar = 250 μm. **C.** Vein density of MT and *Well* leaves (n = 12 images from six terminal leaflet). Data are mean±s.e.m.. ** indicates significant differences by Student t test ($p<0.01$).

The hydraulic conductance of xylem vessels is strongly dependent on anatomical parameters (Zimmermann, 1983; Ewers et al., 1990; Hacke et al., 2006; Sperry et al. 2006). Positive correlations have been found between xylem hydraulic conductivity and vessel lumen area, vessel number, length and diameter, indicating that hydraulic conductivity was strongly associated with vessel size (Legge, 1985; Hacke et al., 2006; Sperry et al. 2006; Zach et al., 2010; Lens et al., 2011; Hajek et al., 2014; Scoffoni et al., 2017b). Based on this, an anatomical analysis of cross-sections of MT and *Well* stems was performed. No difference in xylem cross-sectional areas were verified (Figure 5A). Analysis focusing in the primary xylem revealed that the development protoxylem and metaxylem were similar between genotypes (data not shown). On the other hand, differences were observed in the secondary xylem. *Well* plants present a higher vessel density than MT, approximately 570 vessels per mm^2, which corresponds to an increase of 22% (Figure 5B). However, this genotype shown a significant reduction in the mean vessel size

(14% compared to MT) (Figure 5C). According to Poiseuille´s law, an increase in conduit diameter leads to an increase of fourth power in the hydraulic conductivity, which is confirmed by several works that highlight a great gain in conducting capacity from a slight increase in vessel diameter (Zimmermann, 1983; Ewers, 1985; Tyree and Ewers, 1991; Sperry et al. 2006, Zach et al., 2010). Therefore, the reduction in leaf and stem hydraulic conductance observed in *Well* is probably associated to xylem vessel size.

Moreover, vessel size distributions were analyzed and a reduction in the incidence of larger vessels (more than 2000 mm^2) in *Well* plants compared to MT (Figure 5D) was verified. Larger conduits provide greater xylem water flow and K_{leaf} but are more vulnerable to embolism (Sack and Scoffoni, 2013). Ahmad et al. (2018) found a strong negative correlation between vessel density and the xylem pressure inducing loss of hydraulic conductance, indicating that higher vessel density promotes a greater embolism resistance and reduces a substantial loss of conductance in adverse conditions, such as drought. This resistant to air entrance into the xylem and loss of conductance may play a crucial role delaying wilting and promoting a faster recovery of *Well* plants after exposed to drought stress.

Together, the results suggest that in *Well* plants the water lost in conditions of higher transpiration rate on the leaf is probably not fully refilled by xylem water. In turn, this may promote a disturbance of the soil/plant/atmosphere continuum, leading to stomatal closure. We demonstrated that the stomatal closure and subsequent recovery of leaf turgor occur at the hottest hours of the day, *i.e.*, in the period where transpiration rate is higher (Figure 3D) and when normally there is a high vapor pressure deficit. Therefore, stomatal closure may affect wilting (Figure 1 and S2), and probably the WUE determined by Vicente et al. (2015), since it limits water loss and carbon isotope discrimination. Linked with this, we observed that most developed stem of *Well* plants may act as water storage and could maintain a basal metabolism allowing these plants to survive to severe drought stress.

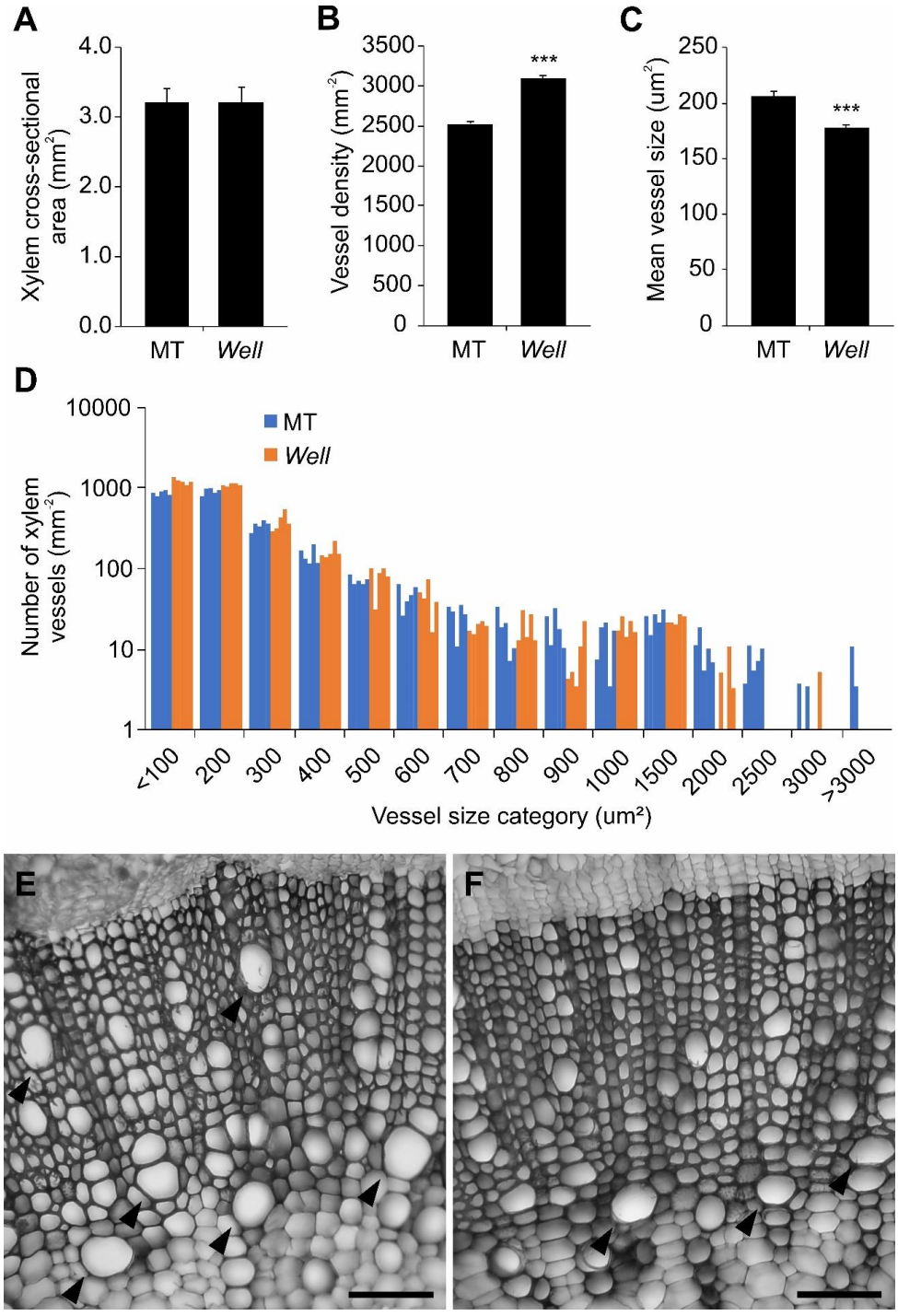

Figure 5 - Anatomic characterization of cross-sections of MT and *Well* xylem. **A.** Xylem cross-sectional area of MT and *Well* stem (n=10 cross-sections). **B and C.** Vessel density (B) and mean vessel size (C) in MT and *Well* xylem. Data are mean±s.e.m.. Statistical significance was determined by Student t test ($p<0.001$). **D.** Vessel size distribution in the xylem of MT and *Well*. The x axis shows the upper values of cross-sectional area for each vessel size category. Blue (MT) and orange (*Well*) bars within each category represent a single individual plant (n = 5 per genotype). **E and F**. Representative cross-sections of the fifth internode of MT (E) and *Well* (F) taken at 45 dag. Scale bar = 100 μm. The black arrow heads indicate the largest vessels in each genotype. Note that MT genotype presents a greater occurrence of large vessels compared to *Well*.

2.4. CONCLUSION

In this work, we characterized the water relations in an introgression line with delayed wilting, greater recovery after a severe drought stress, and that had already been reported as more efficient in water use (Vicente et al., 2015). The lower hydraulic conductance found in *Well* plants may be a possible mechanism for such effects. We also presented evidences indicating that the greater stomatal sensitivity observed in *Well* plants occurs in response to lower hydraulic conductance, which correlates to the reduction in the size of the xylem vessels. The further molecular identification of the *Well* locus may favor its incorporation in breeding programs, aiming to improve water use efficiency and minimize plant losses due to drought stress in seedling transplant.

REFERENCES

Ahmada HB, Lensb F, Capdevillea G, Burletta R, Lamarque LJ, Delzona S. 2018. Intraspecific variation in embolism resistance and stem anatomy across four sun-flower (*Helianthus annuus* L.) accessions. Physiologia Plantarum, 163, 59-72.

Basu S, Ramegowda V, Kumar A, Pereira A. 2016. Plant adaptation to drought stress. F1000Research, 5. DOI: 10.12688/f1000research.7678.1.

Blum A. 2005. Drought resistance, water-use efficiency, and yield potential - are they compatible, dissonant, or mutually exclusive? Australian Journal of Agricultural Research, 56, 1159-68.

Blum A. 2009. Effective use of water (EUW) and not water-use efficiency (WUE) is the target of crop yield improvement under drought stress, Field Crops Research, 112, 119-23.

Bolger A, Scossa F, Bolger ME, Lanz C, Maumus F, Tohge T. et al. 2014. The genome of the stress-tolerant wild tomato species *Solanum pennellii*. Nature Genetics, 46, 1034-1038.

Boyer JS. 1976. Water deficits and photosynthesis. In Kozlowski TT. ed, Water Deficits and Plant Growth IV. Academic Press, New York, pp 153-190.

Boyer JS. 1982. Plant productivity and environment (crop genetic improvement). Science, 218, 443-448.

Bramley H, Ehrenberger W, Zimmermann U, Palta JA, Rüger S, Siddique, KHM. 2013. Non-invasive pressure probes magnetically clamped to leaves tomonitor the water status of wheat. Plant Soil, 369, 257-268.

Brix H. 1962. The effect of water stress on the rates of photosynthesis and respiration in tomato plants and loblolly pine seedlings. Physiologia Plantarum, 15, 10-20.

Brodribb TJ, Holbrook NM. 2003. Stomatal closure during leaf dehydration, correlation with other leaf physiological traits. Plant Physiology, 132, 2166-2173.

Brodribb TJ, Holbrook NM. 2004. Stomatal protection against hydraulic failure: a comparison of coexisting ferns and angiosperms. New Phytologist, 162, 663-670.

Buckley TN, Sack L, Gilbert ME. 2011. The role of bundle sheath extensions and life form in stomatal responses to leaf water status. Plant Physiology, 156, 962-973.

Buckley TN, Mott KA, Farquhar GD. 2003. A hydromechanical and biochemical model of stomatal conductance. Plant Cell and Environment, 26, 1767-1785.

Carvalho RF, Aidar ST, Azevedo RA, Dodd IC, Peres LEP. 2011. Enhanced transpiration rate in the *high pigment 1* tomato mutant and its physiological significance. Plant Biology, 13, 546-550.

Cochard H, Coll L, Le Roux X, Améglio T. 2002. Unraveling the effects of plant hydraulics on stomatal closure during water stress in walnut. Plant Physiology, 128, 282-290.

Darwin F. 1898. Observations on stomata. Philosophical Transactions of the Royal Society of London, Series B, 190, 531-621.

Doebley JF, Gaut BS, Smith BD. 2006. The Molecular Genetics of Crop Domestication. Cell, 127, 1309-1321.

Ehrenberger W, Rüger S, Rodríguez-Domínguez CM, Díaz-Espejo A, Fernández JE, Moreno J, Zimmermann D, Sukhorukov VL, Zimmermann U. 2012. Leaf patch clamp pressure probe measurements on olive leaves in a nearly turgorless State. Plant Biology, 14, 666-674.

Ewers FW, Fisher JB, Chiu ST. 1990. A survey of vessel dimensions in stems of tropical lianas and other growth forms. Oecologia, 84, 544-552.

Farquhar GD, O'Leary MH, Berry JA. 1982. On the relationship between carbon isotope discrimination and the intercellular carbon dioxide concentration in leaves. Australian journal of plant physiology, 9, 121-37.

Farquhar GD, Ehleringer JR, Hubick KT. 1989. Carbon isotope discrimination and photosynthesis. Annual Review of Plant Physiology and Plant Molecular Biology, 40, 503-37.

Farber M, Attia Z, Weiss D. 2016. Cytokinin activity increases stomatal density and transpiration rate in tomato. Journal of Experimental Botany, 67, 6351-6362

Fernández JE. 2014. Plant-based sensing to monitor water stress: applicability to commercial orchards. Agricultural Water Management, 142, 99-109.

Fernández JE, Rodriguez-Dominguez CM, Perez-Martin A, Zimmermann U, Rüger S, Martín-Palomo MJ, Torres-Ruiz JM, Cuevas MV, Sann C, Ehrenberger W, Diaz-Espejo A. 2011. Online-monitoring of tree water stress in a hedgerow olive orchard using the leaf patch clamp pressure probe. Agricultural Water Management, 100, 25-35.

Fletcher AL, Sinclair TR, Allen LH Jr. 2007. Transpiration responses to vapor pressure deficit in well watered 'slow-wilting' and commercial soybean. Environmental and Experimental Botany, 61, 145-151.

Franks PJ, Doheny-Adams WT, Britton-Harper ZJ, Gray JE. 2015. Increasing water use efficiency directly through genetic manipulation of stomatal density. New Phytologist, 207, 188-95.

Gay AP, Hurd RG. 1975. Influence of light on stomatal density in tomato. New Phytologist, 75, 37-46.

Hacke UG, Sperry JS, Wheeler JK, Castro L. 2006. Scaling of angiosperm xylem structure with safety and efficiency. Tree Physiology, 26, 619-701.

Hajek P, Leuschner C, Hertel D, Delzon S, Schuldt B. 2014. Trade-offs between xylem hydraulic properties, wood anatomy and yield in *Populus*. Tree Physiology, 34, 744-756.

Hsiao TC. 1973. Plant responses to water stress. Annual Review Plant Physiology, 24: 519-570.

Juenger TE. 2013. Natural variation and genetic constraints on drought tolerance. Current Opinion in Plant Biology, 2013, 16, 274-281.

Kadioglu A, Terzi R. 2007. A dehydration avoidance mechanism: leaf rolling. The Botanical Review, 73, 290-302.

Kang Y, Khan S, Ma X. 2009. Climate change impacts on crop yield, crop water productivity and food security – a review. Progress in Natural Science, 19, 1665-1674.

Kebede H, Martin B, Nienhuis J, King G. 1994. Leaf anatomy of two *Lycopersicon* species with contrasting gas exchange properties. Crop Science, 34, 108-113.

Koornneef M, Alonso-Blanco C, Vreugdenhil D. 2004. Naturally occurring genetic variation in *Arabidopsis thaliana*. Annual Review Plant Physiology, 55, 141-172.

Kooyers NJ. 2015. The evolution of drought escape and avoidance in natural herbaceous populations Plant Science, 234, 155-162.

Legge NJ. 1985. Anatomical aspects of water movement through stems of mountain ash (*Eucalyptus regnans* F. Muell.). Australian Journal of Botany 33: 287–298.

Lens F, Sperry JS, Christman MA, Choat B, Rabaey D, Jansen S. 2011. Testing hypotheses that link wood anatomy to cavitation resistance and hydraulic conductivity in the genus Acer. New Phytologist, 190, 709-723.

Levitt J. 1972. Responses of Plants to Environmental Stresses. New York, NY: Academic Press, 698.

Li JB, Luan YS, Liu Z. 2015. Overexpression of *SpWRKY1* promotes resistance to *Phytophthora nicotianae* and tolerance to salt and drought stress in transgenic tobacco. Physiology Plantarum, 155: 248e266.

Li J, Wang Y, Wei J, Pan Y, Su C, Zhang X. 2018. A tomato proline-, lysine-, and glutamic-rich type gene *SpPKE1* positively regulates drought stress tolerance. Biochemical and Biophysical Research Communications, 499, 777-782.

Loukehaich R, Wang T, Ouyang B, Ziaf K, Li H, Zhang J, Lu Y, Ye Z. 2012. *SpUSP*, an annexin-interacting universal stress protein, enhances drought tolerance in tomato. Journal of Experimental Botany, 63, 5593-5606.

Martin B, Tauer CG, Lin RK. 1999. Carbon isotope discrimination as a tool to improve water-use efficiency in tomato. Crop Science, 39, 1775-1783.

Martin B, Thorstenson YR. 1988. Stable carbon isotope composition (delta-C-13), water-use efficiency, and biomass productivity of *Lycopersicon esculentum*, *Lycopersicon pennellii*, and the F1 hybrid. Plant Physiology, 88, 213–217.

Meissner R, Jacobson Y, Melamed S, Levyatuv S, ShalevG, Ashri A, Elkind Y, Levy A. 1997. A new model system for tomato genetics. Plant Journal, 12, 1465-1472.

Mueller ND, Gerber JS, Johnston M, Ray DK, Ramankutty N, Foley JA. 2012. Closing yield gaps through nutrient and water management. Nature, 490: 254-257.

Najafi E, Devineni N, Khanbilvardi RM, Kogan F. 2018. Understanding the Changes in Global Crop Yields Through Changes in Climate and Technology. Earth's Future, 6, 410-427.

Padilla-Díaz CM, Rodriguez-Dominguez CM, Hernandez-Santana V, Perez-Martin A, Fernández JE. 2016. Scheduling regulated deficit irrigation in a hedgerow olive orchard from leaf turgor pressure related measurements. Agricultural Water Management. 164, 28-37.

Pasteirnak D, Wilson GL. 1974. Differing effects of water deficit on net photosynthesis, respiration and transpiration of apple leaves. Plant Physiology, 16, 565-583.

Pinheiro HA, DaMatta FM, Chaves ARM, Loureiro ME. 2005. Drought tolerance is associated with rooting depth and stomatal control of water use in clones of *Coffea canephora*. Annals of Botany, 96, 101-108.

Premachandra GS, Saneoka H, Fujita K, Ogata S. 1993. Water stress and potassium fertilization in field grown maize (*Zea mays* L.): Effects of leaf water relations and leaf rolling. Journal of Agronomy and Crop Science, 170, 195-201

Powles JE, Buckley TN, Nicotra AB, Farquhar GD. 2006. Dynamics of stomatal water relations following leaf excision. Plant, Cell and Environment, 29, 981-992.

Puglielli G, Gratani L, Varone L. 2017. Leaf rolling as indicator of water stress in *Cistus incanus* from different provenances. DOI: http://dx.doi.org/10.1101/131508.

Raschke K. 1970. Stomatal responses to pressure changes and interruptions in the water supply of detached leaves of *Zea mays* L. Plant Physiology 45, 415-423.

Rick CM. 1973. Potential genetic resources in tomato species: clues from observations in native habitats. In: Srb AM. (ed.). Genes, Enzymes and Populations. New York, Plenum, 255-269.

Rick CM 1976. Tomato *Lycopersicon esculentum* (Solanaceae). In: Simmonds NW. (ed.). Evolution of Crop Plants, London, Longman, 268-273.

Rick CM 1983. Genetic variability in tomato species. Plant Molecular Biology Reporter, 1, 81-87.

Sack L, Holbrook NM. 2006. Leaf hydraulics. Annual Review of Plant Biology, 57, 361-381.

Sack L, Scoffoni C. 2013. Leaf venation: structure, function, development, evolution, ecology and applications in past, present and future. New Phytologist, 198, 938-1000.

Saglam AA, Kadioglu R, Terzi R, Saruhan N. 2008. Leaf rolling and biochemical changes in them in post-stress emerging *Ctenanthe setosa* plant under drought conditions. Russian Journal of Plant Physiology, 55: 48-53.

Saliendra NZ, Sperry JS, Comstock JP. 1995. Influence of leaf water status on stomatal response to humidity, hydraulic conductance, and soil drought in *Betula occidentalis*. Planta, 196, 357-366.

Scoffoni C, Albuquerque C, Brodersen CR, Townes SV, John GP, Bartlett MK, Buckley TN, McElrone AJ, Sack L. 2017a. Outside-xylem vulnerability, not xylem embolism, controls leaf hydraulic decline during dehydration. Plant Physiology, 173, 1197-1210.

Scoffoni C, Albuquerque C, Brodersen CR, Townes ST, John GP, Cochard H, Buckley TN, McElrone AJ, Sack L. 2017b. Leaf vein xylem conduit diameter influences susceptibility to embolism and hydraulic decline. New Phytologist, 213, 1076-1092.

Serraj R, Sinclair TR. 2002. Osmolyte accumulation: can it really help increase crop yield under drought conditions? Plant, Cell and Environment, 25, 333-341.

Sinclair TR, Zwieniecki MA, Holbrook NM. 2008. Low leaf hydraulic conductance associated with drought tolerance in soybean. Physiologia Plantarum, 132, 446–451.

Sperry JS, Hacke UG, Pittermann J. 2006. Size and function in conifer tracheids and angiosperm vessels. American Journal of Botany, 93, 1490-1500.

Sun F, Roderick ML, Farquhar GD. 2012. Changes in the variability of global land precipitation. Geophysical Research Letters, 39, L19402, DOI:10.1029/2012GL053369.

Treviño MB, O'Connell MA. 1998. Three drought-responsive members of the nonspecific lipid-transfer protein gene family in *Lycopersicon pennellii* show different developmental patterns of expression. Plant Physiology, 116, 1461-1468.

The Tomato Genome Consortium. 2012. The tomato genome provides insights into fleshy fruit evolution. Nature, 485, 635-641.

Tyree MT, Ewers FW. 1991. The hydraulic architecture of trees and other woody-plants. New Phytologist., 119, 345-360.

van Ittersum MK, Cassman KG, Grassini P, Wolf J, Tittonell P, Hochman Z. 2013. Yield gap analysis with local to global relevance – a review, Field Crops Research, 143: 4-17.

Vicente MH, Zsögön A, Sá AFL, Ribeiro RV, Peres LEP. 2015. Semideterminate growth habit adjusts the vegetative-to-reproductive balance and increases productivity and water-use efficiency in tomato (*Solanum lycopersicum*). Journal of Plant Physiology, 177, 11-19.

Xu X, Martin B, Comstock J, Vision T, Tauer C, Zhao B, Pausch R, Knapp S. 2008. Fine mapping a QTL for carbon isotope composition in tomato. Theoretical and Applied Genetics, 117, 221-233.

Xu Z, Zhou G. 2008. Responses of leaf stomatal density to water status and its relationship with photosynthesis in a grass. Journal of Experimental Botany, 59, 3317-3325.

Wei T, O'Connell MA. 1996. Structure and characterization of a putative drought-inducible H1 histone gene. Plant Molecular Biology, 30, 255-68.

Westhoff M, Reuss R, Zimmermann D, Netzer Y, Gessner A, Gessner P, Zimmermann G, Wegner LH, Bamberg E, Schwartz A, Zimmermann U. 2009. A non-invasive probe for online monitoring of turgor pressure changes under field conditions. Plant Biology, 11,701-712.

Yu ATT. 1972. The genetics and physiology of water usage in *Solanum pennellii* Corr. and its hybrids with *Lycopersicon esculentum* Mill.. Thesis (Doctor of Philosophy), Davis, University of California, 122p.

Zach A, Schuldt B, Brix S, Horna V, Culmsee H, Leuschner C. 2010. Vessel diameter and xylem hydraulic conductivity increase with tree height in tropical rainforest trees in Sulawesi, Indonesia. Flora, 205, 506-512.

Zamir D. 2001. Improving plant breeding with exotic genetic libraries. Nature Reviews Genetics, 2, 983-989.

Ziaf K, Loukehaich R, Gong P, Liu H, Han Q, Wang T, Li H, Ye Z. 2011. A multiple stress responsive gene *ERD15* from *Solanum pennellii* confers stress tolerance in tobacco. Plant Cell Physiology, 52, 1055-1067.

Zimmermann MH. 1983. Xylem structure and the ascent of sap. Berlin/Heidelberg, Germany: Springer Berlin Heidelberg, 143 p.

Zimmermann U, Bitter R, Ribeiro-Marchiori PE, Rüger S, Ehrenberger W, Sukhorukov VL, Schüttler A, Ribeiro RF. 2013. A non-invasive plant-based probe for continuous monitoring of water stress in real time: a new tool for irrigation scheduling and deeper insight into drought and salinity stress physiology. Theoretical and Experimental Plant Physiology, 25, 3-12.

Zimmermann D, Reuss R, Westhoff M, Gessner P, Bauer W, Bamberg E, Bentrup F-W, Zimmermann U. 2008. A novel, non-invasive, online monitoring, versatile and easy plant-based probe for measuring leaf water status. Journal of Experimental Botany 59:3157-3167.

Zsögön A. 2011. Identification and characterization of a tomato introgression line with reduced wilting under drought. Thesis (Doctor of Philosophy). The Australian National University, Canberra, 199p.

Zsögön A, Alves Negrini AC, Peres LEP, Nguyen HT, Ball MC. 2015. A mutation that eliminates bundle sheath extensions reduces leaf hydraulic conductance, stomatal conductance and assimilation rates in tomato (*Solanum lycopersicum*). New Phytologist, 205, 618-626

Zsögön A, Vicente MH, Reartes DS, Peres LEP. 2017. Understanding and improving water-use efficiency and drought resistance in tomato. In: Mattoo A, Handa AK. (Org.). Achieving sustainable cultivation of tomatoes. 1ed.Cambridge: UK: Burleigh Dodds Science Publishing Limited, p. 1-26.